2022

TOWARDS A CIRCULAR ECONOMY: LIQUID-FED FAST PYROLYSIS OF WASTE POLYOLEFIN PLASTICS

Daniel G. Kulas
Michigan Technological University, dgkulas@mtu.edu

TOWARDS A CIRCULAR ECONOMY: LIQUID-FED FAST PYROLYSIS OF WASTE POLYOLEFIN PLASTICS

By

Daniel G. Kulas

A DISSERTATION

Submitted in partial fulfillment of the requirements for the degree of

DOCTOR OF PHILOSOPHY

In Chemical Engineering

MICHIGAN TECHNOLOGICAL UNIVERSITY

2022

This dissertation has been approved in partial fulfillment of the requirements for the Degree of DOCTOR OF PHILOSOPHY in Chemical Engineering.

Department of Chemical Engineering

Dissertation Advisor:	*David Shonnard*
Committee Member:	*Rebecca Ong*
Committee Member:	*Michael Mullins*
Committee Member:	*Ezra Bar Ziv*
Department Chair:	*Pradeep Agrawal*

Table of Contents

List of Figures

List of Tables

Author Contribution Statement

This doctoral dissertation contains material previously reviewed and published in scientific journals along with material currently submitted to scientific journals. Full citation of these are as follows

Chapter 2

Reprinted with permission from Kulas, D. G.; Zolghadr, A.; Shonnard, D., Micropyrolysis of Polyethylene and Polypropylene Prior to Bioconversion: The Effect of Reactor Temperature and Vapor Residence Time on Product Distribution. *ACS Sustainable Chemistry & Engineering* 2021, 9 (43), 14443-14450. Copyright 2021 American Chemical Society.

DOI: 10.1021/acssuschemeng.1c04705

Author Contributions

Kulas:	Conceptualization, Methodology, Investigation, Visualization, Writing – original draft.
Zolghadr:	Conceptualization, Investigation, Writing – review & editing.
Shonnard:	Conceptualization, Writing – review & editing, Supervision, Project administration, Funding acquisition.

Chapter 3

Reprinted with permission from Kulas, D.; Zolghadr, A.; Shonnard, D., Liquid-Fed Waste Plastic Pyrolysis Pilot Plant: Effect of Reactor Volume on Product Yields. *Journal of Analytical and Applied Pyrolysis* 2022, 166, 105601. Copyright 2022 Elsevier.

DOI: 10.1016/j.jaap.2022.105601

Author Contributions

Kulas:	Conceptualization, Methodology, Investigation, Visualization, Writing – original draft.
Zolghadr:	Conceptualization, Investigation, Writing – review & editing.
Shonnard:	Conceptualization, Writing – review & editing, Supervision, Project administration, Funding acquisition.

Chapter 4

In preparation for submission to *ACS Sustainable Chemistry and Engineering*. Kulas, D; Zolghadr, A; Chaudhari, U; Shonnard, D. Economic and Environmental Analysis of Plastics Pyrolysis After Secondary Sortation of Mixed Plastic Waste

Author Contributions

Kulas:	Conceptualization, Methodology, Investigation, Visualization, Writing – original draft.
Zolghadr:	Conceptualization, Investigation, Writing – review & editing.
Chaudhari:	Data Collection, Analysis, Writing – review & editing
Shonnard:	Conceptualization, Writing – review & editing, Supervision, Project administration, Funding acquisition.

Acknowledgements

First, I want to express my utmost gratitude to my advisor Dr. David Shonnard for his constant guidance and advice through my PhD journey. Deep gratitude also goes to my committee members Dr. Rebecca Ong, Dr. Michael Mullins, and Dr. Ezra Bar Ziv for their valuable advice.

I would like to acknowledge the financial support from Defense Advanced Research Projects Agency ReSource program (cooperative agreement HR00112020033). I also thank the Department of Chemical Engineering for the opportunity to work as a teaching assistant for the Unit Operations Lab.

I would also like to thank my entire research group, especially to Dr. Olumide Winjobi, Dr. Ulises Gracida Alvarez, Dr. Sharath Ankathi, and Dr. Ali Zolghadr for taking their time to teach me the techniques necessary to conduct both laboratory and modeling research, and to Utkarsh Chaudhari and Saketh Merugu for the fun times hanging out in the office and at conferences. I also recognize the effort and help from the undergraduate researchers Lina Espejo Ramirez, Topher Taylor, Libby Umlor, Jessie Lyons, Emily Mattson, Elizabet Schumann, Kristen Kautz, Emmeline Beck, Jim Smith, Mahlon Bare, John Baughn, Matthew Fooy, and Kristina Mills. Special thanks also goes to all my researchers collaborators for making the DARPA project a fascinating project to work on.

I also want to thank the Faculty and Staff of the Department of Chemical Engineering, specially to Dr. Pradeep Agrawal for giving me the opportunity to gain experience in teaching, to Dr. Julie King and Dr. Jeana Collins, for their constant and valuable advice, to Dr. Michael Mullins for the opportunity to work in their laboratory and use their equipment, to Taana Blom, Alexis Snell, and Kristi Pieti, for all the help with the administrative paperwork and to Steve Wisniewski and Jerry Norkol for their constant and valuable technical support with fabricating and repairing the laboratory equipment used for my research.

My deepest thanks to my parents, Greg and Kathy Kulas, for their constant love and support as well as my siblings: Michael and Sarah for everything. Thank you for all your sacrifices and all you have done for me throughout the years. A special mention goes to my cat, Shadow, for her hours of attempting to “help” me with computer work. I would also like to express my gratitude to all my friends from St. Albert the Great University Parish and intramural sports. Thank you for giving me a variety of extracurricular activities to keep my mind and body healthy.

And finally, I would like to thank God Almighty for giving me the strength, knowledge, ability, and opportunity to undertake this research study and to persevere and complete it satisfactorily.

List of Abbreviations

A: Frequency factor

C: Carbon

CED: Cumulative energy demand

CEPCI: Chemical Engineering plant cost index

CSBR: Continuous spouted bed reactor

DCF: Discounted cash flow

Ea: Activation Eenrgy

EVA: Ethylene-vinyl acetate

EVOH: Ethylene-vinyl alcohol

FBR: Fluidized bed reactor

FCI: Fixed capital investment

FCOP: Fixed operation costs

GC-MS: Gas chromatography/mass spectrometry

GHG: Greenhouse gas

GWP: Global warming potential

h: Heat transfer coefficient

HDPE: High-density polyethylene

HI: Heat integration

IRR: Internal rate of return

kt: Kiloton

LCA: Life cycle assessment

LDPE: Low-density polyethylene

MACRS: Modified accelerated cost recovery system

MAE: Mean absolute error

MT: Metric ton

MRF: Material recovery facility

MSP: Minimum selling price

MSW: Municipal solid waste

NPV: Net present value

PE: Polyethylene

PET: Polyethylene terephthalate

POLs: Petroleum, oils, and lubricants

PP: Polypropylene

PS: Polystyrene

PVC: Polyvinyl chloride

ROI: Return on Investment

TEA: Techno-economic analysis

TSMR: Two-stage micropyrolysis reactor

VCOP: Variable operating costs of production

VRT: Vapor residence time

WC: Working Capital

Abstract

Plastic usage has quickly grown in recent years as plastics have become an essential part of everyday life. Unfortunately, recycling rates have not matched the increased growth, with the majority of waste plastic landfilled. The strategy of circular economy has been proposed to reuse the waste plastic to create new polymers, thus avoiding both landfilling and the use of virgin raw materials. Achieving a circular economy for plastics requires the development of new technologies capable of recycling plastic waste under a circular economy perspective. In this dissertation, a novel liquid-fed fast pyrolysis process is introduced towards achieving a circular economy. Recycled pyrolysis wax is used to dissolve waste polyolefin plastic and create a liquid feed to the pyrolysis reactor. The oil product from the pyrolysis reaction is naphtha-like in appearance and could be used as a feedstock for petro-chemical facilities for the production of new polymers.

The fundamental pyrolysis reaction kinetics are investigated using a novel two-stage micropyrolysis reactor accessory to a commercial pyroprobe unit. A practical lumped kinetic model was created using generated micropyrolysis data to predict the effect of temperature (550-600 °C) and vapor residence time (VRT; 1-6 seconds) on product distribution. The presented kinetic model shows strong agreement with known degradation mechanisms and was applied for scaling-up the pyrolysis process to a 250 g/hr pilot plant. By testing three different reactor volumes, it was found that VRT had a significant effect on wax, liquid, and gas product distribution. A multiphysics model was developed and predicted reactor temperature, pyrolysis product species, and velocity profiles. The trends for product distribution as a function of VRT were found to be consistent between both the pilot plant and micropyrolysis systems, demonstrating that the pilot system can be tuned to produce the desired pyrolysis product. Finally, the data generated using the pilot plant was used to guide a process simulation for an 84,000 tonne/yr waste plastic pyrolysis facility. A techno-economic analysis and life cycle assessment of the process found favorable economic and environmental results for pyrolysis oil when compared to fossil naphtha.

1 Introduction

1.1 Current state of plastic waste generation, disposal, and recycling

Over the past century, plastics have become an essential part of human life. Valued for their durability and versatility[1], plastics serve as key components of the packaging, construction, transportation, electronics and healthcare sectors.[2] The properties that make plastics so useful also create challenges for the end-of-life phase of plastics. The low production cost of plastics[3, 4] has created a take-make-dispose approach to plastics. It is easier and cheaper to produce new virgin single-use plastics then to reuse and recycle waste plastics. In the United States, around 35.7 million U.S. tons of waste plastic was generated in 2018[5], representing a 20-fold growth in the past 50 years.[6] Approximately 64% of the total waste plastic generated was comprised of polyolefins, including high density polyethylene (HPDE - 17%), low density polyethylene (LDPE - 24%), and polypropylene (PP - 23%).[5] Most of these plastics are single use products[7, 8], becoming a waste stream soon after being generated. In 2018, the majority of waste plastics (75%) were landfilled at the end of life while a minority were incinerated for energy (15.8%) or collected for recycle (8.5%).[5] Collection for recycling is primarily driven by the recycling of polyethylene terephthalate (PET) bottles. The numbers are much worse for polyolefins, with 9% of HDPE, 4% of LDPE, and only 1% of PP recycled in 2018.[5] One study calculated that this take-make-dispose approach, in which plastic is primarily landfilled after use, represents a loss of materials worth $10 billion/year.[9] The linear economy also hurts the environment, with estimated greenhouse gas (GHG) emissions of 1.1 to 3.0 tonne (MT) of CO_2 eq. of GHG emissions above that which could be achieved if recycling were to replace landfilling.[1] In recent years, many researchers have proposed moving away from a linear economy towards a circular economy for plastics.[5, 10-12] In a circular economy, the waste plastic is reused to create new polymers. This avoids both the landfilling of the waste plastic and the use of virgin materials to create the new virgin-quality polymer resins.[13] Current commercial plastic recycling technologies are not capable of recycling waste plastic under a circular economy perspective. There is a need to develop new recycling technologies to achieve a circular economy for plastics.[5, 11]

The majority of plastics collected for recycling are prepared for mechanical recycling. One major issue with mechanical recycling is that it struggles to handle post-consumer materials that contain either a mixture of plastic types or high levels of contamination.[14] Polyolefins have a large range of polymer structure, molecular weight, and additives. This variation causes unpredictable physical properties and can lead to downcycling, meaning that the recycled plastic resin is used to make a different product compared to the original.[15] Another issue is the inability to control the final color, with different color plastic inputs usually combining to produce an undesirable grey color after reprocessing into pellets.[16] Extrusion has also been found to cause crosslinking in chains,[17] increasing the viscosity in plastic. One study found a fivefold increase in viscosity of HDPE after sixty extrusion cycles, suggesting that HDPE cannot be recycled in this manner over many cycles. The downcycling of recycled plastics prevents mechanical recycling from achieving a circular economy. Another concern is the presence of small plasticizer and stabilizer additives left

over in the recycled HDPE that could diffuse into food products and be toxic, limiting the potential applications of the recycled polymers.[18] A strategy to overcome this includes multilayered packaging with virgin layers on the surfaces to prevent diffusion. Other feasible options for recycled HDPE include plastic lumber, detergent bottles, plastic benches, etc.[15, 19] Environmentally, life cycle assessment (LCA) results are favorable for mechanical recycling when compared to virgin resin production, chemical recycling, and incineration, showing lower GHG emissions and energy consumption.[5, 12, 20-22]

Since mechanical recycling cannot tolerate high levels of contamination or plastic mixtures,[14] it is unable to recycle all the plastic that exits a materials recovery facility (MRF). MRFs typically sort the plastic into a relatively pure PET and HDPE bales that are a high quality feedstock for mechanical recycling.[23] The rest of the plastics typically end up in a product called #1-7 mixed plastic bale, which are considered low-value and often incinerated or landfilled.[24] Surveys of MRFs in the U.S. have found that on average 25% of the plastic entering a MRF ends up in this mixed plastic bale.[25] This bale contains a combination of PET, HDPE, PP, LDPE, PS, and PVC[26] plus non-plastic contaminant levels up to 5 wt.% total.[23] Both of these qualities eliminate mechanical recycling as an option to recycle the #1-7 bale. At the industrial level, the lack of commercial recycling technologies capable of processing the #1-7 bale relegate it to being treated as a waste stream through landfilling or incineration. Landfilled plastic takes decades to centuries in order to fully breakdown due to its high durability.[27] This creates the potential for plastic to leak from mismanaged landfills into the rivers and oceans.[28, 29]

Incineration converts municipal solid waste (MSW) into energy by combusting MSW at temperatures above 750 °C, releasing heat that can be used to produce steam for heating and electricity at efficiencies up to 80%.[30] Despite having the benefit of generating energy while avoiding landfill disposal, incineration also has its drawbacks. The emissions from MSW incinerations can be toxic to humans, commonly containing dioxins and furans.[31] Of the treatment options available for plastics, incineration has the highest greenhouse gas (GHG) emissions, ranging from 1.8-3.0 kg CO_2 eq/kg plastic wastes.[21, 32] Taking a credit for the electricity produced lowers the GHG emissions to 1.4 kg CO_2 eq/kg plastic wastes, making it more comparable to some chemical recycling technologies.[21, 32] Incineration also has higher air pollution and acidification potential than landfilling, mechanical recycling, or chemical recycling.[23]

Despite being treated as a waste stream commercially, there is untapped value in post-use mixed plastics that can be used to incentivize collection and reprocessing.[33] Mixed plastic has become an attractive feedstock for developing chemical recycling technologies.[34] Chemical recycling technologies that have been developed to recycle waste polyolefin plastic include hydrogenolysis, gasification, dissolution with purification, liquefaction, and pyrolysis.[23]

Hydrogenolysis uses a noble metal catalyst (such as Ru, Pt, etc.) in the presence of hydrogen to cleave the plastics carbon-carbon bonds and produce hydrocarbons. The reaction is similar to slow pyrolysis in that it is completed at moderate temperatures (200-350 ℃) and pressures (20-60 bar) with long residence times (1-24 hours).[23] Hydrogenolysis

of polyolefins creates light gases,[35-37] liquid fuels,[38-40] and lubricants,[35, 39, 41, 42] suggesting that varying the operating conditions and catalyst provides some selective control in product distribution. This research is still at the research scale, with consumption of expensive H_2 being a primary barrier to commercialization.[43]

Gasification converts plastic waste into synthesis gas (CO, H_2), which can serve as a feedstock to produce a range of chemicals and fuels.[44] Occurring above 550 ℃, gasification also produces ash as a byproduct.[45] Commercially, roughly 100 waste gasification facilities are in operation across the globe which produce electricity and heat.[23] The next generation of gasification facilities, however, appear to be headed towards producing biofuels (when plastics are mixed with biogenic wastes), aviation fuels, and chemicals.[23]

Dissolution uses solvents to recover and recycle plastics without any chemical reactions. An advantage of dissolution is that it doesn't require a high-purity input stream.[46, 47] An effective solvent selectively dissolves only a single target plastic, ignoring other plastic types, additives, and other impurities. The undissolved solids are filtered out before an antisolvent precipitates the now pure and high-quality polymer resin. Using a sequence of multiple solvents and antisolvents can selectively separate both multilayer plastics and waste plastic mixtures. This process has been demonstrated by researchers at the University of Wisconsin-Madison, who used dissolution to recycle post-industrial films composed of PE, EVOH, PET, and EVA.[48, 49] Their process, called Solvent-Targeted Recovery and Precipitation (STRAP), was found to produce plastic resins at costs similar to virgin resins. One barrier to commercialization is the cost to separate the solvent and anti-solvent after precipitation. A recent study found that when precipitation is induced via temperature instead of antisolvents the process becomes more economically feasible.[48]

Liquefaction converts plastic into a liquid oil using pressurized gases and/or solvents between 200-450 ℃. Of particular interest is the use of supercritical solvents, such as acetone and ethanol,[50-53] which can drastically increase reaction rates.[54, 55] Liquefaction of HDPE/PP with acetone solvent at 450-470 ℃ was found to produce a 90% yield of aliphatic hydrocarbon oil after 1 hour of residence time.[50] Operationally, reaction temperature and residence time are key variables to controlling liquefaction yields. Recent research has observed that increasing the temperature increased reaction rates, with more cracking of liquid products to gases and increased formation of aromatics.[56] Increasing reaction time also increases the conversion and allows secondary reactions to occur. This can be counterproductive, with Shabtai, et al.[56] finding that while conversion improved from 82.5% to 100% at a longer residence time, the oil yield actually decreased from 92.8% to 60.2% due to increased cracking at the extended residence time. Research looking at real-world waste plastic has concluded that feedstock heterogeneity is a critical obstacle to commercialization.[57] Williams and Slaney[57] found oil yields from mixed plastics were significantly less than for the individual plastics, concluding that plastic interactions detrimentally decrease volatiles formation and promote solid residue. Contaminants found in the waste plastics can also hinder the effect of the catalyst, decreasing oil yields.[58]

Pyrolysis uses high temperatures and an inert atmosphere to break down plastics into hydrocarbon products. Pyrolysis can be carried out either with or without the use of solid

heterogeneous catalysts. Typical products include gas, aromatics, pyrolysis oil, and wax along with a solid residue char that can occur, especially when contaminants are present.[4, 23, 59, 60] The pyrolysis oil can be cracked down and further refined for new plastics production in petrochemical facilities,[33] making it a circular economy technology. The pyrolysis oil, after additional refining, can also be used as a gasoline or diesel alternative.[61] The pyrolysis gas can be combusted for energy or fed to a separation train to produce ethylene and propylene.[13] Polyolefin pyrolysis tends to favor the generation of olefins over paraffins, with one study finding a range of olefin/paraffin respective yields from 1.3 to 5 depending on reaction conditions for HDPE pyroylsis.[62]

In addition to producing fuels and chemicals, pyrolysis can also serve as a chemical pretreatment step for microbial growth to produce proteins.[63] Research conducted by Byrne, et al.[63] found that microbes derived from environmental consortia were able to grow on pyrolysis oil derived from waste plastics. The oil, which contained C10-C20 alkenes, served as the energy and carbon source for the oil-degrading microorganisms to produce biomass. It has been proposed that this biomass could be recovered as a value-added compound such as protein.[63-65] This is in contrast to natural biodegradation of plastics, which is very slow and inefficient due to plastic's structural complexity and ultra-high molecular weight.[27, 66, 67] Muhonja, et al. found that even in the optimum case, microorganisms only achieved 35% degradation of polyethylene plastics over sixteen weeks.[68] Using pyrolysis to pretreat the plastic and break it down considerably accelerates the biological process, with extensive microbial growth observed over the course of five days.[63]

1.2 Kinetics of polyolefin pyrolysis

Due to the high number of potential products from polyolefin pyrolysis, considerable research has been devoted to understanding pyrolysis reaction kinetics. Through understanding the kinetics, the pyrolysis operating conditions can then be manipulated to produce the desired products. The pyrolysis kinetics can also be used to assist in reactor design and scaling-up of pyrolysis.[69] Pyrolysis reactions can generally be split into two steps: primary and secondary thermal degradation. Primary thermal degradation occurs right away when the plastic is broken down into mostly high molecular weight compounds.[62] Secondary degradation occurs in the vapor phase as the pyrolysis products continue to react with each other and break down into lighter molecular weight compounds.

A coil pyrolyzer is a typical device used by researchers to study the primary reactions and products from pyrolysis through an approach called micropyrolysis. By immediately sweeping any primary products formed out of the reaction zone by an inert gas, the occurrence of any secondary reactions is inhibited.[62] An electrically controlled platinum spiral resistance wire is used to provide a flash increase of temperature (~1000 °C/s)[59] to a very small sample (0.5-5 mg)[59, 62] to achieve fast pyrolysis. A study by del Remedio Hernandez, et al.[62] et al. found that fast primary thermal pyrolysis of HDPE produced primarily wax compounds at temperatures from 500-700 °C. Liquid and gas products were only significantly produced by raising the pyrolysis temperature to 800 °C, adding a catalyst, or using a fluidized bed reactor to allow both primary and secondary reactions to

occur. Research conducted by Gracida-Alvarez, et al.[59] added a unique second stage tubular reactor to the conventional micropyroylsis system. The primary pyrolysis vapors produced from the coil pyroylzer were carried into a hot tubular reactor by an inert carrier gas where secondary reactions occurred. The temperature of both the coil pyroylzer and the tubular reactor are controllable, along with the inert gas flow rate, which is correlated to the vapor residence time. Both the reactor temperature and vapor residence time have been found to have a significant impact on product distribution, making control of them essential to understanding the fundamental pyrolysis kinetics. High temperatures increase bond breakage, leading to a faster free-radical chain reaction (eq. 1-6).[70] Increasing residence time increases the extent of the reaction, which in turn leads to lighter molecular weight products.[4, 71]

Three types of kinetic models have been used to describe the pyrolysis reaction:[72] mechanistic,[70, 73] probabilistic,[74, 75] and lumped-species phenomenological.[60, 69, 76] Mechanistic models aim to understand the intrinsic reaction kinetics by accounting for every plausible reaction pathway, intermediate species, and final product.[70] Past mechanistic research has concluded that free-radical mechanisms dominate the pyrolysis reaction.[70, 73] The reactions are initiated in two ways by either end initiation (eq. 1) or random initiation (eq. 2), where radicals (R) of length i (having i monomer units) are created from a polymer chain (P) of length n. The formed radicals continue to react and decompose via hydrogen abstraction (eq. 3) and β-scission (eq. 4). The radical reaction is terminated when two radicals react with each other via either disproportionation (eq. 5) and recombination (eq. 6).[70] The termination reactions forms carbon-carbon double bonds (C=C) in the structure, leading to a high production of alkenes.[57]

$$P_n \rightarrow R_{n-1} + R_1 \quad (1)$$

$$P_n \rightarrow R_{n-i} + R_i \quad (2)$$

$$R_i + P_n \rightarrow P_i + R_n \quad (3)$$

$$R_n \rightarrow P_{n-j} + R_j \quad (4)$$

$$R_i + R_j \rightarrow P_i + P_j \quad (5)$$

$$R_i + R_j \rightarrow P_{i+j} \quad (6)$$

More detailed mechanistic models also incorporate radical addition and backbiting reactions such as 1,5- and 1,4-hydrogen transfer.[73, 77-79] It is not always practical or possible, however, for researchers to track every molecule and reaction while creating a kinetic model. A study by Harmon, et al.[70] found that both phenomenological and probabilistic models can capture experimental results with strong agreement while being less complex than mechanistic models.

Probabilistic models simplify the reaction network to one key reaction: β-scission (eq. 4).[74] Although this simplification loses mechanistic details, it can still capture the most

important aspects of the reaction mechanism.[70] By assuming that β-scission randomly breaks the polymer chain, a probability distribution can be used to predict the product distribution by carbon number. The reaction rate is modeled as a function of temperature while the reaction extent depends on residence time.[74] A weakness of probabilistic models is that it ignores all other reaction pathways. These reaction pathways can differ quite a bit from random chain scission and be significant, such as the Diels−Alder, unimolecular cyclization, and dehydrogenation reaction pathways proposed for aromatic generation from gases (eq. 7).[59, 80] As such, a probabilistic model focusing on random chain scission would fail to predict any aromatic formation.

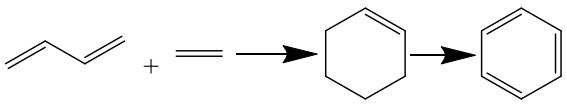

(7)

Phenomenological models use mechanisms based on observation instead of the underlying free radical chemistry.[64] Typical phenomenological models account for around a dozen reactions[70] between several intermediate and end product lumped species. The individual species are lumped together by a common parameter, avoiding the need to measure and track every molecule.[81, 82] Common lumping parameters include molecular weight, carbon number, density and boiling point.[60, 76] Kinetic parameters for the lumped reaction pathways are fitted to experimental data using nonlinear regression.[69, 76] A review of the literature shows that phenomenological reaction networks include irreversible first-order reactions that crack large molecules into smaller ones.[69, 76] These reactions are similar to those found from hydrocracking of heavy petroleum fractions and pyrolysis of rubber.[83-86]

Fundamental knowledge of the reaction mechanisms and how product distribution is affected by vapor residence time and temperature will help to propose reactor operating conditions that favor the yield of pyrolysis oil at the pilot scale level. As discussed in Chapter 2, the research program included the formation of a lumped kinetic model fitted to experimental data produced from a novel micropyrolysis apparatus with control of both vapor residence time and temperature.

1.3 Pyrolysis reactor design and scale-up

Pilot scale pyrolysis reactors can be categorized by reactor type and the presence of catalysts. This section gives a brief overview of the different type of pyrolysis reactors found in the literature along with a discussion of the pros and cons of using catalysts. It then concludes with discussion on the innovative pilot scale reactor used in this research program.

A recent review article on plastic pyrolysis[4] identified that researchers primarily use fluidized bed,[71, 87-90] fixed-bed,[91-95] and conical spouted bed reactors (CSBR)[96-99] for plastic pyrolysis. Fluidized bed reactors are typically chosen when working with catalysts because the catalyst can be reused many times within the fluidized media without needing to discharge. They have high rates of heat transfer, making them a common choice for industrial reactors for pyrolyzing plastic waste.[100] The catalyst is continuously circulated

between the pyrolysis and a regeneration zone to remove any coke formation.[23] Fluidized bed reactors can face the issue bed defluidization, which occurs when melted plastics stick on the fluidized bed itself.[61] Fixed-bed reactors, on the other hand are limited due to the low catalyst surface area available for reaction and issues with handling solid feedstock.[4] A few researchers have proposed using a fixed-bed reactor as a second stage to further breakdown the primary pyrolysis product.[94, 95] While this avoids the issue of solid feedstock, the addition of a second reactor has not been found to be cost effective compared to a single-stage process. Designed to have better versatility for handling solid feed, the CSBR has been found to be particularly effective for low temperature pyrolysis to obtain wax.[99] Technical challenges of the CSBR encountered during research include catalyst entrainment and product collection.[101] In addition, the complicated design of a CSBR requires many pumps which is expensive compared to simpler systems.[4]

Fluidized bed, fixed-bed, and CSBR reactors all make use of catalysts, which increase rates of reaction and requiring lower temperatures for degradation which decreases energy consumption.[4, 61, 102, 103] A study by Anene, et al.[2] found that catalytic pyrolysis of LDPE/PP at 460 °C produced larger amounts of liquid and gas product when compared to thermal pyrolysis at the same conditions. Research by del Remedio Hernández, et al.[62] also found that catalytic pyrolysis of HDPE at 500-600 °C created gases in high proportions (>80% wt%) with low amounts of liquid product (<10 wt%). They did find, however, that high temperatures and coke deposition can deactivate the catalyst, which led to reduced gas fraction between 700–800 °C and required catalyst regeneration.[62] Other researchers have observed similar trends on the effect of catalyst to liquid and gas product yields.[104-109] Catalytic pyrolysis also provides increased selectivity, with Anene, et al. finding that while thermal pyrolysis produced a mixture of C_7-C_{40} compounds, using the catalyst narrowed the carbon distribution range to C_7-C_{12} with no compounds above C_{13} measured.[2] This selectivity gives it an advantage over thermal pyrolysis in terms of product quality. While thermal pyrolysis products are typically restricted to being sold to oil refineries for additional upgrading, catalysts can produce gasoline and diesel range products that do not need further upgrading.[61] Disadvantages to catalytic pyrolysis include increased complexity to the system, increased operating costs for regeneration, and potential poisoning of the catalyst by impurities/contaminations.[23]

In Chapter 3, an innovative pyrolysis reactor is proposed for the pyrolysis of waste plastics. Novelties include a liquid feed that flows into a simple tubular reactor. The liquid feed is achieved through a dissolution pretreatment step which dissolves waste plastic in a recycled pyrolysis wax solvent.[110] One advantage with the liquid-fed system over traditional Archimedes screw feeders[111, 112] is that avoiding solid feeding into a hot reactor environment prevents the formation of clogs or jams at the reactor entrance. Previous research has shown that dissolving polyolefin plastic into a paraffin wax solvent at a 1:1 ratio (wt.) reduces the viscosity and improves the mixture's flow properties.[110] Creating a low viscosity molten feed is preferable to create uninterrupted flow into the reactor.[60] Another advantage is the ability to create a continuous feed with uniform properties. Mixed plastic waste has much variation in plastic composition from bale to bale.[26] Dissolving the plastic in a large well-mixed tank before pyrolysis minimizes the effect of composition variations between individual bales, assuming all plastic types can be dissolved. Using the

liquid feed also eliminates the need to use an inert gas, such as nitrogen, as the fluidizing medium.[4] Finally, the simple tubular reactor design creates advantages in scaling-up, with the secondary tubular micropyrolysis reactor presented in Chapter 2 having many similarities to the tubular pilot plant reactor presented in Chapter 3.

1.4 Sustainable process design for thermochemical conversion of polyolefins

Given the growth in research of waste plastic pyrolysis, it is important to understand the environmental, economic, and social impacts of commercializing this technology. While the capitalistic nature of the United States economy is quite effective at evaluating and improving the economic profitability of chemical processes, environmental and societal concerns are often relegated to secondary considerations.[13] The concept of sustainable development has been introduced to reduce the impact on the environment from chemical processes and products.[113] Sustainable development of a technology includes addressing the environmental, economic, and social concerns. It is important to incorporate sustainable development at the early stages of process design, where process modifications and optimizations are many times cheaper than making modifications to a facility in operation. At the heart of the method to assess sustainability for new technologies is process simulation.[5] Process simulations are often created using laboratory or pilot-scale data and use commercial software packages to model process operations at a commercial scale. Simulation outputs, including material and energy balances and product yields, serve as the inputs to economic, environmental and societal sustainability analyses.

Techno-economic analysis (TEA) and life cycle assessments (LCA) are two powerful tools to evaluate the economic and environmental impacts of a chemical recycling process.[114] TEA builds off of a process simulation by estimating the economic costs associated with the entire production pathway. With a scope from feedstock acquisition to bringing the product to market, TEA serves as an essential tool to understand which stages of production have the highest capital and operating costs. For developing technologies such as pyrolysis, this type of analysis highlights what the economic barriers to commercialization are and can guide the direction of future research. A TEA often uses a discounted cash flow analysis to generate economic indicators such as minimum selling price (MSP), net present value (NPV), payback period, and internal rate of return (IRR)[5] as well as socioeconomic indicators including number of jobs added.[115]

Similar to TEA, an LCA uses process simulation data to evaluate the environmental impacts of the process while also accounting for the upstream and downstream processes. Key outputs of LCA include environmental impacts corresponding to climate change, fossil energy consumption, air pollution, toxic emissions, and water usage.[5, 116] For chemical recycling, the environmental impacts are typically compared either to other waste management scenarios like landfilling or incineration[20, 117, 118] or to alternative technologies such as creating fossil fuels.[119, 120] A thorough review of the current literature for TEA/LCA analysis of waste plastics pyrolysis is provided in Chapter 4.

While both TEA and LCA are valuable individually, combining them allows for a more complete understanding of a technology's environmental and economic impacts.[10, 13, 115, 121-126] Often during the development stage of a technology, it is useful to incorporate scenario analysis within TEA and LCA. Scenario analysis ask the question of how changes on the process level (e.g., process intensification, energy integration, changes in product yield) affect the economic and environmental performance.[5] There may be economic and environmental trade-offs to a process change that require careful consideration by researchers and potential stakeholders.

Recently, researchers have begun to apply TEA and LCA results to a system level. It can be challenging to identify the best recycling option when the environmental and economic results depend on a wide-range of factors such as locally available technologies, capacities, specific waste compositions, and the state of the local electric grid.[124, 126, 127] A systems analysis framework can be created that considers the effect of scaling new technologies to regional, national, or global scales.[5] Systems analysis may also assess the effect of circular economy chemical recycling technologies to the plastic waste supply chain, which is outside the scope of traditional TEA and LCA studies. A recent systems analysis by Chaudhari, et al.[5] found that there is a need in the literature for high quality LCA and TEA studies for new chemical recycling technologies. In this research, we present the novel idea of combining liquid-phase pyrolysis with a post-MRF secondary sort of mixed plastic waste bales. Advanced sorting technologies can separate the valuable plastic out of these mixed bales, creating a lower cost mixed feedstock of HDPE and PP for pyrolysis. A preliminary TEA and LCA, complete with a full scenario analysis of key input variables, is presented in Chapter 4 to evaluate the economic and environmental impacts of this developing technology.

1.5 Research Objectives

According to the information presented above, this dissertation addresses the current gaps in knowledge on the fast pyrolysis of waste polyolefins through the following objectives and their corresponding research tasks.

1. To extend the utility of conventional micropyrolysis through the addition of a tubular vapor residence time reactor downstream of the pyroprobe.
    a) Perform micropyrolysis on HDPE, LDPE, and PP at reactor conditions of 550-600 °C and 1.4 to 5.6 second vapor residence time
    b) Develop a plastics pyrolysis kinetic model that predicts reactor products as a function of vapor residence time and temperature for the polymer resins HDPE, LDPE, and PP
    c) Determine the effect of temperature on reaction rates for pyrolysis kinetics.
2. To scale-up from the micropyrolysis apparatus to a pilot scale system capable of continuously pyrolyzing waste polyolefins
    a) Demonstrate that pyrolysis wax can be used as a dissolution solvent to prepare waste plastics for pyrolysis

b) Develop a multiphysics model combining kinetics, momentum, mass, and heat transport within the pyrolysis tubular reactor to predict vapor residence time within the pyrolysis reactor.
c) Investigate scale-up from micropyrolysis to pilot plant systems at comparable residence times.

3. To evaluate the economic and environmental feasibility of the analyzed liquid-fed pyrolysis process
    a) Use the yields from the pilot scale experiments to propose the conceptual design of a refinery that produces naphtha-like pyrolysis oil from the pyrolysis of waste HDPE/PP.
    b) Carry out a TEA and LCA to evaluate the economic and environmental burdens of the designed refinery and perform a robust scenario analysis on the key input variables.

This dissertation is divided in three parts: Chapter 2 addresses objective 1 and the corresponding research tasks, Chapter 3 accomplishes objective 2 and it's corresponding research tasks, and Chapter 4 presents the progress on objective 3. Finally, Chapter 5 presents the conclusions and future work derived from the results of the performed research.

1.6 References

1. MacArthur, D. E.; Waughray, D.; Stuchtey, M. R. In *The new plastics economy, rethinking the future of plastics*, World Economic Forum, Ellen MacArthur Foundation and McKinsey & Company London, UK: 2016.

2. Anene, A. F.; Fredriksen, S. B.; Sætre, K. A.; Tokheim, L.-A., Experimental study of thermal and catalytic pyrolysis of plastic waste components. *Sustainability* **2018,** *10* (11), 3979.

3. Ahmad, I.; Khan, M. I.; Khan, H.; Ishaq, M.; Tariq, R.; Gul, K.; Ahmad, W., Pyrolysis study of polypropylene and polyethylene into premium oil products. *International journal of green energy* **2015,** *12* (7), 663-671.

4. Sharuddin, S. D. A.; Abnisa, F.; Daud, W. M. A. W.; Aroua, M. K., A review on pyrolysis of plastic wastes. *Energy conversion and management* **2016,** *115*, 308-326.

5. Chaudhari, U. S.; Lin, Y.; Thompson, V. S.; Handler, R. M.; Pearce, J. M.; Caneba, G.; Muhuri, P.; Watkins, D.; Shonnard, D. R., Systems analysis approach to polyethylene terephthalate and olefin plastics supply chains in the circular economy: A review of data sets and models. *ACS Sustainable Chemistry & Engineering* **2021,** *9* (22), 7403-7421.

6. Lord, R.; Kao, G.; Joshi, S.; Gautham, P.; Bartlett, C.; Bullock, S.; Burks, B.; Baldock, C.; Aird, S. *Plastics and sustainability: a valuation of environmental benefits, costs and opportunities for continuous Improvement*; Trucost: 2016.

7. Geyer, R.; Jambeck, J. R.; Law, K. L., Production, use, and fate of all plastics ever made. *Science advances* **2017,** *3* (7), e1700782.

8. Di, J.; Reck, B. K.; Miatto, A.; Graedel, T. E., United States plastics: Large flows, short lifetimes, and negligible recycling. *Resources, Conservation and Recycling* **2021,** *167*, 105440.

9. Sherwin, G. The Circular Shift: Four Key Drivers of Circularity in North America. https://www.closedlooppartners.com/wp-content/uploads/2021/01/The-Circular-Shift_Closed-Loop-Partners-2020.pdf.

10. Bora, R. R.; Wang, R.; You, F., Waste polypropylene plastic recycling toward climate change mitigation and circular economy: energy, environmental, and technoeconomic perspectives. *ACS Sustainable Chemistry & Engineering* **2020,** *8* (43), 16350-16363.

11. Hong, M.; Chen, E. Y.-X., Chemically recyclable polymers: a circular economy approach to sustainability. *Green Chemistry* **2017,** *19* (16), 3692-3706.

12. Schwarz, A.; Ligthart, T.; Bizarro, D. G.; De Wild, P.; Vreugdenhil, B.; Van Harmelen, T., Plastic recycling in a circular economy; determining environmental performance through an LCA matrix model approach. *Waste Management* **2021,** *121*, 331-342.

13. Gracida-Alvarez, U. R.; Winjobi, O.; Sacramento-Rivero, J. C.; Shonnard, D. R., System analyses of high-value chemicals and fuels from a waste high-density polyethylene refinery. Part 1: Conceptual design and techno-economic assessment. *ACS Sustainable Chemistry & Engineering* **2019,** *7* (22), 18254-18266.

14. Ignatyev, I. A.; Thielemans, W.; Vander Beke, B., Recycling of polymers: a review. *ChemSusChem* **2014,** *7* (6), 1579-1593.

15. Singh, N.; Hui, D.; Singh, R.; Ahuja, I.; Feo, L.; Fraternali, F., Recycling of plastic solid waste: A state of art review and future applications. *Composites Part B: Engineering* **2017,** *115*, 409-422.

16. Malik, N.; Kumar, P.; Shrivastava, S.; Ghosh, S. B., An overview on PET waste recycling for application in packaging. *International Journal of Plastics Technology* **2017,** *21* (1), 1-24.

17. Schyns, Z. O.; Shaver, M. P., Mechanical recycling of packaging plastics: A review. *Macromolecular rapid communications* **2021,** *42* (3), 2000415.

18. Bhunia, K.; Sablani, S. S.; Tang, J.; Rasco, B., Migration of chemical compounds from packaging polymers during microwave, conventional heat treatment, and storage. *Comprehensive Reviews in Food Science and Food Safety* **2013,** *12* (5), 523-545.

19. Awoyera, P.; Adesina, A., Plastic wastes to construction products: Status, limitations and future perspective. *Case Studies in Construction Materials* **2020,** *12*, e00330.

20. Perugini, F.; Mastellone, M. L.; Arena, U., A life cycle assessment of mechanical and feedstock recycling options for management of plastic packaging wastes. *Environmental Progress* **2005,** *24* (2), 137-154.

21. Khoo, H. H., LCA of plastic waste recovery into recycled materials, energy and fuels in Singapore. *Resources, Conservation and Recycling* **2019,** *145*, 67-77.

22. Demetrious, A.; Crossin, E., Life cycle assessment of paper and plastic packaging waste in landfill, incineration, and gasification-pyrolysis. *Journal of Material Cycles and Waste Management* **2019,** *21* (4), 850-860.

23. Li, H.; Aguirre-Villegas, H. A.; Allen, R. D.; Bai, X.; Benson, C. H.; Beckham, G. T.; Bradshaw, S. L.; Brown, J. L.; Brown, R. C.; Castillo, M. A. S.,

Expanding Plastics Recycling Technologies: Chemical Aspects, Technology Status and Challenges. *ChemRxiv* **2022**.

24. Yadav, G.; Singh, A.; Nicholson, S. R.; Beckham, G. T. *Techno-Economic Analysis and Life Cycle Assessment for Pyrolysis of Mixed Waste Plastics*; National Renewable Energy Lab.(NREL), Golden, CO (United States): 2022.

25. Dimino, R.; Timpane, M. *Economic Impact of Beverage Container Deposits on Municipal Recycling Processing Costs*; National Waste & Recycling Association, 2022.

26. Kurzynowski, B.; Dimino, R.; Goodal, C. *#3-7 Bale Audit Results*; RRS: 2021.

27. Albertsson, A. C.; Karlsson, S., The three stages in degradation of polymers—polyethylene as a model substance. *Journal of Applied Polymer Science* **1988,** *35* (5), 1289-1302.

28. Jambeck, J. R.; Geyer, R.; Wilcox, C.; Siegler, T. R.; Perryman, M.; Andrady, A.; Narayan, R.; Law, K. L., Plastic waste inputs from land into the ocean. *Science* **2015,** *347* (6223), 768-771.

29. Eriksen, M.; Lebreton, L. C.; Carson, H. S.; Thiel, M.; Moore, C. J.; Borerro, J. C.; Galgani, F.; Ryan, P. G.; Reisser, J., Plastic pollution in the world's oceans: more than 5 trillion plastic pieces weighing over 250,000 tons afloat at sea. *PloS one* **2014,** *9* (12), e111913.

30. Mutz, D.; Hengevoss, D.; Hugi, C.; Gross, T. *Waste-to-energy options in municipal solid waste management a guide for decision makers in developing and emerging countries*; Deutsche Gesellschaft für Internationale Zusammenarbeit (GIZ) GmbH: 2017.

31. Mukherjee, A.; Debnath, B.; Ghosh, S. K., A review on technologies of removal of dioxins and furans from incinerator flue gas. *Procedia environmental sciences* **2016,** *35*, 528-540.

32. Rudolph, N.; Kiesel, R.; Aumnate, C., *Understanding plastics recycling: Economic, ecological, and technical aspects of plastic waste handling*. Carl Hanser Verlag GmbH Co KG: 2020.

33. Krüger, C.; Russ, M.; Gonzalez, M.; Horlacher, M. *Evaluation of pyrolysis with LCA–3 case studies*; BASF: 2020.

34. Fivga, A.; Dimitriou, I., Pyrolysis of plastic waste for production of heavy fuel substitute: A techno-economic assessment. *Energy* **2018,** *149*, 865-874.

35. Kots, P. A.; Liu, S.; Vance, B. C.; Wang, C.; Sheehan, J. D.; Vlachos, D. G., Polypropylene plastic waste conversion to lubricants over Ru/TiO2 catalysts. *ACS Catalysis* **2021,** *11* (13), 8104-8115.

36. Rorrer, J. E.; Beckham, G. T.; Román-Leshkov, Y., Conversion of polyolefin waste to liquid alkanes with ru-based catalysts under mild conditions. *JACS Au* **2020,** *1* (1), 8-12.

37. Rorrer, J. E.; Troyano-Valls, C.; Beckham, G. T.; Román-Leshkov, Y., Hydrogenolysis of Polypropylene and Mixed Polyolefin Plastic Waste over Ru/C to Produce Liquid Alkanes. *ACS Sustainable Chemistry & Engineering* **2021,** *9* (35), 11661-11666.

38. Nakaji, Y.; Tamura, M.; Miyaoka, S.; Kumagai, S.; Tanji, M.; Nakagawa, Y.; Yoshioka, T.; Tomishige, K., Low-temperature catalytic upgrading of waste polyolefinic plastics into liquid fuels and waxes. *Applied Catalysis B: Environmental* **2021,** *285*.

39. Jia, C.; Xie, S.; Zhang, W.; Intan, N. N.; Sampath, J.; Pfaendtner, J.; Lin, H., Deconstruction of high-density polyethylene into liquid hydrocarbon fuels and lubricants by hydrogenolysis over Ru catalyst. *Chem Catalysis* **2021,** *1* (2), 437-455.

40. Liu, S.; Kots, P. A.; Vance, B. C.; Danielson, A.; Vlachos, D. G., Plastic waste to fuels by hydrocracking at mild conditions. *Science Advances* **2021,** *7* (17).

41. Celik, G.; Kennedy, R. M.; Hackler, R. A.; Ferrandon, M.; Tennakoon, A.; Patnaik, S.; LaPointe, A. M.; Ammal, S. C.; Heyden, A.; Perras, F. A., Upcycling single-use polyethylene into high-quality liquid products. *ACS central science* **2019,** *5* (11), 1795-1803.

42. Jaydev, S. D.; Martín, A. J.; Pérez-Ramírez, J., Direct Conversion of Polypropylene into Liquid Hydrocarbons on Carbon-Supported Platinum Catalysts. *ChemSusChem* **2021,** *14* (23), 5179-5185.

43. Hou, Q.; Zhen, M.; Qian, H.; Nie, Y.; Bai, X.; Xia, T.; Rehman, M. L. U.; Li, Q.; Ju, M., Upcycling and catalytic degradation of plastic wastes. *Cell Reports Physical Science* **2021,** *2* (8), 100514.

44. Arena, U., Process and technological aspects of municipal solid waste gasification. A review. *Waste management* **2012,** *32* (4), 625-639.

45. Seo, Y.-C.; Alam, M. T.; Yang, W.-S., Gasification of municipal solid waste. In *Gasification for Low-Grade Feedstock*, Yun, Y., Ed. IntechOpen: 2018.

46. Billiet, S.; Trenor, S. R., 100th anniversary of macromolecular science viewpoint: needs for plastics packaging circularity. *ACS Macro Letters* **2020,** *9* (9), 1376-1390.

47. Triebert, D.; Hanel, H.; Bundt, M.; Wohnig, K., Solvent-Based Recycling. In *Circular Economy of Polymers: Topics in Recycling Technologies*, ACS Publications: 2021; pp 33-59.

48. Sánchez-Rivera, K. L.; Zhou, P.; Kim, M. S.; González Chávez, L. D.; Grey, S.; Nelson, K.; Wang, S. C.; Hermans, I.; Zavala, V. M.; Van Lehn, R. C., Reducing Antisolvent Use in the STRAP Process by Enabling a Temperature-Controlled Polymer Dissolution and Precipitation for the Recycling of Multilayer Plastic Films. *ChemSusChem* **2021,** *14* (19), 4317-4329.

49. Walker, T. W.; Frelka, N.; Shen, Z.; Chew, A. K.; Banick, J.; Grey, S.; Kim, M. S.; Dumesic, J. A.; Van Lehn, R. C.; Huber, G. W., Recycling of multilayer plastic packaging materials by solvent-targeted recovery and precipitation. *Science advances* **2020,** *6* (47), eaba7599.

50. Hwang, G.-C.; Choi, J.-H.; Bae, S.-Y.; Kumazawa, H., Degradation of polystyrene in supercritical n-hexane. *Korean Journal of Chemical Engineering* **2001,** *18* (6), 854-861.

51. Pei, X.; Yuan, X.; Zeng, G.; Huang, H.; Wang, J.; Li, H.; Zhu, H., Co-liquefaction of microalgae and synthetic polymer mixture in sub-and supercritical ethanol. *Fuel processing technology* **2012,** *93* (1), 35-44.

52. Baloch, H. A.; Nizamuddin, S.; Siddiqui, M.; Mubarak, N.; Mazari, S.; Griffin, G.; Srinivasan, M., Co-liquefaction of synthetic polyethylene and polyethylene bags with sugarcane bagasse under supercritical conditions: A comparative study. *Renewable Energy* **2020,** *162*, 2397-2407.

53. Baloch, H. A.; Siddiqui, M. T. H.; Nizamuddin, S.; Mubarak, N.; Khalid, M.; Srinivasan, M.; Griffin, G., Solvothermal co-liquefaction of sugarcane bagasse and polyethylene under sub-supercritical conditions: optimization of process parameters. *Process Safety and Environmental Protection* **2020,** *137*, 300-311.

54. Murty, M.; Rangarajan, P.; Grulke, E.; Bhattacharyya, D., Thermal degradation/hydrogenation of commodity plastics and characterization of their liquefaction products. *Fuel Processing Technology* **1996,** *49* (1-3), 75-90.

55. Seshasayee, M. S.; Savage, P. E., Oil from plastic via hydrothermal liquefaction: Production and characterization. *Applied Energy* **2020,** *278*.

56. Shabtai, J.; Xiao, X.; Zmierczak, W., Depolymerization− liquefaction of plastics and rubbers. 1. Polyethylene, polypropylene, and polybutadiene. *Energy & fuels* **1997,** *11* (1), 76-87.

57. Williams, P. T.; Slaney, E., Analysis of products from the pyrolysis and liquefaction of single plastics and waste plastic mixtures. *Resources, Conservation and Recycling* **2007,** *51* (4), 754-769.

58. Shah, N.; Rockwell, J.; Huffman, G. P., Conversion of waste plastic to oil: direct liquefaction versus pyrolysis and hydroprocessing. *Energy & fuels* **1999,** *13* (4), 832-838.

59. Gracida-Alvarez, U. R.; Mitchell, M. K.; Sacramento-Rivero, J. C.; Shonnard, D. R., Effect of temperature and vapor residence time on the micropyrolysis products of waste high density polyethylene. *Industrial & Engineering Chemistry Research* **2018,** *57* (6), 1912-1923.

60. Lechleitner, A. E.; Schubert, T.; Hofer, W.; Lehner, M., Lumped Kinetic Modeling of Polypropylene and Polyethylene Co-Pyrolysis in Tubular Reactors. *Processes* **2021,** *9* (1), 34.

61. Al-Salem, S.; Antelava, A.; Constantinou, A.; Manos, G.; Dutta, A., A review on thermal and catalytic pyrolysis of plastic solid waste (PSW). *Journal of environmental management* **2017,** *197*, 177-198.

62. del Remedio Hernández, M.; Gómez, A.; García, Á. N.; Agulló, J.; Marcilla, A., Effect of the temperature in the nature and extension of the primary and secondary reactions in the thermal and HZSM-5 catalytic pyrolysis of HDPE. *Applied Catalysis A: General* **2007,** *317* (2), 183-194.

63. Byrne, E.; Schaerer, L. G.; Kulas, D. G.; Ankathi, S. K.; Putman, L. I.; Codere, K. R.; Schum, S. K.; Shonnard, D. R.; Techtmann, S. M., Pyrolysis-Aided Microbial Biodegradation of High-Density Polyethylene Plastic by Environmental Inocula Enrichment Cultures. *ACS Sustainable Chemistry & Engineering* **2022**.

64. Kulas, D. G.; Zolghadr, A.; Shonnard, D., Micropyrolysis of Polyethylene and Polypropylene Prior to Bioconversion: The Effect of Reactor Temperature and Vapor Residence Time on Product Distribution. *ACS Sustainable Chemistry & Engineering* **2021,** *9* (43), 14443-14450.

65. Hubbard, B. R.; Putman, L. I.; Techtmann, S.; Pearce, J. M., Open Source Vacuum Oven Design for Low-Temperature Drying: Performance Evaluation for Recycled PET and Biomass. *Journal of Manufacturing and Materials Processing* **2021,** *5* (2), 52.

66. Tran, N. H.; Urase, T.; Ngo, H. H.; Hu, J.; Ong, S. L., Insight into metabolic and cometabolic activities of autotrophic and heterotrophic microorganisms in the biodegradation of emerging trace organic contaminants. *Bioresource technology* **2013,** *146*, 721-731.

67. Sivan, A.; Szanto, M.; Pavlov, V., Biofilm development of the polyethylene-degrading bacterium Rhodococcus ruber. *Applied microbiology and biotechnology* **2006,** *72* (2), 346-352.

68. Muhonja, C. N.; Makonde, H.; Magoma, G.; Imbuga, M., Biodegradability of polyethylene by bacteria and fungi from Dandora dumpsite Nairobi-Kenya. *PloS one* **2018,** *13* (7), e0198446.

69. Bin Jumah, A.; Malekshahian, M.; Tedstone, A. A.; Garforth, A. A., Kinetic Modeling of Hydrocracking of Low-Density Polyethylene in a Batch Reactor. *ACS Sustainable Chemistry & Engineering* **2021,** *9* (49), 16757-16769.

70. Harmon, R. E.; SriBala, G.; Broadbelt, L. J.; Burnham, A. K., Insight into Polyethylene and Polypropylene Pyrolysis: Global and Mechanistic Models. *Energy & Fuels* **2021,** *35* (8), 6765-6775.

71. Mastral, F.; Esperanza, E.; Berrueco, C.; Juste, M.; Ceamanos, J., Fluidized bed thermal degradation products of HDPE in an inert atmosphere and in air–nitrogen mixtures. *Journal of Analytical and Applied Pyrolysis* **2003,** *70* (1), 1-17.

72. Klein, M. T.; Neurock, M.; Broadbelt, L.; Foley, H. C., Reaction Pathway Analysis: Global Molecular and Mechanistic Perspectives. ACS Publications: 1993.

73. Kruse, T. M.; Wong, H.-W.; Broadbelt, L. J., Mechanistic modeling of polymer pyrolysis: polypropylene. *Macromolecules* **2003,** *36* (25), 9594-9607.

74. Zhao, D.; Wang, X.; Miller, J. B.; Huber, G. W., The Chemistry and Kinetics of Polyethylene Pyrolysis: A Feedstock to Produce Fuels and Chemicals. *ChemSusChem* **2019,** *13* (7), 1764-1774.

75. FakhrHoseini, S. M.; Dastanian, M., Predicting pyrolysis products of PE, PP, and PET using NRTL activity coefficient model. *Journal of Chemistry* **2013**, 1-5.

76. Eidesen, H.-K.; Khawaja, H.; Jackson, S., Simulation of the HDPE Pyrolysis Process. *Int. Jnl. of Multiphysics* **2018,** *12* (1), 79-88.

77. Kruse, T. M.; Levine, S. E.; Wong, H.-W.; Duoss, E.; Lebovitz, A. H.; Torkelson, J. M.; Broadbelt, L. J., Binary mixture pyrolysis of polypropylene and polystyrene: A modeling and experimental study. *Journal of analytical and applied pyrolysis* **2005,** *73* (2), 342-354.

78. De Witt, M. J.; Dooling, D. J.; Broadbelt, L. J., Computer generation of reaction mechanisms using quantitative rate information: Application to long-chain hydrocarbon pyrolysis. *Industrial & engineering chemistry research* **2000,** *39* (7), 2228-2237.

79. Levine, S. E.; Broadbelt, L. J., Detailed mechanistic modeling of high-density polyethylene pyrolysis: Low molecular weight product evolution. *Polymer Degradation and Stability* **2009,** *94* (5), 810-822.

80. Lopez, A.; De Marco, I.; Caballero, B.; Laresgoiti, M.; Adrados, A., Influence of time and temperature on pyrolysis of plastic wastes in a semi-batch reactor. *Chemical Engineering Journal* **2011,** *173* (1), 62-71.

81. Singh, J.; Kumar, M.; Saxena, A. K.; Kumar, S., Reaction pathways and product yields in mild thermal cracking of vacuum residues: A multi-lump kinetic model. *Chemical Engineering Journal* **2005,** *108* (3), 239-248.

82. Del Bianco, A.; Panariti, N.; Anelli, M.; Beltrame, P.; Carniti, P., Thermal cracking of petroleum residues: 1. Kinetic analysis of the reaction. *Fuel* **1993,** *72* (1), 75-80.

83. Fuentes-Ordóñez, E. G.; Salbidegoitia, J. A.; Gonzalez-Marcos, M. P.; Gonzalez-Velasco, J. R., Transport phenomena in catalytic hydrocracking of polystyrene in solution. *Industrial & Engineering Chemistry Research* **2013,** *52* (42), 14798-14807.

84. Nguyen, T. S.; Tayakout-Fayolle, M.; Ropars, M.; Geantet, C., Hydroconversion of an atmospheric residue with a dispersed catalyst in a batch reactor: Kinetic modeling including vapor–liquid equilibrium. *Chemical Engineering Science* **2013,** *94*, 214-223.

85. Miranda, M.; Cabrita, I.; Pinto, F.; Gulyurtlu, I., Mixtures of rubber tyre and plastic wastes pyrolysis: a kinetic study. *Energy* **2013,** *58*, 270-282.

86. Quitian, A.; Ancheyta, J., Experimental methods for developing kinetic models for hydrocracking reactions with slurry-phase catalyst using batch reactors. *Energy & Fuels* **2016,** *30* (6), 4419-4437.

87. Kaminsky, W., Chemical recycling of plastics by fluidized bed pyrolysis. *Fuel Communications* **2021,** *8*, 100023.

88. Williams, P. T.; Williams, E. A., Fluidised bed pyrolysis of low density polyethylene to produce petrochemical feedstock. *Journal of Analytical and Applied Pyrolysis* **1999,** *51* (1-2), 107-126.

89. Luo, G.; Suto, T.; Yasu, S.; Kato, K., Catalytic degradation of high density polyethylene and polypropylene into liquid fuel in a powder-particle fluidized bed. *Polymer Degradation and Stability* **2000,** *70* (1), 97-102.

90. Jung, S.-H.; Cho, M.-H.; Kang, B.-S.; Kim, J.-S., Pyrolysis of a fraction of waste polypropylene and polyethylene for the recovery of BTX aromatics using a fluidized bed reactor. *Fuel processing technology* **2010,** *91* (3), 277-284.

91. Bagri, R.; Williams, P. T., Catalytic pyrolysis of polyethylene. *Journal of analytical and applied pyrolysis* **2002,** *63* (1), 29-41.

92. Saad, J. M.; Nahil, M. A.; Williams, P. T., Influence of process conditions on syngas production from the thermal processing of waste high density polyethylene. *Journal of analytical and applied pyrolysis* **2015,** *113*, 35-40.

93. Renzini, M. S.; Lerici, L. C.; Sedran, U.; Pierella, L. B., Stability of ZSM-11 and BETA zeolites during the catalytic cracking of low-density polyethylene. *Journal of analytical and Applied Pyrolysis* **2011,** *92* (2), 450-455.

94. Onu, P.; Vasile, C.; Ciocılteu, S.; Iojoiu, E.; Darie, H., Thermal and catalytic decomposition of polyethylene and polypropylene. *Journal of Analytical and Applied Pyrolysis* **1999,** *49* (1-2), 145-153.

95. Vasile, C.; Pakdel, H.; Mihai, B.; Onu, P.; Darie, H.; Ciocâlteu, S., Thermal and catalytic decomposition of mixed plastics. *Journal of analytical and Applied Pyrolysis* **2001,** *57* (2), 287-303.

96. Elordi, G.; Olazar, M.; Castano, P.; Artetxe, M.; Bilbao, J., Polyethylene cracking on a spent FCC catalyst in a conical spouted bed. *Industrial & engineering chemistry research* **2012,** *51* (43), 14008-14017.

97. Artetxe, M.; Lopez, G.; Amutio, M.; Elordi, G.; Bilbao, J.; Olazar, M., Cracking of high density polyethylene pyrolysis waxes on HZSM-5 catalysts of different acidity. *Industrial & Engineering Chemistry Research* **2013,** *52* (31), 10637-10645.

98. Elordi, G.; Olazar, M.; Aguado, R.; Lopez, G.; Arabiourrutia, M.; Bilbao, J., Catalytic pyrolysis of high density polyethylene in a conical spouted bed reactor. *Journal of analytical and applied pyrolysis* **2007,** *79* (1-2), 450-455.

99. Arabiourrutia, M.; Elordi, G.; Lopez, G.; Borsella, E.; Bilbao, J.; Olazar, M., Characterization of the waxes obtained by the pyrolysis of polyolefin plastics in a conical spouted bed reactor. *Journal of Analytical and Applied Pyrolysis* **2012,** *94*, 230-237.

100. Kunii, D.; Levenspiel, O., *Fluidization engineering*. Butterworth-Heinemann: 1991.

101. Fogler, H. S., *Elements of Chemical Reaction Engineering*. 5th ed.; Prentice Hall PTR: Upper Saddle River, N.J., 2016.

102. Miandad, R.; Barakat, M.; Aburiazaiza, A. S.; Rehan, M.; Nizami, A., Catalytic pyrolysis of plastic waste: A review. *Process Safety and Environmental Protection* **2016,** *102*, 822-838.

103. Kim, S. C.; Kang, B. S.; Kim, B.-S.; Kim, Y.-M.; Joen, J.-K.; Park, Y.-K., Catalytic pyrolysis of municipal plastic film wastes over nanoporous Al-MCM-41. *Journal of Nanoscience and Nanotechnology* **2018,** *18* (2), 1078-1082.

104. Ateş, F.; Miskolczi, N.; Borsodi, N., Comparision of real waste (MSW and MPW) pyrolysis in batch reactor over different catalysts. Part I: Product yields, gas and pyrolysis oil properties. *Bioresource technology* **2013,** *133*, 443-454.

105. Donaj, P. J.; Kaminsky, W.; Buzeto, F.; Yang, W., Pyrolysis of polyolefins for increasing the yield of monomers' recovery. *Waste management* **2012,** *32* (5), 840-846.

106. Aguado, J.; Serrano, D.; San Miguel, G.; Castro, M.; Madrid, S., Feedstock recycling of polyethylene in a two-step thermo-catalytic reaction system. *Journal of Analytical and Applied Pyrolysis* **2007,** *79* (1-2), 415-423.

107. Lin, Y.-H.; Yen, H.-Y., Fluidised bed pyrolysis of polypropylene over cracking catalysts for producing hydrocarbons. *Polymer degradation and Stability* **2005,** *89* (1), 101-108.

108. Seo, Y.-H.; Lee, K.-H.; Shin, D.-H., Investigation of catalytic degradation of high-density polyethylene by hydrocarbon group type analysis. *Journal of Analytical and Applied Pyrolysis* **2003,** *70* (2), 383-398.

109. Syamsiro, M.; Saptoadi, H.; Norsujianto, T.; Noviasri, P.; Cheng, S.; Alimuddin, Z.; Yoshikawa, K., Fuel oil production from municipal plastic wastes in sequential pyrolysis and catalytic reforming reactors. *Energy Procedia* **2014,** *47*, 180-188.

110. Zolghadr, A.; Foroozandehfar, A.; Kulas, D. G.; Shonnard, D., Study of the Viscosity and Thermal Characteristics of Polyolefins/Solvent Mixtures: Applications for Plastic Pyrolysis. *ACS omega* **2021,** *6* (48), 32832-32840.

111. Marculescu, C.; Antonini, G.; Badea, A.; Apostol, T., Pilot installation for the thermo-chemical characterisation of solid wastes. *Waste management* **2007,** *27* (3), 367-374.

112. Fekhar, B.; Miskolczi, N., Stability and storage properties of hydrocarbons obtained by pilot scale pyrolysis of real waste HDPE-PVC in tubular reactor. *Chemical Engineering Transactions* **2018,** *70*, 1141-1146.

113. Allen, D. T.; Shonnard, D. R., *Green engineering: environmentally conscious design of chemical processes*. Pearson Education: 2001.

114. Nicholson, S. R.; Rorrer, J. E.; Singh, A.; Konev, M. O.; Rorrer, N. A.; Carpenter, A. C.; Jacobsen, A. J.; Román-Leshkov, Y.; Beckham, G. T., The critical role of process analysis in chemical recycling and upcycling of waste plastics. *Annual Review of Chemical and Biomolecular Engineering* **2022,** *13*, 301-324.

115. Singh, A.; Rorrer, N. A.; Nicholson, S. R.; Erickson, E.; DesVeaux, J. S.; Avelino, A. F.; Lamers, P.; Bhatt, A.; Zhang, Y.; Avery, G., Techno-economic, life-cycle, and socioeconomic impact analysis of enzymatic recycling of poly (ethylene terephthalate). *Joule* **2021,** *5* (9), 2479-2503.

116. Zhao, X.; You, F., Consequential life cycle assessment and optimization of high-density polyethylene plastic waste chemical recycling. *ACS Sustainable Chemistry & Engineering* **2021,** *9* (36), 12167-12184.

117. Al-Salem, S.; Evangelisti, S.; Lettieri, P., Life cycle assessment of alternative technologies for municipal solid waste and plastic solid waste management in the Greater London area. *Chemical Engineering Journal* **2014,** *244*, 391-402.

118. Alston, S. M.; Arnold, J. C., Environmental impact of pyrolysis of mixed WEEE plastics part 2: life cycle assessment. *Environmental science & technology* **2011,** *45* (21), 9386-9392.

119. Benavides, P. T.; Cronauer, D. C.; Adom, F.; Wang, Z.; Dunn, J. B., The influence of catalysts on biofuel life cycle analysis (LCA). *Sustainable Materials and Technologies* **2017,** *11*, 53-59.

120. Iribarren, D.; Dufour, J.; Serrano, D. P., Preliminary assessment of plastic waste valorization via sequential pyrolysis and catalytic reforming. *Journal of Material Cycles and Waste Management* **2012,** *14* (4), 301-307.

121. Kulas, D.; Winjobi, O.; Zhou, W.; Shonnard, D., Effects of Coproduct Uses on Environmental and Economic Sustainability of Hydrocarbon Biofuel from One-and Two-Step Pyrolysis of Poplar. *ACS Sustainable Chemistry & Engineering* **2018,** *6* (5), 5969-5980.

122. Winjobi, O.; Zhou, W.; Shonnard, D. R., Production of Hydrocarbon Fuel using Two-Step Torrefaction and Fast Pyrolysis of Pine. Part 1: Techno-economic Analysis *ACS Sustainable Chemistry & Engineering* **2017**.

123. Winjobi, O.; Zhou, W.; Kulas, D.; Nowicki, J.; Shonnard, D. R., Production of Hydrocarbon Fuel using Two-Step Torrefaction and Fast Pyrolysis of Pine. Part 2: Life-Cycle Carbon Footprint. *ACS Sustainable Chemistry & Engineering* **2017**.

124. Gracida-Alvarez, U. R.; Winjobi, O.; Sacramento-Rivero, J. C.; Shonnard, D. R., System Analyses of High-Value Chemicals and Fuels from a Waste High-Density Polyethylene Refinery. Part 2: Carbon Footprint Analysis and Regional Electricity Effects. *ACS Sustainable Chemistry & Engineering* **2019,** *7* (22), 18267-18278.

125. Kulas, D. G.; Thies, M. C.; Shonnard, D. R., Techno-Economic Analysis and Life Cycle Assessment of Waste Lignin Fractionation and Valorization Using the ALPHA Process. *ACS Sustainable Chemistry & Engineering* **2021,** *9* (15), 5388-5395.

126. Volk, R.; Stallkamp, C.; Steins, J. J.; Yogish, S. P.; Müller, R. C.; Stapf, D.; Schultmann, F., Techno-economic assessment and comparison of different plastic recycling pathways: A German case study. *Journal of industrial ecology* **2021,** *25* (5), 1318-1337.

127. Van Eygen, E.; Laner, D.; Fellner, J., Integrating high-resolution material flow data into the environmental assessment of waste management system scenarios: The case of plastic packaging in Austria. *Environmental science & technology* **2018,** *52* (19), 10934-10945.

2 Micropyrolysis of Polyethylene and Polypropylene Prior to Bioconversion: The Effect of Reactor Temperature and Vapor Residence Time on Product Distribution[1]

Abstract

The rapid thermal degradation of olefin plastics is a promising chemical recycling technology to create useful products from waste plastics. In this study, pyrolysis vapors from polyethylene (HDPE and LDPE) and polypropylene were subjected to secondary degradation using a new two-stage micropyrolysis reactor (TSMR) accessory to a commercial micropyrolysis unit. Variations in reactor temperature (550-600 °C) and vapor residence time (VRT) (1.4-5.6 seconds) showed a strong effect on the product distribution, which was comprised of mostly alkene hydrocarbons over a broad carbon number range, with minor production of alkanes and alkadienes. Based on the generated micropyrolysis data, a very practical lumped kinetic model comprised of 10 reactions and 6 lumped "species" was created to describe the plastic pyrolysis and to understand how temperature and VRT turn product distribution into different product classes of compounds (plastic, wax, heavy oil, light oil, gas, and aromatics). Kinetic parameters, such as activation energy and frequency factor, were solved for using the method of least squares. The presented kinetic model shows good agreement with the data and with known degradation mechanisms.

---

[1] Reprinted with permission from Kulas, D. G.; Zolghadr, A.; Shonnard, D., Micropyrolysis of Polyethylene and Polypropylene Prior to Bioconversion: The Effect of Reactor Temperature and Vapor Residence Time on Product Distribution. *ACS Sustainable Chemistry & Engineering* 2021, 9 (43), 14443-14450. Copyright 2021 American Chemical Society.

2.1 Introduction

With increasing volumes of excess plastic waste, there is a critical need for a timely means of upcycling structurally complex plastic debris to aid waste management initiatives and valorization of plastic waste. The rapid thermal degradation of waste plastics is a promising chemical recycling technology that both addresses the waste management issues of landfill disposal and ocean debris, produces useful products, and has the potential to close material loops in a circular economy of plastics. Primary thermal degradation of polymers usually yields a large quantity of high molecular weight compounds with limited applicability. This makes secondary degradation necessary to improve the quality of pyrolysis products. To address sustainability issues, recent studies have found that monomers, aromatics, gasoline and diesel produced from waste plastic pyrolysis have favorable economic[1] and environmental[2-4] results when compared to comparable products from fossil resources.

In addition to gasoline and diesel obtained from plastics pyrolysis, another product of particular interest is waste plastic-derived alkenes with carbon chain lengths from C5-C15. We have found that this product can be used as a feedstock for microbial biodegradation in enrichment cultures derived from environmental consortia.[5] Oil-degrading microorganisms colonize and break down the liquid alkenes, using the alkenes as carbon and energy source to produce microbial biomass or other value-added compounds. Biodegradation of plastic in the environment tends to be very slow and inefficient due to their length or structural complexity.[6-8] Even under ideal culture conditions, isolated microorganisms were only able to break down approximately 35% of polyethylene plastics over sixteen weeks.[9] By coupling a chemical pretreatment step, such as fast pyrolysis, with the biological process, the breakdown of waste plastic to bio-derived products can be considerably accelerated. Microbial communities from six different environmental inocula sources in enrichment cultures were found to achieve extensive biodegradation of polyethylene pyrolysis products over the course of five days, exhibiting signs of growth on pyrolysis products quantified in the form of carbon dioxide production and protein production.[5]

The plastics of primary interest in this research are polyethylene (PE) and polypropylene (PP). Theoretically, PP degrades faster than PE since half of the carbon in the PP chain is tertiary carbon, which consequently eases the formation of tertiary carbocation during the degradation.[10] Comparing PE types, LDPE should have slightly quicker degradation than HDPE as it has more branching, resulting in a weaker intermolecular force.[10] Reactor temperature controls the cracking reaction of the polymer chain. Increasing this temperature of the system causes the energy induced by Van der Waals force along the polymer chains to be greater than the enthalpy of the C-C bond in the chain, resulting in the carbon chain breaking.[11] High temperatures also cause intense vibrations of C-C bonds and increased collisions between different molecules, which leads to further bond breakage. Increasing residence time increases the conversion of high molecular weight primary pyrolysis products to low molecular weight liquid hydrocarbons and non-condensable hydrocarbon gases.[10, 12] High temperatures and long residence times have

been found to be the best conditions for maximizing hydrocarbon gas production and also for aromatics production in the pyrolysis process.[10, 13] Random chain scission has been proposed as the dominant thermal degradation mechanism, which leads to the formation of a large number of hydrocarbon species.[14, 15] The stabilization of the resultant radical after chain scission leads to the formation of carbon-carbon double bonds (C=C) in the structure as well as the production of alkanes.[15] Previous research on pyrolysis of PP and PE shows that waxes and heavy oil olefins are produced at low-temperatures with gases and light oils at high temperatures.[14, 16] In one study, fast pyrolysis of waste HDPE at temperatures of 625°C produced 30 wt % light oil and 60 wt % gases.[16]

Three methods of modeling to describe plastic fast pyrolysis have been proposed in the literature: mechanistic,[17, 18] probabilistic,[19] and complex phenomenological.[20, 21] Mechanistic models attempt to account for every reaction pathway and species present in pyrolysis. For example, a mechanistic model created by Kruse and Broadbelt[17] included over 24,000 reactions and tracked 213 species during polyethylene plastic pyrolysis. They found that the overall decomposition of a long hydrocarbon chain occurs via free-radical mechanisms that can generally be described by 3 steps: initiation, radical reaction, and termination.[17, 18] The radical reactions include hydrogen abstraction and β-scission, and the reactions are terminated via disproportionation and recombination.[18] Probabilistic models use random chain scission as the reaction pathway.[19] Since the random chain scission pathway assumes that linkages are randomly broken within the polymer, a probability distribution can be used to predict product distribution. The rate at which the linkages are broken is dependent on temperature while the extent to which the reaction occurs is dependent on residence time.[19] A weakness here is that by focusing on only one reaction pathway, any other reaction pathways are ignored. Phenomenological models use mechanisms based on observation instead of the underlying free radical chemistry. This type of model tracks different intermediate and end product lumped species instead of tracking every single molecule. Lumping is a common strategy in refinery calculations since it is challenging to measure and track every single molecule.[22, 23] The lumps are classified by a main parameter, such as molecular weight, density, or boiling point,[20] however carbon number is a common lumping parameter for this type of model.[20, 21] For example, when grouping based off carbon number range, C6-C10 alkenes, alkanes, and alkadienes are all treated as one lumped species.

The reason for using the phenomenological model in this work is that we are more interested in product distribution than the exact mechanisms that occurred when achieving said product distribution. The model's purpose is to identify the operating conditions of pyrolysis temperature and vapor residence time that produce the desired product distribution between gaseous, liquid, and wax hydrocarbons. This work builds off of the previous phenomenological models[21] by modeling the reaction kinetics as a function of both residence time and temperature, including aromatics as a distinct product group of interest. The phenomenological model developed here is valid for any vapor residence time and temperature combination within the typical fast pyrolysis range (550-600 °C, and 1-6 second vapor residence time). It should be used cautiously when operating outside these ranges. The carbon number was used as the lumping parameter and six "lumped" species

were created: waste plastic, gas (C1-C4), light oil (C5-C10), heavy oil (C11-C20), wax (C21+), and aromatics.

The objectives of this research are to perform micropyrolysis on HDPE, LDPE, and PP at reactor conditions of 550-600 °C and 1.4 to 5.6 s VRT and to create a kinetic model that predicts pyrolysis reaction product distribution as a function of vapor residence time and temperature for the polymer resins HDPE, LDPE, and PP. The primary product of interest is alkenes with carbon chain lengths from C5-C15 for use as a feedstock for microbial biodegradation. This research brings further understanding to the fundamental kinetics of plastic pyrolysis which will increase the sustainability of this technology.

2.2 Methods

2.2.1 HDPE, LDPE and PP Sample Preparation

The HDPE and LDPE samples were purchased from Carl's Industrial Salvage Store and the PP samples (density 0.901 g/cm^3) purchased from Poly Plastics (Michigan, USA). The plastics samples were finely sliced into pieces of approximately 0.5 mm width and 3 mm length and weighed in a microbalance (Mettler AJ100) with an accuracy of +/- 10 ug. Each sample was prepared to be within the weight range of 400-600 µg. The small weight of the sample was used to overcome heat transfer limitations of the CDS pyroprobe that a larger sample would face. The prepared samples were centered in a quartz tube (CDS Analytical), covered with glass wool from both sides, and inserted into the probe of a CDS 5200 HP pyroprobe (CDS Analytical) instrument.

2.2.2 Micropyrolysis Reactor

The two-stage micropyrolysis reactor (TSMR) used in this research previously appeared in Figure 1 of Gracida-Alveraz, et al.[13] A schematic of the TSMR system can be found in Figure A.1 of Appendix A. Similar to Gracida-Alvarez's research, the CDS probe was inserted into an accessory tubular reactor which was connected to the interface of the CDS pyroprobe to carry out both primary and secondary pyrolysis. Primary thermal degradation was achieved within in the CDS probe at a heating rate of 1000 °C/s until the target temperature (550-600 ℃). The target temperature was then sustained within the CDS probe for a period of 20 secs. The secondary degradation of the primary vapors was carried out within the tubular reactor that was 22.25 inches (0.57 m) long and ¼ in ID stainless steel tubing. A heating tape (model BWH051040L by BriskHeat), manually controlled with a rheostat (Powerstat), covered the outside of the tubular reactor from position 3.875 to 20.25 in from the point of insertion of the probe to provide the heat required to increase the temperature of the vapor inside the reactor up to the desired value. A second heated zone covered the remaining two inches of the reactor and its union of the pyroprobe interface to avoid condensation of the pyrolysis vapors. The temperature of this second heated zone was kept at 300 °C to avoid further degradation before being transported to the gas chromatograph/mass spectrometer (GC-MS) through a heated transfer line also operated at 300 °C. Insulation of the reactor was achieved with a braided fiberglass sleeve (DARCO southern). The reactor temperature was monitored with two type-K thermocouples (Omega) positioned at 10 and 16 inches from the reactor inlet edge and connected to a

temperature recorder (Omega). The vapor residence time (VRT) was controlled by modifying the carrier gas (ultra-high purity helium) flow rate coming through the reactor during pyrolysis (25-100 ml/min). All pyrolysis experiments were run in duplicate, ensuring in all cases complete degradation of the plastic sample through visual inspection of the quartz tube before and after pyrolysis. In addition, a gravimetric mass balance was performed pre and post pyrolysis, as described in Table A.1 in Appendix A.

2.2.3 Analytical Methods

The pyrolysis products were separated in a gas chromatograph (gc) (model K8880181 by ThermoFisher) with a Restek RXI-5MS fused silica column (low polarity phase, crossbond 5% diphenyl/95% dimethyl polysiloxane, 30m × 0.25 mm, 0.25 μm film thickness) which can observe up to compounds up to C30. Compounds were sent to a mass spectrometer (ms) (model DSQII by Thermo Scientific) which captured ion fragments in a range of 15-600 m/z. Further details of the analytical methods can be found in a prior publication by Gracida-Alveraz, et al.[13]

The pyrolysis products were identified from the ms results with the aid of the Xcalibur software from Thermo Fisher. Compound identification was performed by mass spectra comparison with the database available in the Xcalibur software. For each identified compound, the response factor relating the compound's mass to its gc peak area was determined by using controlled amounts of standards with known concentrations of the compound of interest as described in Russell, et al.[16] The standard mixtures were chosen to represent chemical species that are present in pyrolysis products. A power law correlation was then obtained for the relationship between response factor and carbon number for each compound class (alkene, alkadiene, alkane). Once calculated, each compound mass was divided by the total mass of all detected compounds and multiplied by 100% to determine product composition in mass percentage. These results were then grouped by C number to determine mass fraction of lumped compound classes.

2.2.4 Kinetic Modeling

As shown in Figure 2.1, the proposed pyrolysis reaction mechanism is comprised of the initial polymer plus five thermal-degradation products. The primary products of pyrolysis are wax (with a first-order reaction constant = k_1), heavy oil (k_2), light oil (k_3), and gas (k_4). Aromatic products have not been found in past research of primary pyrolysis of HDPE and thus was not included as a possible primary reaction pathway in the model.[24] Secondary reaction pathways include the conversion of the wax into heavy oil (k_5), light oil (k_9), and gas (k_6), as well as the conversion of heavy oil into light oil (k_8), and the light oil into gas (k_7). Finally, the gas is converted into aromatics (k_{10}) through a Diels-Alder reaction, followed by the dehydrogenation and unimolecular cyclation reactions, followed by dehydrogenation.[13] This model was chosen to describe the pyrolysis reactions, based upon the work by Eidesen, et al.[21] All of the reactions are assumed to be irreversible, with a reaction order of 1, to reduce the complexity of the system. The reaction equations (Eq. 2-7) are mass balances, assuming that the primary vapors from primary pyrolysis in the pyroprobe generate a vapor cloud that is conveyed by the inert He gas down the length of the tubular reactor, where secondary pyrolysis reactions occur. The vapor-residence time

was controlled by changing the inert He gas flowrate, which changes the speed of the vapor cloud though the reactor. The vapor cloud is assumed to behave similarly to a plug-flow reactor, with no input of species into the cloud, or flow of the species out of the vapor cloud. Therefore, the rate of accumulation of each species within the vapor cloud is equal to the rate of generation by reaction, as a result of all the different reactions.

The temperature dependencies of the ten reaction rate constants are described by the Arrhenius law (Eq. 1). Each lumped species in the proposed mechanisms is subject to multiple reactions, yielding first order ordinary differential equations (Eq. 2-7) which were solved simultaneously in MATLAB using numerical integration with a time step of 0.01 seconds.

$$k_i = A_i * e^{-\frac{E_{a,i}}{RT}} \tag{1}$$

where i represents one of the ten reactions in the reaction pathway. The activation energy (E_a) and Arrhenius constant (A) parameters are unknown for each of the ten specified reactions, leading to 20 unknown parameters that have to be obtained. The unknown kinetic parameters were solved for in MATLAB using the method of least squares which finds a local or global minima using reasonable starting points obtained from the literature.[20, 21] For each polymer species, the best fit of the kinetic model was made to the entire set of micropyrolysis data, including all temperatures and all VRT values.

$$\frac{dP}{dt} = -k_1 * P - k_2 * P - k_3 * P - k_4 * P \tag{2}$$

$$\frac{dW}{dt} = k_1 * P - k_5 * W - k_6 * W - k_9 * W \tag{3}$$

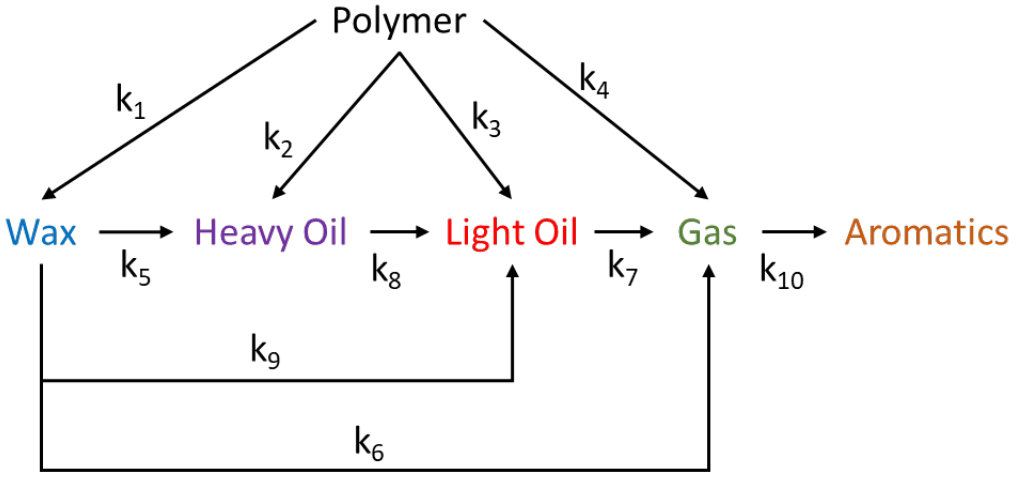

Figure 2.1 Reaction pathways in the kinetic model. Polymer is the plastic feedstock (LDPE, HDPE, or PP), wax is C21+, heavy oil is C11-C20, light oil is C5-C10, and gas is C1-C4.

$$\frac{dH_{Oil}}{dt} = k_2 * P + k_5 * W - k_8 * H_{Oil} \quad (4)$$

$$\frac{dL_{Oil}}{dt} = k_4 * P + k_9 * W + k_8 * H_{Oil} - k_7 * L_{Oil} \quad (5)$$

$$\frac{dGas}{dt} = k_3 * P + k_6 * W + k_7 * L_{Oil} - k_{10} * Gas \quad (6)$$

$$\frac{dA}{dt} = k_{10} * Gas \quad (7)$$

P is the mass fraction (expressed as percent) of plastic, dP/dt represents the rate at which the plastic is being consumed in primary pyrolysis, W is the wax product, H_{oil} is the heavy oil product, L_{oil} is the light oil product, Gas is C1-C4 hydrocarbon product, and A is the aromatics product. The effect of temperature on the reaction constant was accounted for using the Arrhenius equation (Eq. 1).

2.3 Results

The effect of pyrolysis temperature and VRT on the distribution of pyrolysis products for HDPE, LDPE, and PP are presented in Figure 2.2. Each lumped category was found to contain mostly alkenes, with alkanes and alkadienes also present in minor amounts on both a peak area and mass basis, as compared to alkenes (Figure A.4 in Appendix A). This matches observations by other investigators, who found that the pyrolysis of PE and PP produces mainly alkenes.[15] For the ranges in pyrolysis temperatures and VRT, the C5-C10 group has the highest mass percentage (30-50 wt %) for every polymer type. The C1-C4, C11-C15, and C16-C20 groups all have similar mass percentages (10-30 wt %) while C21+ and aromatics have the smallest mass percentage (0-10 wt %). The trends for how the mass percentage of each lumped category changes with temperature and VRT are relatively consistent for all three plastic types. Compounds lighter than C11 have an increase in mass percentage with an increase in temperature. Molecules heavier than C11 have a decrease in mass percentage with an increase in temperature. The same trend holds true for the effect of VRT. An exception to this trend occurs for the C1-C4 group, which sees a decrease in mass percentage with an increase in VRT. This decrease is most likely explained by the production of aromatics from the gaseous compounds through the Diels−Alder reaction mechanism.[13]

2.3.1 Mass Percentages

The results in Figure 2.2 provide information on temperature and VRT to manipulate product distribution to favor a preferred product. For example, if the preferred product is gas, increasing pyrolysis temperature will be more effective than increasing residence time. Going from 550 to 600 °C increased the gas yield from 20 to 30 wt %. Further increases of reactor temperature up to 675 °C have been found to increase gas yield up to 80 wt % at a VRT of 1.4 s for waste HDPE.[16] Similar to gas, aromatic production is also favored at high reaction temperatures (> 600 °C). In addition, long VRT's were found to increase

production of aromatics, specifically for polypropylene pyrolysis. A strategy for producing more light oil product is to lengthen the vapor residence time in the pyrolysis reactor. Increasing the reactor temperature was also found to help in this regard. Going from 575 °C to 600 °C only produced a minor increase in light oil production, suggesting that further increases in temperature would provide negligible or even detrimental changes as reactor temperatures above 600 °C tend to favor the gas product. A process aimed towards producing the heavier hydrocarbon fractions (> C16) would benefit from operating at short reaction times and low temperatures. Increasing the VRT from 1.4 to 5.6 s was found to have a significant detrimental effect on > C16 mass fractions.

Aromatics, specifically benzene, are a major concern for this work due to the intended microbial application for the pyrolysis oil. While microbial consortia can metabolize aromatics, any aromatics, especially benzene, that are not metabolized in the culture media may remain in the dried recovered biomass. This would limit the use of the biomass as a possible food source as benzene is carcinogenic to humans[25]. In our experiments, polypropylene was found to have higher aromatic production than HDPE and LDPE for nearly all combinations of temperature and VRT, especially at long residence times (5.6 s) and high temperatures (600 °C). This can be explained by polypropylene degrading faster than polyethylene and forming more gaseous products compared to HDPE and LDPE under the same pyrolysis conditions.[10] Aromatic production was relatively minor (<2 wt %) at short VRTs (1.4 and 2.8 s) and low temperatures (550 and 575 °C). The combination of high temperature (600 °C) and long residence time (5.6 s) produced the highest wt % of aromatics (Figure A.5 in Appendix A). This suggests that both high pyrolysis temperatures and longer residence times are required for aromatic production, which also agrees with the reaction mechanism. The formation of aromatics is a secondary reaction with non-condensable gases as the intermediate reactants. Pyrolysis temperatures above 600 °C are required to produce high quantities of non-condensable gases.[24] The long residence times are required to give the gases time to react to form aromatics. This conclusion is supported by the research of Russell, et al.[16] who found that micropyrolysis of waste HDPE at 675 °C and 5.6 s VRT produced 15 wt % aromatics.

Although concentrations of benzene were very small (0 – 1.2 wt %), its production appears to increase with increased pyrolysis temperature and VRT (Figure A.6 in Appendix A). Among the different plastic types, benzene production appears to be highest for PP and lowest for HDPE, although distinct trends are difficult to confirm at such low concentrations. Due to the branching structure, PP also produced benzene derivatives (i.e. methylbenzene) at 0 – 0.5 wt % in addition to benzene.

Mass percentages presented here are based on the pyrolysis vapors collected and detected using GC-MS. It is important to stress that these vapors do not represent a closed mass balance on the micro-pyrolysis experiments. Table A.1 in Appendix A presents a mass balance closure for these experiments and an indication on the molecular weight distribution of the primary pyrolysis products. We assume in this work that the pyrolysis vapors detected in GC-MS are representative of all pyrolysis vapors generated, had they all transited through the tubular reactor.

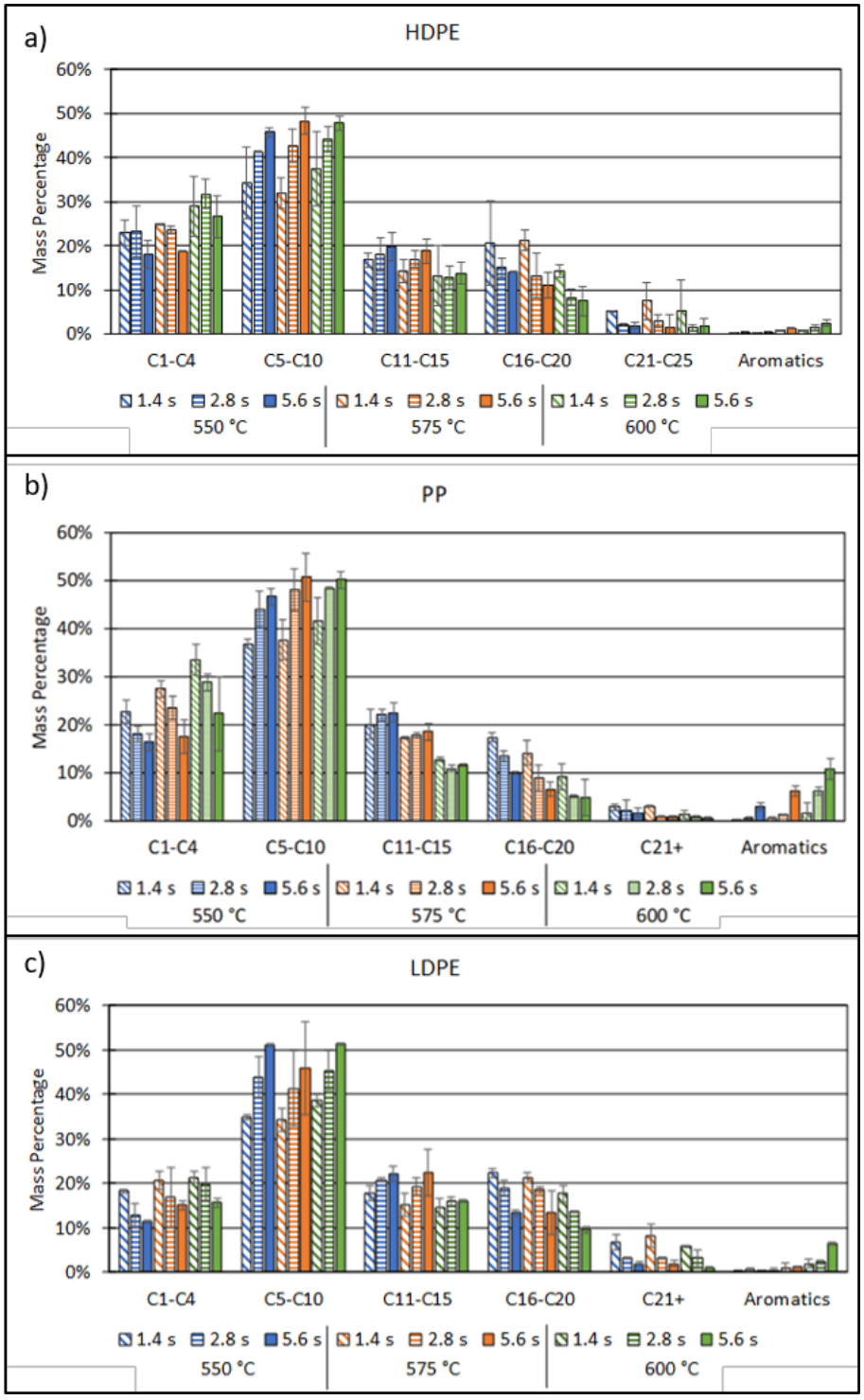

Figure 2.2 Experimental data showing the effect of vapor residence time (1-4 to 2.8 s) and reactor temperature (550-600 °C) on HDPE (a), PP (b) and LDPE (c) pyrolysis product distribution. Each lumped carbon range (i.e. C1-C4) contains alkenes, alkanes, and alkadienes.

2.3.2 Kinetic Model

The kinetic model equations 1-6 were fitted to the experimental micropyrolysis data at 550, 575, and 600 °C and with VRT from 1.4 – 5.6 s. The fitted reaction constants and their respective Arrhenius parameters are summarized in Table 2.1 and section A.5 of Appendix A. Reaction k_7 (light oil to gas) has the lowest frequency factor, and thus reaction constant, for all three plastic types. This is consistent with the findings of Eidesen, et al.[21] which found the reaction pathway of oil to gas to have a much lower reaction constant than the other reaction pathways that were analyzed. The presented data shows that the primary thermal degradation of both polyethylene and polypropylene (<1 sec. VRT) produce a large range of hydrocarbon species (from wax to gas) which is in line with what is expected from random scission. Secondary reactions (k_5-k_{10}) continue to break down the hydrocarbons at a much slower rate than the primary degradation. In order to confirm that primary thermal degradation is much faster than secondary degradation, the pyrolysis probe was examined to see how long it took to vaporize the sample. We found that it took less than 5 seconds for each of the three plastic samples to fully degrade (disappear by visual inspection, see Figure A.7 of Appendix A). Considering heat transfer limitations (i.e. it takes time to fully heat up the probe and the sample, even with the very high heating rate), it is clear that the primary degradation does occur very rapidly and generated primary vapors over about 5 seconds in the probe, which then transit through the hot tubular reactor in which secondary reactions occur. Focusing on the Arrhenius parameters (Table 2.1), k_7 and k_{10} have very low activation energies compared to the other reactions. This means that these reaction pathways have a very low temperature dependence. This is unexpected for k_{10}, as the literature shows that increasing temperature has a significant positive effect on aromatic production.[13, 16]

A recent study by Lechleitner, et al. solved the kinetic parameters for a similar lumped model.[20] They found that the activation energy, Ea, ranged from 80 to 700 kJ/mol for the different reactions while the frequency factor, A, ranges from 1e5 to 1e15. With the exception of k_7 and k_{10}, the values for Ea presented in Table 2.1 are within that range. A possible explanation for this is that k_7 reaction was found to be negligible for this system and k_{10} reaction (gas -> aromatics) was not modeled in Lechleitner's work. The presented values for A are on the lower side of the literature values. One possible reason for this is that the literature model was of slow pyrolysis instead of fast pyrolysis (T from 400-500 °C, residence time from 1-50 minutes) which may account for the differences in A.

Table 2.1 Arrhenius parameters of the kinetic model fit for each reaction constant 'k'

Reaction Constant	PP		HDPE		LDPE	
	A, 1/s	**Ea, kJ/mol**	**A, 1/s**	**Ea, kJ/mol**	**A, 1/s**	**Ea, kJ/mol**
k_1 (Polymer -> Wax)	1.3E+14	2.0E+02	2.6E+11	1.6E+02	1.1E+12	1.6E+02
k_2 (Polymer -> Heavy Oil)	2.4E+04	3.9E+01	1.9E+05	5.5E+01	4.8E+03	2.8E+01
k_3 (Polymer -> Light Oil)	9.9E+08	1.2E+02	8.7E+06	8.4E+01	2.3E+08	1.1E+02
k_4 (Polymer -> Gas)	1.3E+03	2.1E+01	1.1E+03	2.2E+01	6.9E+03	3.4E+01
k_5 (Wax -> Heavy Oil)	5.3E+00	7.2E+00	1.1E+02	2.8E+01	2.8E+03	4.6E+01
k_6 (Wax -> Gas)	2.3E+11	2.8E+02	4.2E-01	5.1E+01	4.2E+24	5.0E+02
k_7 (Light Oil -> Gas)	1.4E-02	9.2E-01	9.9E-02	4.3E+00	1.8E-01	3.2E+01
k_8 (Heavy Oil -> Light Oil)	1.1E+09	1.5E+02	6.3E+03	6.3E+01	3.3E+00	1.1E+01
k_9 (Wax -> Light Oil)	1.9E+10	1.5E+02	4.6E+04	6.3E+01	2.9E+01	1.1E+01
k_{10} (Gas -> Aromatics)	4.6E-01	4.1E-03	1.9E-01	8.1E-04	5.2E-01	1.4E-03

The best-fit of the kinetic model equations 1-6 to the experimental micropyrolysis data at 550, 575, and 600 °C and with VRT from 1.4 – 5.6 s are shown in Figures 3-5 for LDPE, HDPE, and PP, respectively. Error bars represent standard deviations for duplicate trials. For the LDPE dataset, the best fit of the kinetic model does a good job in predicting general trends of the gas, light oil, and wax species (Figure 2.3). The model, however, overpredicts production of aromatics at low temperatures. The heavy oil mass percentages at 575 °C do have large error bars, which may contribute to the less favorable fit. The mean absolute error (MAE) of the LDPE model is 0.0156 kg/kg.

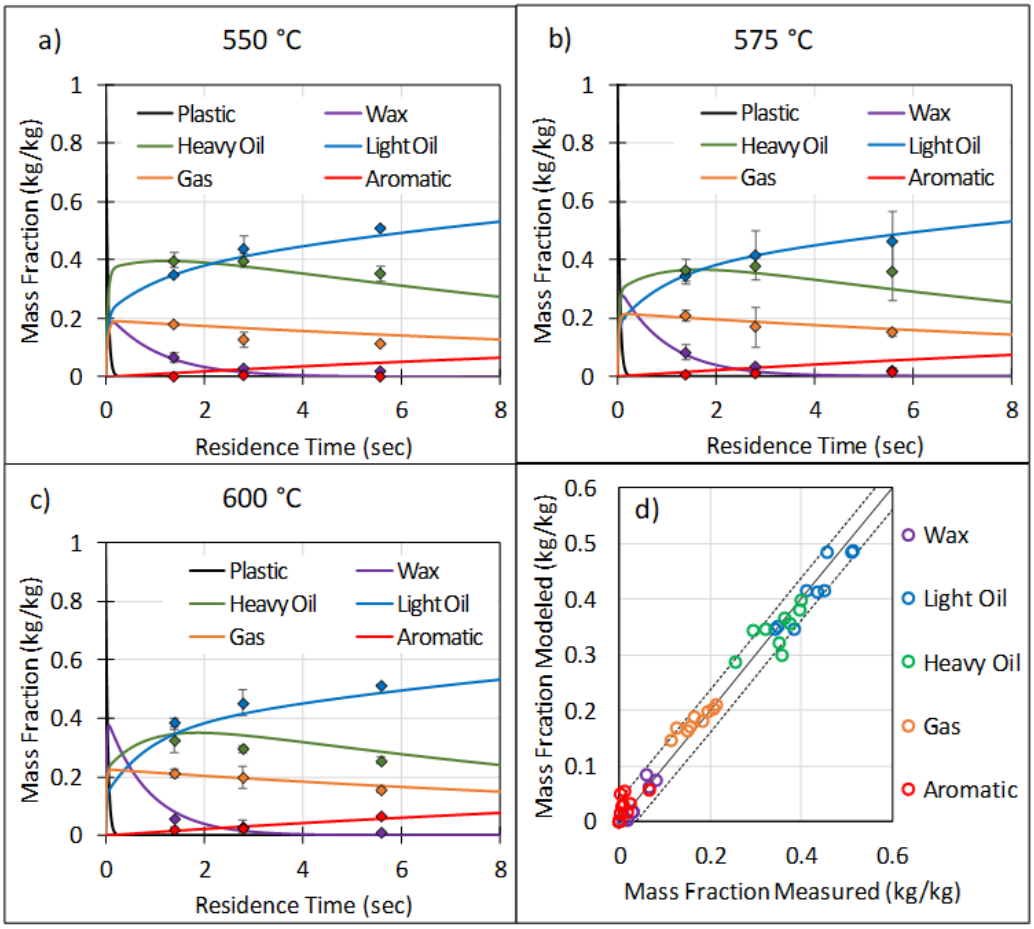

Figure 2.3 LDPE kinetic model results. For parts a, b, and c the line is the model results while the points are measured values. Part d shows the deviation of the modeled and measured values for pyrolysis of LDPE. The dashed lines show the 95% confidence interval (CI) (+/- 3.8 wt %).

Similar to the LDPE model, the HDPE model does a very good job predicting the light oil product along with the wax and aromatics (Figure 2.4). The model struggles to match the data more with the heavy oil and gas products, particularly at 600 °C. The mean absolute error (MAE) of the HDPE model is 0.0152 kg/kg.

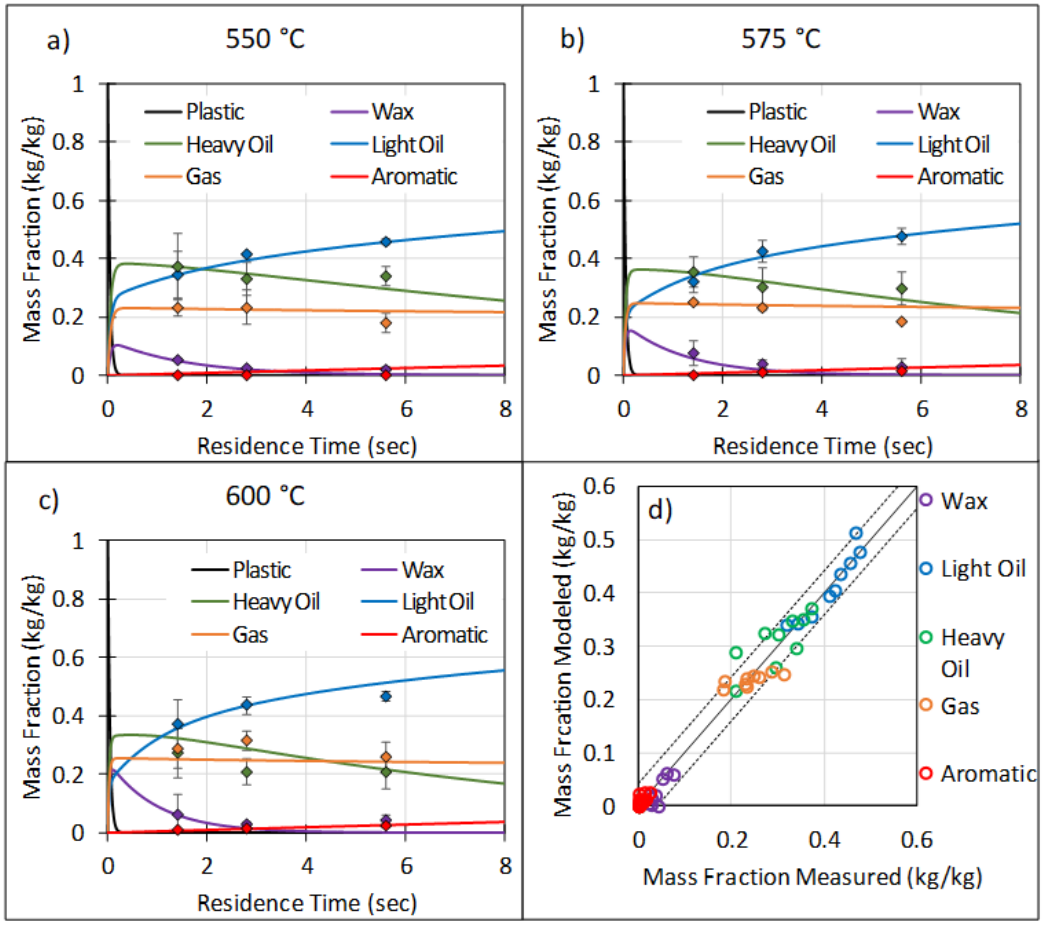

Figure 2.4 HDPE kinetic model results. For part a, b, and c the line is the model results while the points are measured values. Part d shows the deviation of the modeled and measured values for pyrolysis of HDPE. The dashed lines show the 95% CI (+/- 4.1 wt %).

The model fit and deviations between the measured and modeled results for the polypropylene experiments is presented in Figure 2.5. The model fits the 550 and 575 °C data better than the 600 °C experimental data, specifically for the light oil product which is overpredicted at 600 °C. The mean absolute error (MAE) of the PP model is 0.0147 kg/kg.

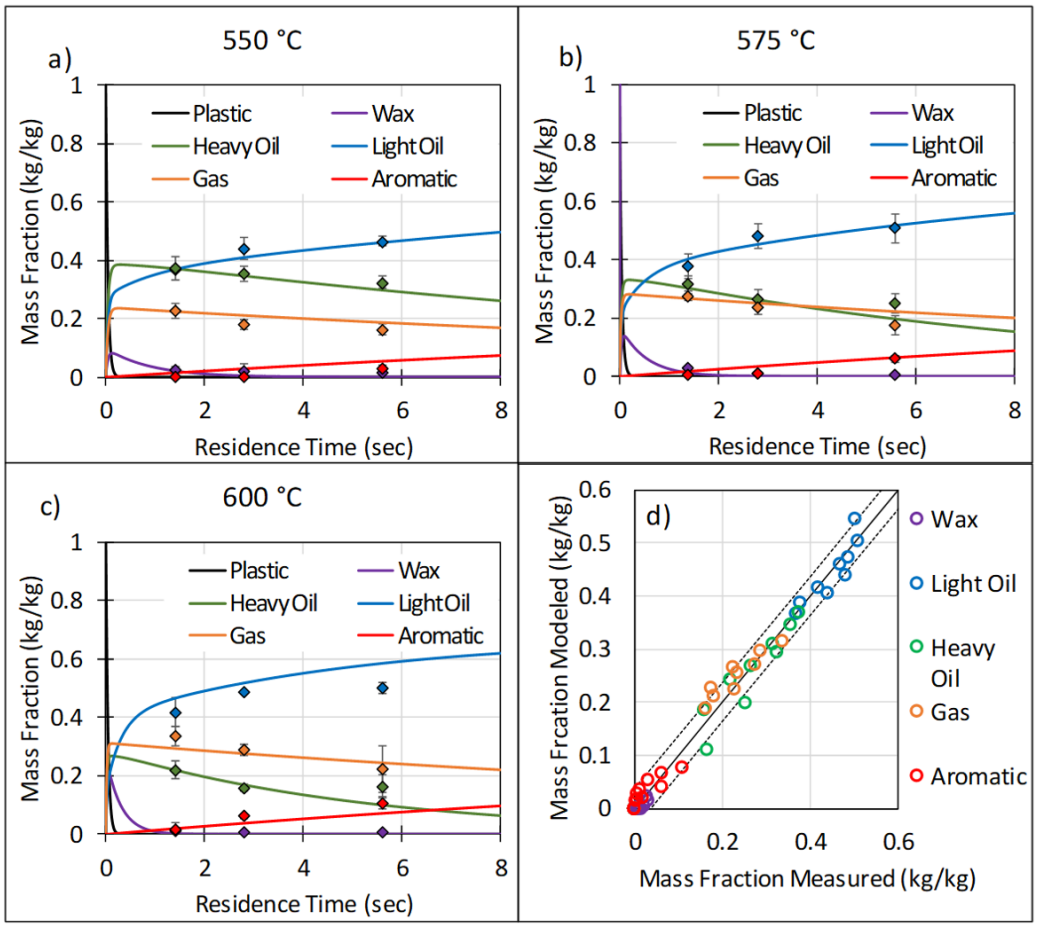

Figure 2.5 Polypropylene kinetic model results. For part a, b, and c the line is the model results while the points are measured values. Part d shows the deviation of the modeled and measured values for pyrolysis of polypropylene. The dashed lines show the 95% CI (+/- 3.7 wt %).

2.4 Conclusions

In this study, a new vapor residence time reactor accessory to a commercial micropyrolysis apparatus was employed. Micropyrolysis reactor temperature (550-600 °C) and vapor residence time (1.4 – 5.6 s) were found to affect the product distribution among compound classes. At a low temperature (550°C) and short VRT (1.4 s), a wide range of liquid (C5-C20 hydrocarbons) and wax products (C21-C30 hydrocarbons) were produced. Increasing temperature and VRT caused higher proportions of gas (C2-C4 hydrocarbons) and the generation of aromatics products. Polypropylene was found to break down faster than polyethylene (HDPE and LDPE), producing lower molecular weight compounds under identical reactor conditions. A very practical lumped kinetic model comprising of 10 reactions and 6 “lumped species” was created to describe the plastic pyrolysis and to understand how the temperature and VRT affect product distribution across different product classes of compounds (plastic, wax, heavy oil, light oil, gas, and aromatics). The

solved kinetic parameters, such as activation energy and frequency factor, match up well with the literature. The lumped species kinetic model appears to accurately represent trends in products with temperature and VRT and could be a good model to utilize for reactor design, in which in addition to the intrinsic reaction kinetics, heat and momentum transfer could be included.

2.5 Acknowledgments

Funding for this work was provided by the Defense Advanced Research Projects Agency ReSource program cooperative agreement HR00112020033. The views, opinions and/or findings expressed are those of the author and should not be interpreted as representing the official views or policies of the Department of Defense or the U.S. Government.

2.6 References

1. Gracida-Alvarez, U. R.; Winjobi, O.; Sacramento-Rivero, J. C.; Shonnard, D. R., System analyses of high-value chemicals and fuels from a waste high-density polyethylene refinery. Part 1: Conceptual design and techno-economic assessment. *ACS Sustainable Chemistry & Engineering* **2019,** *7* (22), 18254-18266. DOI: 10.1021/acssuschemeng.9b04763

2. Gracida-Alvarez, U. R.; Winjobi, O.; Sacramento-Rivero, J. C.; Shonnard, D. R., System Analyses of High-Value Chemicals and Fuels from a Waste High-Density Polyethylene Refinery. Part 2: Carbon Footprint Analysis and Regional Electricity Effects. *ACS Sustainable Chemistry & Engineering* **2019,** *7* (22), 18267-18278. DOI: 10.1021/acssuschemeng.9b04764

3. Iribarren, D.; Dufour, J.; Serrano, D. P., Preliminary assessment of plastic waste valorization via sequential pyrolysis and catalytic reforming. *Journal of Material Cycles and Waste Management* **2012,** *14* (4), 301-307. DOI: 10.1007/s10163-012-0069-6

4. Gracida-Alvarez, U. R.; Keenan, L. M.; Sacramento-Rivero, J. C.; Shonnard, D. R., Resource and greenhouse gas assessments of the thermochemical conversion of municipal solid waste in Mexico. *Acs Sustainable Chemistry & Engineering* **2016,** *4* (11), 5972-5978. DOI: 10.1021/acssuschemeng.6b01143

5. Byrne, E.; Schaerer, L. G.; Kulas, D. G.; Ankathi, S. K.; Putman, L. I.; Codere, K. R.; Schum, S. K.; Shonnard, D. R.; Techtmann, S. M., Pyrolysis-Aided Microbial Biodegradation of High-Density Polyethylene Plastic by Environmental Inocula Enrichment Cultures. *ACS Sustainable Chemistry & Engineering* **2022**. DOI: 10.1021/acssuschemeng.1c05318

6. Tran, N. H.; Urase, T.; Ngo, H. H.; Hu, J.; Ong, S. L., Insight into metabolic and cometabolic activities of autotrophic and heterotrophic microorganisms in the biodegradation of emerging trace organic contaminants. *Bioresource technology* **2013,** *146*, 721-731. DOI: 10.1016/j.biortech.2013.07.083

7. Albertsson, A. C.; Karlsson, S., The three stages in degradation of polymers—polyethylene as a model substance. *Journal of Applied Polymer Science* **1988,** *35* (5), 1289-1302. DOI: 10.1002/app.1988.070350515

8. Sivan, A.; Szanto, M.; Pavlov, V., Biofilm development of the polyethylene-degrading bacterium Rhodococcus ruber. *Applied microbiology and biotechnology* **2006,** *72* (2), 346-352. DOI: 10.1007/s00253-005-0259-4

9. Muhonja, C. N.; Makonde, H.; Magoma, G.; Imbuga, M., Biodegradability of polyethylene by bacteria and fungi from Dandora dumpsite Nairobi-Kenya. *PloS one* **2018,** *13* (7), e0198446. DOI: 10.1371/journal.pone.0198446

10. Sharuddin, S. D. A.; Abnisa, F.; Daud, W. M. A. W.; Aroua, M. K., A review on pyrolysis of plastic wastes. *Energy conversion and management* **2016,** *115*, 308-326. DOI: 10.1016/j.enconman.2016.02.037

11. Sobko, A. In *Generalized van der Waals-Berthelot equation of state*, Doklady Physics, Springer: 2008; pp 416-419.

12. Mastral, F.; Esperanza, E.; Berrueco, C.; Juste, M.; Ceamanos, J., Fluidized bed thermal degradation products of HDPE in an inert atmosphere and in air–nitrogen mixtures. *Journal of Analytical and Applied Pyrolysis* **2003,** *70* (1), 1-17. DOI: 10.1016/S0165-2370(02)00068-2

13. Gracida-Alvarez, U. R.; Mitchell, M. K.; Sacramento-Rivero, J. C.; Shonnard, D. R., Effect of temperature and vapor residence time on the micropyrolysis products of waste high density polyethylene. *Industrial & Engineering Chemistry Research* **2018,** *57* (6), 1912-1923. DOI: 10.1021/acs.iecr.7b04362

14. FakhrHoseini, S. M.; Dastanian, M., Predicting pyrolysis products of PE, PP, and PET using NRTL activity coefficient model. *Journal of Chemistry* **2013**, 1-5. DOI: 10.1155/2013/487676

15. Williams, P. T.; Slaney, E., Analysis of products from the pyrolysis and liquefaction of single plastics and waste plastic mixtures. *Resources, Conservation and Recycling* **2007,** *51* (4), 754-769. DOI: 10.1016/j.resconrec.2006.12.002

16. Russell, J. M.; Gracida-Alvarez, U. R.; Winjobi, O.; Shonnard, D. R., Update to "Effect of Temperature and Vapor Residence Time on the Micropyrolysis Products of Waste High Density Polyethylene". *Industrial & Engineering Chemistry Research* **2020,** *59* (22), 10716-10719. DOI: 10.1021/acs.iecr.0c01134

17. Kruse, T. M.; Wong, H.-W.; Broadbelt, L. J., Mechanistic modeling of polymer pyrolysis: polypropylene. *Macromolecules* **2003,** *36* (25), 9594-9607. DOI: 10.1021/ma030322y

18. Harmon, R. E.; SriBala, G.; Broadbelt, L. J.; Burnham, A. K., Insight into Polyethylene and Polypropylene Pyrolysis: Global and Mechanistic Models. *Energy & Fuels* **2021,** *35* (8), 6765-6775. DOI: 10.1021/acs.energyfuels.1c00342

19. Zhao, D.; Wang, X.; Miller, J. B.; Huber, G. W., The Chemistry and Kinetics of Polyethylene Pyrolysis: A Feedstock to Produce Fuels and Chemicals. *ChemSusChem* **2019,** *13* (7), 1764-1774. DOI: 10.1002/cssc.201903434

20. Lechleitner, A. E.; Schubert, T.; Hofer, W.; Lehner, M., Lumped Kinetic Modeling of Polypropylene and Polyethylene Co-Pyrolysis in Tubular Reactors. *Processes* **2021,** *9* (1), 34. DOI: 10.3390/pr9010034

21. Eidesen, H.-K.; Khawaja, H.; Jackson, S., Simulation of the HDPE Pyrolysis Process. *Int. Jnl. of Multiphysics* **2018,** *12* (1), 79-88. DOI: 10.21152/1750-9548.12.1.79

22. Singh, J.; Kumar, M.; Saxena, A. K.; Kumar, S., Reaction pathways and product yields in mild thermal cracking of vacuum residues: A multi-lump kinetic model. *Chemical Engineering Journal* **2005,** *108* (3), 239-248. DOI: 10.1016/j.cej.2005.02.018

23. Del Bianco, A.; Panariti, N.; Anelli, M.; Beltrame, P.; Carniti, P., Thermal cracking of petroleum residues: 1. Kinetic analysis of the reaction. *Fuel* **1993,** *72* (1), 75-80. DOI: 10.1016/0016-2361(93)90379-G

24. del Remedio Hernández, M.; Gómez, A.; García, Á. N.; Agulló, J.; Marcilla, A., Effect of the temperature in the nature and extension of the primary and secondary reactions in the thermal and HZSM-5 catalytic pyrolysis of HDPE. *Applied Catalysis A: General* **2007,** *317* (2), 183-194. DOI: 10.1016/j.apcata.2006.10.017

25. Huff, J., Benzene-induced cancers: abridged history and occupational health impact. *International journal of occupational and environmental health* **2007,** *13* (2), 213-221. DOI: 10.1179/oeh.2007.13.2.213

3 Liquid-Fed Waste Plastic Pyrolysis Pilot Plant: Effect of Reactor Volume on Product Yields[2]

Abstract

A unique waste plastic pyrolysis pilot plant was used for fast pyrolysis (1-5 seconds vapor residence time) of HDPE at 600 °C. A dissolution pre-treatment step dissolved the high-density polyethylene (HDPE) in recycled pyrolysis wax to create a liquid feed to the pyrolysis reactor, avoiding clogging and bridging of the plastic particles that is common in alternative feeding strategies. Three different reactor volumes were tested to determine the effect of residence time on product distribution. Pyrolysis products were cooled through a series of two condenser to separate the products into three groups: a heavy, waxy product (> C15), a lighter liquid product (C6-C15), and a gaseous product (C1-C6). GC-MS analysis was used to characterize the composition of each product. Multiphysics modeling was conducted to estimate the residence time in the reactor and compare the pilot plant results to previously published micropyrolysis research. It was found that residence time had a significant effect on product distribution, with an increase from 1 to 4.5 seconds of residence time causing a 9 wt. % drop in wax (C20-C30) production and a 11 wt. % increase in light oil (C5-C10) production. The trends for product distribution as a function of residence time were found to be consistent between both the pilot plant and micropyrolysis systems, demonstrating that the pilot plant system can be "tuned" to produce the desired pyrolysis product.

[2] Reprinted with permission from Kulas, D.; Zolghadr, A.; Shonnard, D., Liquid-Fed Waste Plastic Pyrolysis Pilot Plant: Effect of Reactor Volume on Product Yields. *Journal of Analytical and Applied Pyrolysis* 2022, 166, 105601. Copyright 2022 Elsevier.

3.1 Introduction

In 2018, the United States generated 5.715 million metric tons of HDPE waste, of which only 9% was collected for sorting and recycling.[1] The remaining HDPE waste was either landfilled (75%) or incinerated (16%).[1] This problem is exacerbated within the US military, especially in field expeditionary operations where burn pits are used to dispose of waste plastics. Wrappers, containers, and other packaging elements are generated throughout military operations at a rate of 0.3 kg per meal.[2] Precious resources are dedicated to both shipping the packaging to a base and then disposing of it after use. In addition, improper disposal methods such as burn pits inflict long-lasting damage on both the environment and the humans who breathe burn pit fumes.[3] Recently, the DARPA ReSource program directed research efforts toward creating valuable materials out of plastic waste, such as edible macronutrients, tactical fibers, adhesives, and petroleum, oils, and lubricants (POLs).

Pyrolysis is a commonly researched chemical deconstruction method which transforms waste plastic into useful products.[4-9] By heating HDPE in the absence of oxygen to temperatures ranging from 400-700 °C, the high-density polyethylene is broken down into straight chain olefins and paraffins. The products can range from C1-C30, depending on reaction conditions such as temperature, residence time, reactor type, and catalyst.[5]

A recent review article on plastic pyrolysis identified that most lab scale pyrolysis reactions were conducted either in batch, semi-batch, or continuous-flow reactors.[5] The continuous flow reactors primarily included fluidized bed[10], fixed-bed, and conical spouted bed reactors (CSBR). Fluidized bed reactors were found to be the best for catalytic plastic pyrolysis because the catalyst can be reused many times without discharging. One issue with fluidized bed reactors is handling the sticky solid feed, specifically with the possibility of bed defluidization when melted plastics stick on the fluidized bed itself.[4] The CSBR is designed to have better versatility for handing the solid feed and is particularly suitable for low temperature pyrolysis to obtain wax.[11] Issues with the CSBR include catalyst feeding and entrainment and product collection. In the work reported here we employ an innovative tubular pyrolysis reactor design using a liquid feed. A dissolution pretreatment step dissolves the plastic in a pyrolysis wax solvent at a 1:1 ratio. The liquid plastic/solvent mixture then flows into a tubular reactor using a mild pressure drop. Previous research with tubular reactors have used Archimedes screw for solid feeding.[12, 13] The advantage with the proposed system is that there is no solid feeding into a hot reactor environment, avoiding any clogs or jams forming at the reactor entrance. Using a liquid feed also allows preheating of the feed, with it being fed into the reactor at a temperature above 300 °C. The simple tubular reactor design avoids both the costs and complexities of having catalysts as well as fluidizing media. Finally, the liquid feed avoids using an inert fluidizing gas during the reaction.

Previous work has shown that petroleum residue can be used as a solvent for dissolution of certain plastics.[14] This requires a plastic pyrolysis plant to be coupled with a petroleum plant and is not as environmentally friendly since it requires a fossil fuel as a solvent. Using recycled pyrolysis wax allows the pyrolysis system to be fully self-sufficient. Catalysts are

not required as it is not necessary to achieve high liquid yields. The wax product is desired in addition to the liquid product for use as the solvent.

The designed pyrolysis process creates 3 main products: gas, liquid, and wax. The gas product is intended to be used for power generation while the liquid product is to be used as a bioconversion feedstock.[15] Previous research has demonstrated that the pyrolysis liquid product contains microbially biodegradable intermediate compounds. Several different environmental inocula were found to achieve extensive biodegradation of polyethylene pyrolysis products over the course of 5 days,[15] demonstrating that microorganisms capable of metabolizing pyrolysis products are widely distributed in the environment. The wax product is recycled as the dissolution solvent for the plastic feedstock. Previous research has shown that a paraffin wax solvent, when mixed with polyolefin plastic at a 1:1 ratio (wt.), reduces the viscosity and improves the mixture's flow properties.[16] A molten plastic feed with a low viscosity is preferable since it can be pumped consistently and uninterrupted into the reactor.[14]

The end goal of this project is to create a modular tunable pyrolysis system where product distribution can be easily manipulated. Our hypothesis is that vapor residence time in the reactor can be used to manipulate the product distribution. Previous research has found that increasing vapor residence time shifts the product distribution from high molecular weight primary pyrolysis products to low molecular weight liquid hydrocarbons and non-condensable hydrocarbon gases.[5, 17-22] For micropyrolysis of HDPE at 600 °C, a change in residence time from 1.4 to 5.6 seconds resulted in 10 wt. % lower C16+ products and 10 wt. % more C5-C10 products.[17] While in a commercial system the pyrolysis residence time would probably be controlled by changing the flowrate for fixed equipment volume, in this work the residence time was controlled by changing the diameter of the tubular reactor while using a constant feed rate. In this way the reactor volume, and thus the residence time, could be controlled while keeping all the other variables consistent across the entire experimental design. The pyrolysis reactor residence time is estimated using a multiphysics model that accounts for mass transfer, heat transfer, and reaction kinetics.

There are two primary objectives for this work: 1) to demonstrate that pyrolysis wax can be used as a dissolution solvent to prepare waste plastics for pyrolysis, and 2) to investigate scale-up from micropyrolysis to pilot plant systems at comparable residence times. Using the wax as a pretreatment solvent for HDPE is an innovative approach to introducing waste plastics to a hot pyrolysis reactor as a liquid without introducing an outside material, such as waste oil as reported in other studies. To the best of our knowledge, no one has previously reported utilizing the pyrolysis wax in this manner. For the second objective, three reactor diameters were chosen which corresponded closely to the three vapor residence times tested previously in the micropyrolysis system. We are not aware of any other research with experimental data at both the micro- and pilot-scale with controllable residence time and temperature. This deliberate approach in which we have performed the scale-up is both novel and very useful on an application basis.

3.2 Material and Methods

3.2.1 Pyrolysis Pilot Plant

The methods for operation of the plastic pyrolysis pilot plant were first described in Byrne, et al.[15] A 2.5 gallon (1 gallon = 3.78 L) agitated tank (Coating Atomization Technologies) was used to dissolve HDPE chips (~1 cm in size) obtained from Idaho National Laboratory (research collaborator) in a wax solvent at a 1:1 mass ratio. The wax solvent used in this work is recycled pyrolysis wax from Condenser 1 (Figure 3.1) which contains a carbon range from C9-C33 normal alkenes (Figure B.1 of Appendix B). The liquid HDPE/wax mixture was heated up to 240 °C where it has a measured viscosity of 26744 Cp (1 Cp = 0.001 Pa*s). The system is operated in semi-batch, where the dissolution tank is loaded before the experimental campaign and then the same feed mixture is used throughout the experiments to prevent variations in the feed. The pyrolysis reactor and condenser systems operate in steady-state continuous mode during each experiment.

Flow of feed HDPE/solvent solution into the plug-flow pyrolysis reactor was pressure-driven by the dissolution tank headspace N_2 pressure (15 psig (1 psi = 6894.76 Pa)) and controlled with a calibrated needle valve (McMaster-Carr) at approx. 250 g/hr. The needle valve was calibrated using pail and scale method to find the correct valve opening for the desired flow rate. Three different reactor sizes were employed: ¼ inch (1 inch = 2.54 cm) sch 40 pipe (0.364 inch ID, 0.540 inch OD), ½ inch sch 40 pipe (0.622 inch ID, 0.840 inch OD), and ¾ inch sch 40 pipe (0.824 inch ID, 1.050 inch OD). All three reactors were 20 inches long made of stainless steel and each new diameter was tested in duplicate for one hour with a target flow rate of 250 g/hr. The temperature set point within the pyrolysis reactor was maintained at 600 °C for all experiments.

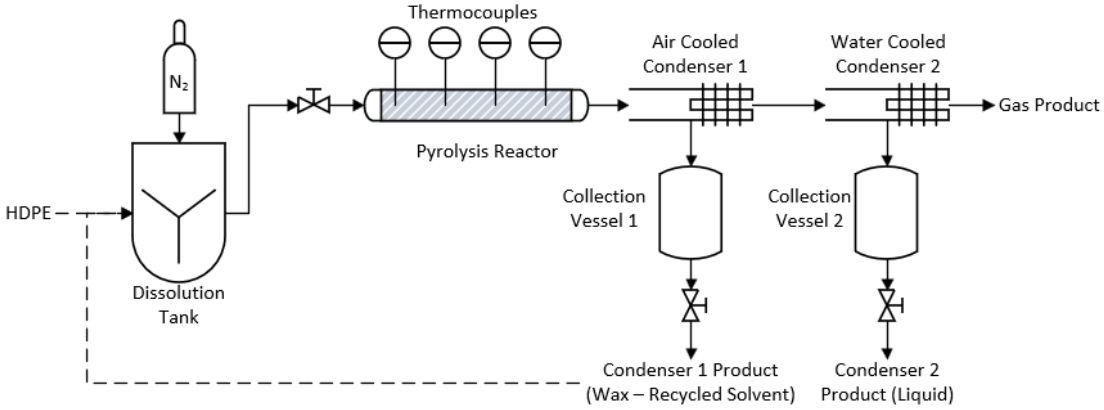

Figure 3.1 Process flow diagram of the waste plastics pyrolysis pilot plant. The dashed lines represent steps that occurred before the campaign of experiments began. The gas product is intended to be burned for power and the liquid product is to be sent to a bioconversion stage.

Four dual element thermocouple probes (Omega Engineering) were installed at 2, 7, 12, and 17 inches down the length of the pyrolysis reactor to monitor and control the reaction temperature. All thermocouples were installed so that the sensing tip was in the center of the reactor diameter. The dual element allows each thermocouple to send a signal both to an 1/8 DIN 7 Channel Universal Process Ramp & Soak Controller (OMEGA Engineering) and to a Programmable Portable Data Logger (OMEGA Engineering) which records the temperature every 30 seconds throughout the experiment. Unlike previously published work[15] with this system, no carrier gas is used in this research, although a N_2 purge gas was employed during process heat up prior to introducing the feed into the pyrolysis reactor. The pyrolysis products were cooled through a series of two condensers to separate the products into three groups: a heavy, waxy product (> C15), a lighter, liquid product (C5-C15), and a gaseous product (C1-C4). The conical condenser 1 contains an aerosol collector comprised of plug of grade #000 steel wool. The droplets collected by the steel wool drip down and collect in the bottom of the condenser where they are then drained at the end of the run. A cooling coil on the exterior surface of condenser 1 uses compressed air as the heat transfer media to control the condenser temperature to 150 °C. Condenser 2 was a double pipe heat exchanger with cooling water on the shell side of the exchanger, keeping the condenser at room temperature (~25 °C). The heat exchanger was tilted downwards so that the condensed droplets drain down into a collection vessel. The gas product flows out of the second condenser and was collected for analysis using a Tedlar bag (SKC Inc). A detailed schematic of the condenser design can be found in Figure B.4 of Appendix B.

3.2.2 Gas Chromatography–Mass Spectrometry (GC-MS)

The pyrolysis samples were collected and analyzed using a coupled Trace 1310 gas chromatograph/ITQ 1100 ion trap mass spectrometer (Thermo Fisher Scientific, Waltham, MA, USA) equipped with a TriPlus RSH autosampler (Thermo Fisher Scientific, Waltham, MA, USA). For each sample the mass spectrometer ion source temperature was heated to 275 ℃ and a full scan was conducted with an m/z ratio of 20-300 and a max ion time of 75 μS. Injection volumes of 1 μL per sample were used for the analysis of each liquid product and all samples were run in a series of duplicates. An autosampler was used for liquid injections and rinsed three times with 3 μL of pure solvent between each run. Calibration curves, shown in Figure B.5 of Appendix B, were developed for 1-decene, 1-tetradecene, 1-hexadecene, 1-octadecene, and 1-eicosene using the ratio of their peak area relative to the peak area of the internal standard (10 μL of 1000 μg/L 1,3,5-trichlorobenzene (SPEX Certiprep)). These ratios were used to generate the calibration curves to quantify the amount of each compound in the diluted samples.

The Condenser 1 hydrocarbon samples were diluted to 1% of their initial concentration in n-hexane. Ten microliters of 1000 μg/mL 1,3,5-trichlorobenzene (SPEX Certiprep) was added to each diluted sample as an internal standard to correct for injection error by the autosampler. The GC was heated at 35 ℃, held for 3 minutes, then heated at a rate of 20℃/min until reaching a temperature of 280 ℃ and held for 15 minutes using a TG-5MS column (Thermo Fisher Scientific, Waltham, MA, USA).

The Condenser 2 hydrocarbon samples were diluted to 1% of their initial concentration in dichloromethane (DCM). Ten microliters of 1000 µg/mL 1,3,5-trichlorobenzene (SPEX Certiprep) was added to each diluted sample as an internal standard to correct for injection error by the autosampler. The GC was heated at 35 ℃, held for 3 minutes, then heated from 35℃-280℃, ramping at 30℃/min until reaching a temperature of 280 ℃ and held for 7 minutes using a TG-5MS column (Thermo Fisher Scientific, Waltham, MA, USA).

The gas product samples were collected using a 5-liter Tedlar bag (SKC Inc) and then injected manually with a volume of 200 µL with a gas-tight syringe. The GC-MS was heated to 35 ℃ and held for 3.5 minutes. The contents of the gas sample were calibrated using a gas standard containing butene, hexane, pentene, ethylene, and propylene, all at a concentration of 1000 PPM in helium (Air Liquide America Specialty Gases LLC).

3.2.3 Reactor Modeling

The primary objectives of the reactor modeling are to estimate the vapor residence time within the reactor and predict reactor temperature versus length. In order to do so, a previously published lumped kinetic model[17] was coupled with mass and heat transfer phenomena using the following governing equations. The differential equations were solved in Polymath 6.10 and are all a function of reactor residence time (τ) to be consistent with the lumped kinetic model.[17] This model differs from a previously published reactor model which was a function of reactor length.[14] The reactor model assumes a plug flow system where the individual species mass balance are represented in equations 1-6 where x_P is mass fraction of the HDPE plastic in the system, r_{iP} represents the rates of reactions 1-4 for conversion of plastic to pyrolysis products, and subscript "i" represents each of the reactions 1-4. The four primary pyrolysis products are wax (W), heavy oil (Hoil), light oil (Loil), and gas (Gas) with aromatics (Ar) as a secondary product. Each of the reaction rates is expressed with a rate law assuming elementary first order reactions to convert plastic to products, so $r_{1P} = k_1 x_P$, $r_{2P} = k_2 x_P$, $r_{3P} = k_3 x_P$, and $r_{4P} = k_4 x_P$. Therefore, the reaction network equations are shown in equations 1-7 (see Figure B.6 of Appendix B).

$$\frac{dx_P}{d\tau} = \left[\sum_{i=1}^{N} r_{iP}\right] = -k_1 x_P - k_2 x_P - k_3 x_P - k_4 x_P \quad (1)$$

$$\frac{dx_W}{d\tau} = k_1 * x_P - k_5 * x_W - k_6 * x_W - k_9 * x_W \quad (2)$$

$$\frac{dx_{Hoil}}{d\tau} = k_2 * x_P + k_5 * x_W - k_8 * x_{Hoil} \quad (3)$$

$$\frac{dx_{Loil}}{d\tau} = k_3 * x_P + k_9 * x_W + k_8 * x_{Hoil} - k_7 * x_{Loil} \quad (4)$$

$$\frac{dx_{Gas}}{d\tau} = k_4 * x_P + k_6 * x_W + k_7 * x_{Loil} - k_{10} * x_{Gas} \quad (5)$$

$$\frac{dAr}{d\tau} = k_{10} * Gas \quad (6)$$

$$k_i = A_i * e^{-\frac{E_{a,i}}{R*T}} \quad (7)$$

A_i is the pre-exponential factor, $E_{a,i}$ is the activation energy, R is the universal gas constant, and T is absolute temperature. The kinetic parameters (A_i and $E_{a,i}$) for all ten reactions were presented in a previously published work.[17] The kinetic parameters for reactions 5, 6, and 9 (Figure B.6 of Appendix B) were updated slightly to improve the modeling of the secondary degradation of the wax to heavy oil, light oil, and gas (see Figure 7 in Section 3.4). A limitation of the micropyrolysis set-up used in fitting the original kinetic parameters is that it underestimates the production of heavier species due to condensation in the pyroprobe and GC-MS column. The underestimation caused poor fitting of the wax reaction pathways. The updated kinetic parameters can be found in Table B.3 of Appendix B. The initial conditions are 50% mass fraction of HDPE (x_P=0.5) and 50% mass fraction wax solvent (x_W=0.5) at the entrance of the reactor (τ=0). It is assumed that while the plastic feed mass flow ($\dot{m}$) enters in the liquid phase (eq. 9), all the primary and secondary pyrolysis products (wax, oil, and gas) are in the vapor phase and can be modeled using the ideal gas law (eqn. 11). The phase change from liquid to vapor is assumed to occur during the primary reaction (eq. 1). It is assumed that the HDPE/wax liquid feed density (ρ_P) does not change as a function of temperature within the system. Integrating the total volumetric flow rate (Q_{total}) over residence time (eqn. 12) solves for the local volume (V) which can then be correlated to the local length down the reactor (l) (eq. 13).

$$Q_{total} = Q_{liquid} + Q_{gas} \quad (8)$$

$$Q_{liquid} = \frac{x_P * \dot{m}}{\rho_P} \quad (9)$$

$$Q_{gas} = \frac{\dot{n}_{gas} * R * T}{P} \quad (10)$$

$$\dot{n}_{gas} = \sum_i y_i = \sum_i x_i * \frac{\dot{m}}{MW_i} \quad (11)$$

$$\frac{dV}{d\tau} = Q_{total} \quad (12)$$

$$l = \frac{V}{d} \quad (13)$$

An energy balance is used to predict the temperature change as a function of residence time for a fluid element as it travels down the reactor[14]. The residence time is correlated to the local volume (and thus local length down the reactor) using equation 12. The basic energy balance for PFRs is shown in equation 14.[23] Energy enters the fluid element via the temperature difference between the local fluid and reactor wall temperature. The entering energy goes towards driving the endothermic reaction and raising the local temperature until it eventually reaches the wall temperature. Equation 15 is used to transform T(V) to T(τ).

$$Q * \rho * C_p * \frac{dT}{dV} = \dot{q} + \sum_i \Delta H_{Ri} * r_i \quad (14)$$

$$\frac{dT}{d\tau} = \frac{dT}{dV} * \frac{dV}{d\tau} = \frac{dT}{dV} * Q \quad (15)$$

Q is the total volumetric flow rate, ρ is density, C_p is heat capacity, $\dot{q}$ is heat transfer rate per volume, ΔH_{Ri} is enthalpy change per i^{th} reaction (Table B.2 of Appendix B),[24] and r_i is reaction rate for i^{th} reaction. The heat transfer rate per volume is a function of the thermal heat transfer coefficient (h), the temperature difference, and diameter (d) (eq. 16).

$$\dot{q} = \frac{4*h*(T_w - T)}{d} \quad (16)$$

Equation 14 is rearranged (eq. 17) and then substituted into equation 15 (eq. 18).

$$\frac{dT}{dV} = (\dot{q} + \sum_i \Delta H_{Ri} * r_i)/(Q * \rho * C_p) \quad (17)$$

$$\frac{dT}{d\tau} = \frac{Q}{Q*\rho*C_p} * (\dot{q} + \sum_i \Delta H_{Ri} * r_i) \quad (18)$$

The volumetric flow rates cancel out and equation 16 is substituted in giving the final energy balance equation used in the reactor modeling:

$$\frac{dT}{d\tau} = \frac{1}{\rho*C_p} * (\frac{4*h*(T_w - T)}{d} + \sum_i \Delta H_{Ri} * r_i) \quad (19)$$

The wall temperature (T_w) is assumed to be at 600 ℃. A simplifying assumption is that the pyrolysis reactions do not begin until the local temperature reaches 550 °C. While the literature clearly shows that HDPE can pyrolyze at temperatures below 550 °C,[25-29] the lumped kinetic model used here has only been validated within the temperature range of 550-600 °C. Since the reaction rates below 550 °C are fairly slow (30 to 45 minutes for complete primary pyrolysis of HDPE in a mixture with LDPE and polypropylene at 500 and 525 ℃)[29] in comparison to the time the model predicts it takes the plastic to heat up (1-4 seconds), it was determined that this assumption shouldn't have a significant effect on the model results.

3.3 Results and Discussion

3.3.1 Temperature Profile

Figure 3.2 shows the time-average temperature during the pyrolysis experiment at each monitoring point of the three reactors. For all reactors, the target setpoint of 600 °C was reached by the third monitoring point at 12 inches. The ¾ inch diameter reactor reached the target setpoint by the second monitoring point at 7 inches down the reactor, much earlier than the ½ and ¼ inch diameter reactors. Since the volumetric flow rate is relatively constant for all trials, this can be explained by the larger diameter reactor having a slower fluid velocity. It is difficult to tell if this trend holds for the ½ inch diameter reactor as its thermocouple at the 2-inch monitoring location malfunctioned.

The reactor model (shown on Figure 3.2) was fitted to the experimental data using the heat transfer coefficients (h). The resulting fit was 85 W/m^2*K for the liquid phase and 1000 W/m^2*K for the gas phase which is in line with correlation values for liquids and gases.[30] Overall, the modeled temperature profile fits the experimental data fairly well, especially for the ¼ inch and ¾ inch reactor diameters. All of the model curves have a flat section where the temperature is constant at 550 ℃ over 1-2 inches. This is where the primary pyrolysis reactions that transition the liquid feed to vapor products are calculated to occur. In this section, all the energy that is transferred into the fluid from the temperature differential goes towards driving the endothermic primary pyrolysis reaction instead of increasing the fluid temperature. Once the primary reactions are complete the vapor temperature rises again until it reaches 600 ℃. While endothermic secondary pyrolysis reactions are occurring in the vapor phase, they have considerably slower reaction rates (10-100 times slower)[17] than the primary pyrolysis. This means more energy is transferred by the temperature differential than is required to drive the secondary reactions, which in turn causes the fluid temperature to rise. The predicted product yields from the reactor model (Figure B.7 of Appendix B) match the pilot plant product yields (Figure 6) well.

Limitations of the model fit include the assumption that the reactor wall temperature is 600 °C everywhere from the heating tape which has not been experimentally verified. In the entrance region the reactor wall temperature may be lower than 600 °C due to the heat sink created by the input liquid and colder feed. Farther down the reactor the wall temperature may be higher than 600 °C because the heat transfer coefficient for the vapor phase is relatively low compared to the boiling coefficient used for liquid and since the maximum temperature of these heating tapes is 760 °C. The model also ignores heat losses through insulation which are present in experiments, especially on the ends of the reactor. These and other modeling issues are currently under study.

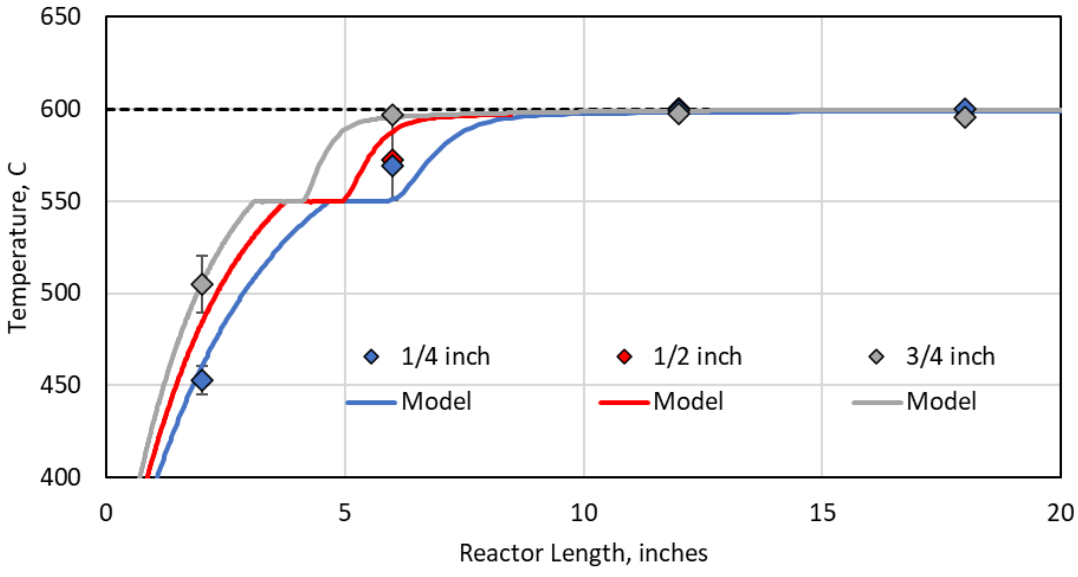

Figure 3.2 Measured pilot plant temperature profile along the reactor length compared to predicted temperature profile from reactor model.

In Figure 3.3, the measured temperature traces at four reactor locations over the hour experiment using the ¾ inch reactor are presented, demonstrating that the system is at steady state for most of the reaction time. Temperature traces for the ¼ inch and ½ inch reactors can be found in Figure B.8 and Figure B.9 of Appendix B. The entrance to the reactor (2 inch) shows lower temperature compared to other measurement locations and has slight variations over time due to small variations with the feed flow. The other three measuring points (7, 12, and 17 inches) are all steady at the setpoint of 600 °C throughout nearly the entire experiment. The dip in temperature at the start of the reaction (specifically at 2 and 7 inches) is due to the sudden introduction of liquid plastic feed to the reactor. After about 10 minutes the temperatures recover back to steady state and are relatively stable for the rest of the experiment.

3.3.2 Product Distribution

Table 3.1 shows the operating parameters, model-predicted vapor residence time, and product distribution from each experiment. Each reactor was run in duplicate with a target flow rate of approximately 250 g/h. The modeled vapor residence time was calculated using the reactor model with the inputs of reactor diameter, flow rate, and reactor temperature (600 °C). It is interesting that although the reactor volume increases by a factor of 9 from ¼ to ¾ inches in diameter, the modeled vapor residence time only changes by a factor of 4 (1.03 s to 4.58 s) for the same flowrate. This is most likely due to the increasing volumetric flow rate down the length of the reactor due to more complete pyrolysis reactions. From the ideal gas law, a decrease in the average MW of the product leads to an increase in the total number of moles present, and thus to an increase in volume (Eqn. 11).

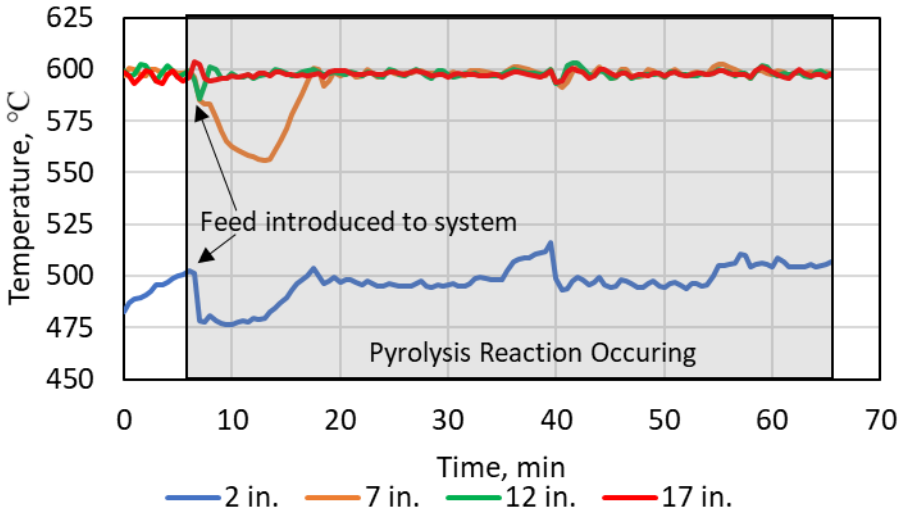

Figure 3.3 Typical reactor temperature profile throughout the length of the reactor for an hour experiment (shaded in gray). The presented data is for pilot plant run #3A using the ¾ inch reactor.

Table 3.1 Detailed information about each pilot plant run. All runs were conducted at 600 °C. Measured yields reflect pyrolysis kinetics as well as separation efficiency in the condensers.

Pilot Plant Run #	Reactor Diameter	Flow g/hr	Modeled VRT, s	Product Yields by Weight %		
				Condenser 1	Condenser 2	Gas
1A	¼ inch	220	0.91	51.9%	21.2%	26.9%
1B	¼ inch	200	1.00	32.8%	27.5%	39.6%
2A	½ inch	350	1.63	28.9%	28.4%	42.7%
2B	½ inch	210	2.64	25.3%	23.6%	51.1%
3A	¾ inch	270	3.50	27.4%	32.2%	40.4%
3B	¾ inch	220	4.21	23.9%	18.4%	57.7%

Increasing reactor size and thus residence time has a significant effect on product distribution (Figure 3.4). The heavier condenser 1 pyrolysis wax product drops in yield as residence time increases, going from an average of 42 wt. % at the ¼" diameter to 25 wt. % at the ¾ inch diameter. The gas product has the opposite trend, with yield rising from 32 wt. % at the ¼ inch diameter to 49 wt. % at the ¾ inch diameter. The middle product from condenser 2 is approximately 25 wt. % for all three reactor sizes with no clear upward or downward trend. These mass yields were measured directly based on gravimetric measurements of feed tank weight loss, mass of each condenser products, and gas by difference. There was no visible char or solid residue remaining in the reactor or condensers in these experiments. The trends shown in Figure 4 match a previous study of HDPE pyrolysis using a fluidized bed reactor, which found a decrease on wax yield and an increase in the gas yield at 650 °C when increasing the VRT from 0.8 to 1.5 s.[20] Another study using a fluidized bed reactor (FBR) to pyrolyze HDPE at 1.5 seconds residence time and 600 ℃, very similar reaction conditions to the ½ inch reactor.[31] At these conditions the FBR produced product distributions of 15.2% gas, 40.9% liquid, and 43.9% wax. The presented system in this work produced similar amount of wax (42 wt. %), less liquid (25 wt. %), and more gas (33 wt. %) than the FBR. Previous research with a solid-fed tubular reactor, operated with a HPDE feedstock and no catalyst, had yields of 55% heavy oil, 35% light oil, and 10% gases at 550-560 ℃.[13] It's clear that the increase in pyrolysis temperature from 550 to 600 ℃ causes a significant increase in gas production, a trend commonly reported in the literature.[5, 17]

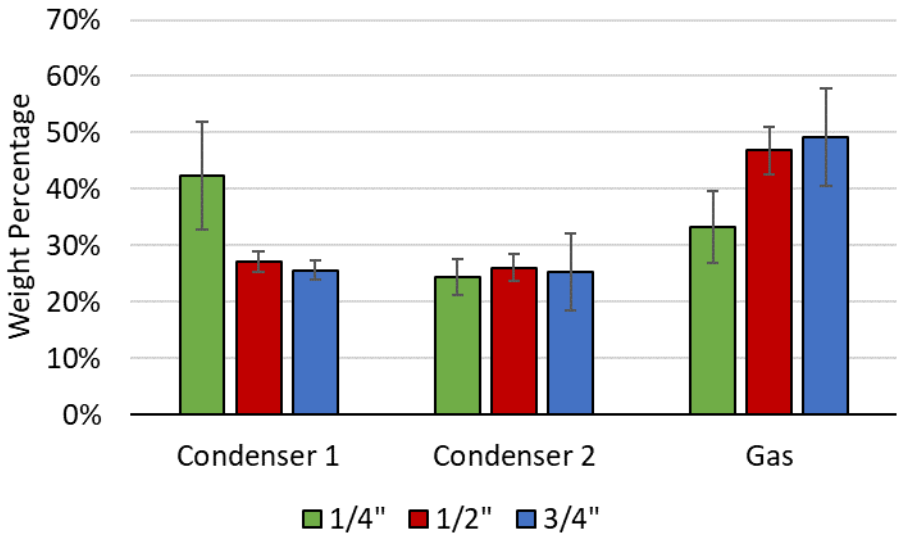

Figure 3.4 Product distribution for the three pilot plant reactor sizes. Condenser 1 product is a pyrolysis wax at room temperature while condenser 2 product is a pyrolysis liquid.

3.3.3 GC-MS Analysis

Using GC-MS calibration curves (Figure B.5 of Appendix B), the pyrolysis products were analyzed for contributions by each individual compound for each carbon number (Figure 3.5). Similar to previous micropyrolysis work,[17] each carbon number is represented by triplicate peaks, with the main center peak being alkene and the two minor side peaks being alkane and alkadiene (Figure B.10 of Appendix B). The pyrolysis gas product contained species from C1-C7. The Condenser 2 product contained species from C6-C30, which contains many "wax" components, while the Condenser 1 product was C9-C33, which likewise contains many "liquid product" components. Considerable overlap is seen between the three products, suggesting that the current condenser system is not achieving an ideal separation. There are distinct trends in these GC-MS results for each main product. As reactor diameter increases from ¼ inch to ¾ inch, yields of gas-range species increase, indicating that the increased vapor residence time leads to more cracking reactions. Conversely, yields of C11-C33 compounds show a decreasing trend. Low amounts (< 1 wt. %) of aromatics, specifically benzene and toluene, are present in the gas and Condenser 2 products. Lastly, an interesting pattern appears when looking at the overall mass contribution of each carbon number. For all three reactor volumes, representing different residence times, C3-C6, C11, and C27-C28 are "peaks" with higher mass percentages. Conversely, C2 and C8-C9 are "valleys" with mass contributions considerably lower than other compounds nearby. The explanation for this pattern is currently unknown, however it is consistent regardless of pyrolysis residence time.

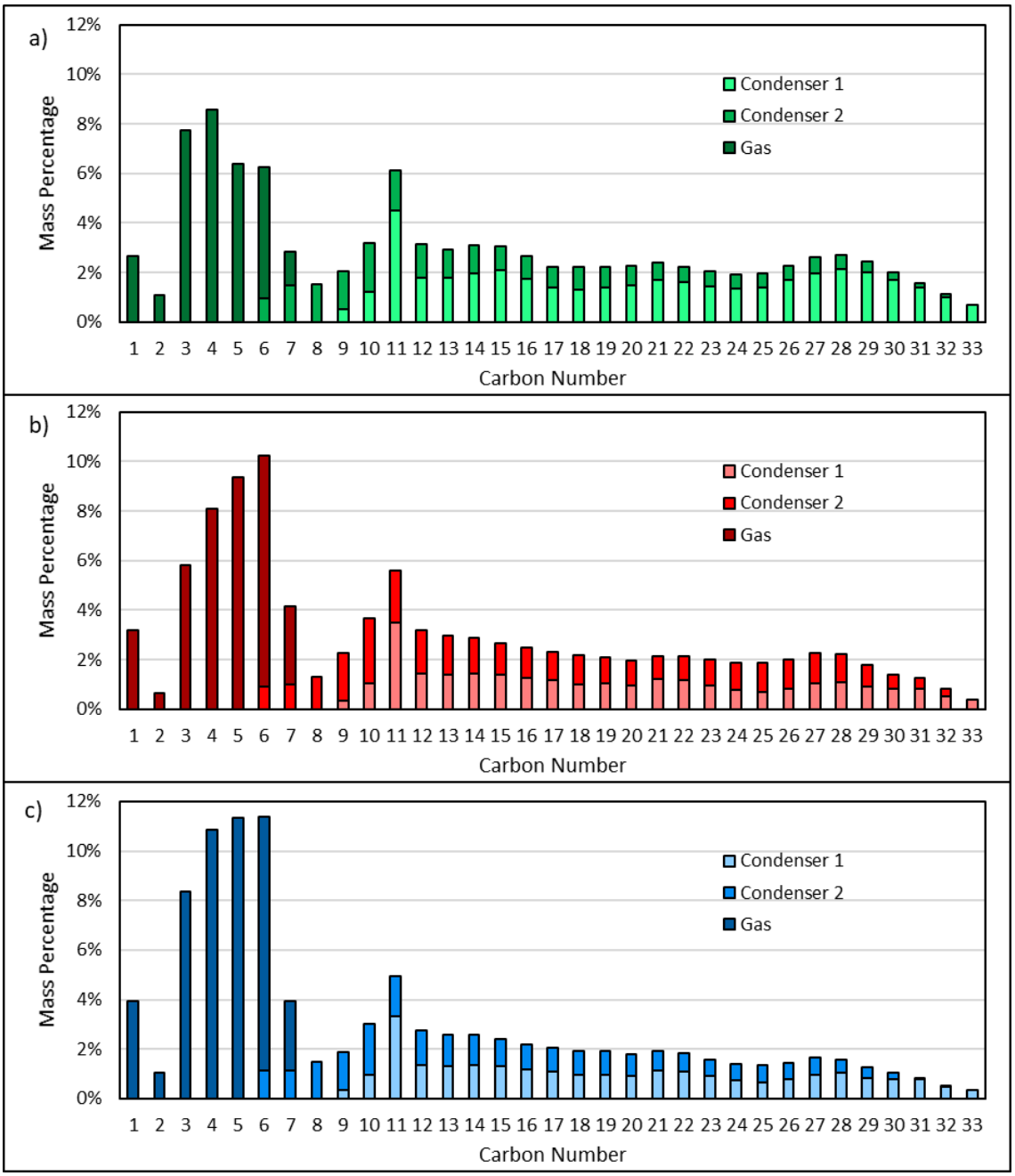

Figure 3.5 Average mass percentage for each carbon number for (a) ¼ inch, (b) ½ inch, and (c) ¾ inch reactor diameters.

3.3.4 Comparison to Micropyrolysis Results

The GC-MS results were lumped into four product categories for comparison to previously published micropyrolysis data[17] (Figure 3.6). The four lumped products are gas (C1-C4), light oil (C5-C10), heavy oil (C11-C19), and wax (C20+). The main trends with increasing reactor residence time are similar in both the pilot plant and micropyrolysis systems. Both

the wax and the heavy oil product wt. % decrease with increased residence time for both pyrolysis systems. The light oil wt. % increases with a corresponding increase in residence time while residence time has a less discernable effect on gas production. Gas production slightly increases with more residence time for the pilot plant but does not for micropyrolysis. In the micropyrolysis work, it was concluded that the gas is converted to aromatics at a similar rate as it was being produced during the secondary pyrolysis reactions, thus keeping the overall mass fraction (x_G) fairly constant over increasing residence time. In the pilot plant work, very low aromatic production was measured, perhaps due to the lower heating rate. The lack of aromatics could explain the increase of gas production from ¼ to ¾ inch reactor (20 to 24 wt. %). Overall, it appears that the micropyrolysis results serve as a good indicator for the pilot plant results.

In order to make a fair comparison between the pilot and micro-reactor, it's worth noting the similarities and differences between the two systems. Both systems have a tubular reactor that is heated by a heating tape with controllable residence time and temperature distribution. On the other hand, there are some notable differences. First, the micropyrolysis apparatus has a considerably faster primary heating rate at 1000 °C/s.[19] The micropyrolysis apparatus also uses Helium as an inert carrier gas which is not present in the pilot plant. It was also previously observed that the micropyrolysis unit underestimates the production of heavier species due to retention of some heavy species in the pyroprobe and the pyrolysis apparatus.[17] This phenomenon was observed but not fully analyzed in that prior work. We believe this underestimation is why the pilot plant produces a higher mass percentage of heavier species (wax, heavy oil) while the micropyrolysis produces more light products (light oil, gas). One last important difference between the micropyrolysis and pilot pyrolysis systems is the feedstock, as the micropyrolysis work studied pure HDPE while the pilot plant uses a 1:1 (wt.) HDPE and pyrolysis wax solvent mixture. The similar trends between the pilot plant and micropyrolysis product distribution results shown in Figure 3.6 provide direct evidence that the addition of the pyrolysis wax solvent to the pilot plant feed does not alter the underlying pyrolysis kinetics.

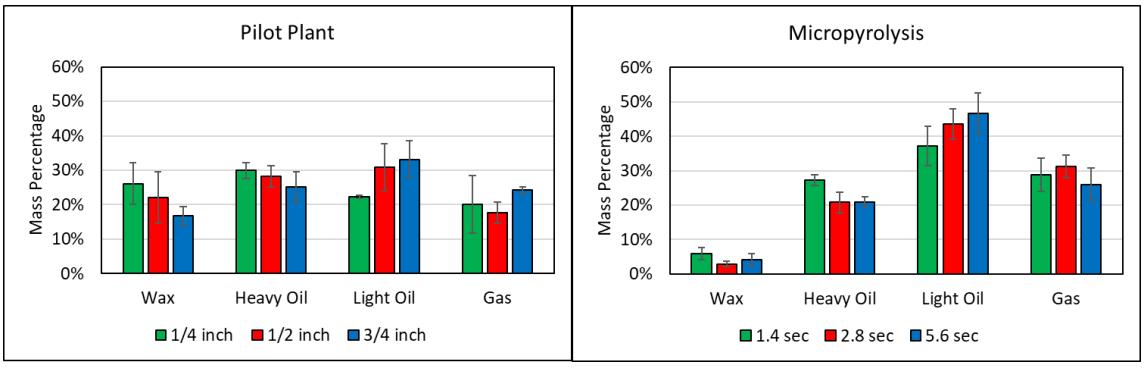

Figure 3.6 Lumped mass percentages for pilot plant (left) and micropyrolysis (right) of HDPE at 600 °C.

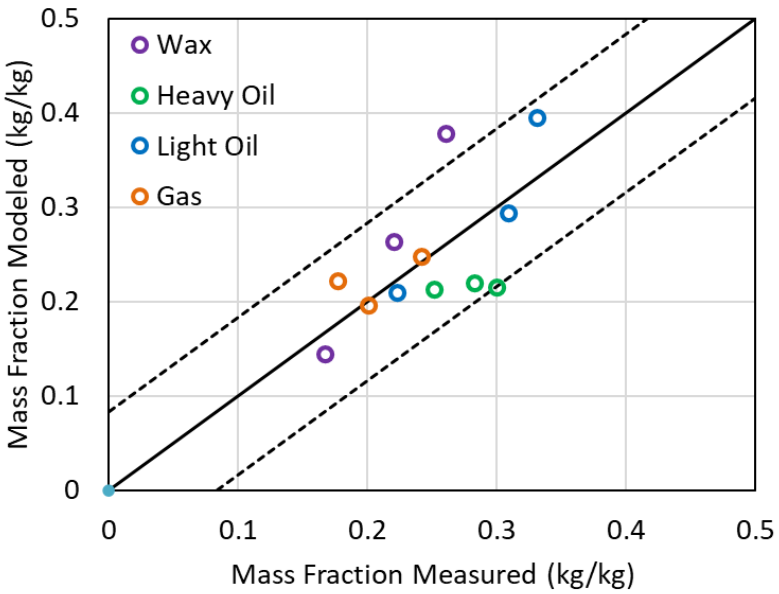

Figure 3.7 Comparison of the lumped mass percentages for the pilot plant (measured) versus the reactor model output (modeled) for the three different reactor volumes. The 95% CI is ± 8 wt. %.

The pilot plant lumped product distribution can also be compared to the reactor model outputs to ensure that the model is accurately predicting the product distribution (Figure 3.7). For the 6 experiments modeled (see Table 3.1), the model product distribution has a 95% confidence interval of ± 12% when compared to the actual product distribution. The wax product has the largest outliers, with the model predicting far more wax product than what was actually produced for a couple of the experiments. Overall, the fit between the model and the measured results is reasonably good considering the limited number of experiments conducted. Since both the model's temperature distribution (Figure 3.2) and product distribution (Figure 3.7) compare well with the pilot plant results, there can be confidence in the accuracy of the predicted vapor residence time.

3.4 Conclusions

An innovative liquid-feed plastic pyrolysis pilot plant was investigated to conduct fast pyrolysis experiments for a mixture of HDPE in a pyrolysis wax solvent at 600 °C. The HDPE was dissolved in recycled pyrolysis wax to create a liquid feed to the pyrolysis reactor. It was found that using the pyrolysis wax as a solvent successfully created a consistent liquid feed, avoiding the bridging issues that can plague solid feeding systems. Three different tubular reactor diameters (volumes) were tested at approximately constant feed rate to determine the effect of residence time on product distribution and multiphysics modeling was conducted to predict the residence times in the reactor as well as temperature profiles. It was found that residence time had a significant effect on product distribution. Increasing pilot plant pyrolysis residence time from 1 to 4.5 seconds caused a 9 wt. % drop in wax production, 5% drop in heavy oil, a 11 wt. % increase in light oil production, and a

4 wt.% increase in gas production. The trends for product distribution as a function of residence time are consistent between both the pilot plant and micropyrolysis systems, suggesting that when micropyrolysis results are obtained using a two-stage pyrolysis mode[17] (primary products generated in the pyroprobe, followed by a constant temperature tubular reactor for vapor phase secondary reactions), the data are useful in correlating to pilot plant yields.

3.5 Acknowledgments

We thank Dr. Simeon Schum (Michigan Technological University) for assisting with maintenance and calibration of the GC-MS. We also thank Jeffrey Lacey of Idaho National Laboratory for providing the waste plastics.

Funding: This work was supported by the Defense Advanced Research Projects Agency ReSource program cooperative agreement HR00112020033. The views, opinions and/or findings expressed are those of the author and should not be interpreted as representing the official views or policies of the Department of Defense or the U.S. Government.

3.6 References

1. EPA, Advancing Sustainable Materials Management: 2018 Fact Sheet Assessing Trends in Material Generation and Management in the United States. Park, U. S. E. P. A. R. T., Ed. Durham, NC, 2020.

2. Barrett, A. H.; Cardello, A. V., *Military food engineering and ration technology*. DEStech Publications, Inc: 2012.

3. Bith-Melander, P.; Ratliff, J.; Poisson, C.; Jindal, C.; Choi, Y. M.; Efird, J. T., Slow burns: a qualitative study of burn pit and toxic exposures among military veterans serving in Afghanistan, Iraq and throughout the Middle East. *Annals of psychiatry and clinical neuroscience* **2021,** *4* (1).

4. Al-Salem, S.; Antelava, A.; Constantinou, A.; Manos, G.; Dutta, A., A review on thermal and catalytic pyrolysis of plastic solid waste (PSW). *Journal of environmental management* **2017,** *197*, 177-198. DOI: 10.1016/j.jenvman.2017.03.084

5. Sharuddin, S. D. A.; Abnisa, F.; Daud, W. M. A. W.; Aroua, M. K., A review on pyrolysis of plastic wastes. *Energy conversion and management* **2016,** *115*, 308-326. DOI: 10.1016/j.enconman.2016.02.037

6. Vollmer, I.; Jenks, M. J.; Roelands, M. C.; White, R. J.; van Harmelen, T.; de Wild, P.; van Der Laan, G. P.; Meirer, F.; Keurentjes, J. T.; Weckhuysen, B. M., Beyond mechanical recycling: Giving new life to plastic waste. *Angewandte Chemie International Edition* **2020,** *59* (36), 15402-15423. DOI: 10.1002/anie.201915651

7. Zeller, M.; Netsch, N.; Richter, F.; Leibold, H.; Stapf, D., Chemical Recycling of Mixed Plastic Wastes by Pyrolysis–Pilot Scale Investigations. *Chemie Ingenieur Technik* **2021,** *93* (11), 1763-1770. DOI: 10.1002/cite.202100102

8. Li, H.; Aguirre-Villegas, H. A.; Allen, R. D.; Bai, X.; Benson, C. H.; Beckham, G. T.; Bradshaw, S. L.; Brown, J. L.; Brown, R. C.; Castillo, M. A. S., Expanding Plastics Recycling Technologies: Chemical Aspects, Technology Status and Challenges. *ChemRxiv* **2022**. DOI: 10.26434/chemrxiv-2022-9wqz0-v2

9. Lubongo, C.; Congdon, T.; McWhinnie, J.; Alexandridis, P., Economic feasibility of plastic waste conversion to fuel using pyrolysis. *Sustainable Chemistry and Pharmacy* **2022,** *27*, 100683. DOI: 10.1016/j.scp.2022.100683

10. Kaminsky, W., Chemical recycling of plastics by fluidized bed pyrolysis. *Fuel Communications* **2021,** *8*, 100023. DOI: 10.1016/j.jfueco.2021.100023

11. Arabiourrutia, M.; Elordi, G.; Lopez, G.; Borsella, E.; Bilbao, J.; Olazar, M., Characterization of the waxes obtained by the pyrolysis of polyolefin plastics in a conical spouted bed reactor. *Journal of Analytical and Applied Pyrolysis* **2012,** *94*, 230-237. DOI: 10.1016/j.jaap.2011.12.012

12. Marculescu, C.; Antonini, G.; Badea, A.; Apostol, T., Pilot installation for the thermo-chemical characterisation of solid wastes. *Waste management* **2007,** *27* (3), 367-374. DOI: 10.1016/j.wasman.2006.02.011

13. Fekhar, B.; Miskolczi, N., Stability and storage properties of hydrocarbons obtained by pilot scale pyrolysis of real waste HDPE-PVC in tubular reactor. *Chemical Engineering Transactions* **2018,** *70*, 1141-1146. DOI: 10.3303/CET1870191

14. Lechleitner, A. E.; Schubert, T.; Hofer, W.; Lehner, M., Lumped Kinetic Modeling of Polypropylene and Polyethylene Co-Pyrolysis in Tubular Reactors. *Processes* **2021,** *9* (1), 34. DOI: 10.3390/pr9010034

15. Byrne, E.; Schaerer, L. G.; Kulas, D. G.; Ankathi, S. K.; Putman, L. I.; Codere, K. R.; Schum, S. K.; Shonnard, D. R.; Techtmann, S. M., Pyrolysis-Aided Microbial Biodegradation of High-Density Polyethylene Plastic by Environmental Inocula Enrichment Cultures. *ACS Sustainable Chemistry & Engineering* **2022**. DOI: 10.1021/acssuschemeng.1c05318

16. Zolghadr, A.; Foroozandehfar, A.; Kulas, D. G.; Shonnard, D., Study of the Viscosity and Thermal Characteristics of Polyolefins/Solvent Mixtures: Applications for Plastic Pyrolysis. *ACS omega* **2021,** *6* (48), 32832-32840. DOI: 10.1021/acsomega.1c04809

17. Kulas, D. G.; Zolghadr, A.; Shonnard, D., Micropyrolysis of Polyethylene and Polypropylene Prior to Bioconversion: The Effect of Reactor Temperature and Vapor Residence Time on Product Distribution. *ACS Sustainable Chemistry & Engineering* **2021,** *9* (43), 14443-14450. DOI: 10.1021/acssuschemeng.1c04705

18. Mastral, F.; Esperanza, E.; Berrueco, C.; Juste, M.; Ceamanos, J., Fluidized bed thermal degradation products of HDPE in an inert atmosphere and in air–nitrogen mixtures. *Journal of Analytical and Applied Pyrolysis* **2003,** *70* (1), 1-17. DOI: 10.1016/S0165-2370(02)00068-2

19. Gracida-Alvarez, U. R.; Mitchell, M. K.; Sacramento-Rivero, J. C.; Shonnard, D. R., Effect of temperature and vapor residence time on the micropyrolysis products of waste high density polyethylene. *Industrial & Engineering Chemistry Research* **2018,** *57* (6), 1912-1923. DOI: 10.1021/acs.iecr.7b04362

20. Mastral, J.; Berrueco, C.; Ceamanos, J., Modelling of the pyrolysis of high density polyethylene: product distribution in a fluidized bed reactor. *Journal of analytical and applied pyrolysis* **2007,** *79* (1-2), 313-322. DOI: 10.1016/j.jaap.2006.10.018

21. Zhao, D.; Wang, X.; Miller, J. B.; Huber, G. W., The Chemistry and Kinetics of Polyethylene Pyrolysis: A Feedstock to Produce Fuels and Chemicals. *ChemSusChem* **2019,** *13* (7), 1764-1774. DOI: 10.1002/cssc.201903434

22. Velghe, I.; Carleer, R.; Yperman, J.; Schreurs, S., Study of the pyrolysis of municipal solid waste for the production of valuable products. *Journal of Analytical and Applied Pyrolysis* **2011,** *92* (2), 366-375. DOI: 10.1016/j.jaap.2011.07.011

23. Rawlings, J. B. a. E., J.G., *Chemical Reactor Analysis and Design Fundamentals*. 2nd ed.; Nob Hill Publishing, LLC: 2022.

24. Elordi, G.; Arabiourrutia, M.; Bilbao, J.; Olazar, M., Energetic viability of a polyolefin pyrolysis plant. *Energy & Fuels* **2018,** *32* (3), 3751-3759. DOI: 10.1021/acs.energyfuels.7b03664

25. Singh, R. K.; Ruj, B.; Sadhukhan, A.; Gupta, P., Impact of fast and slow pyrolysis on the degradation of mixed plastic waste: Product yield analysis and their characterization. *Journal of the Energy Institute* **2019,** *92* (6), 1647-1657. DOI: 10.1016/j.joei.2019.01.009

26. Das, P.; Tiwari, P., Valorization of packaging plastic waste by slow pyrolysis. *Resources, Conservation and Recycling* **2018,** *128*, 69-77. DOI: 10.1016/j.resconrec.2017.09.025

27. Palos, R.; Gutiérrez, A.; Vela, F. J.; Maña, J. A.; Hita, I.; Asueta, A.; Arnaiz, S.; Arandes, J. M.; Bilbao, J., Assessing the potential of the recycled plastic slow pyrolysis for the production of streams attractive for refineries. *Journal of analytical and applied pyrolysis* **2019,** *142*, 104668. DOI: 10.1016/j.jaap.2019.104668

28. Eidesen, H.-K.; Khawaja, H.; Jackson, S., Simulation of the HDPE Pyrolysis Process. *Int. Jnl. of Multiphysics* **2018,** *12* (1), 79-88. DOI: 10.21152/1750-9548.12.1.79

29. Papuga, S. V.; Gvero, P. M.; Vukić, L. M., Temperature and time influence on the waste plastics pyrolysis in the fixed bed reactor. *Thermal science* **2016,** *20* (2), 731-741. DOI: 10.2298/TSCI141113154P

30. Overall Heat Transfer Coefficient Table, Charts, and Equation. https://www.engineersedge.com/thermodynamics/overall_heat_transfer-table.htm (accessed February 2022).

31. del Remedio Hernández, M.; García, Á. N.; Marcilla, A., Catalytic flash pyrolysis of HDPE in a fluidized bed reactor for recovery of fuel-like hydrocarbons. *Journal of analytical and applied pyrolysis* **2007,** *78* (2), 272-281. DOI: 10.1016/j.jaap.2006.03.009

4 Economic and Environmental Analysis of Plastics Pyrolysis After Secondary Sortation of Mixed Plastic Waste[3]

4.1 Introduction

Plastics have become an essential material in our daily lives, with the use of plastic packaging expected to double in the next 20 years.[1] Recycling technologies have failed to keep up with the rise of waste plastics generation, with only 8.5% of waste plastic collected for recycling in the United States as of 2018.[2] The vast majority of that collected material is prepared for mechanical recycling, which requires relatively pure feedstock of a single plastic type. Mechanical recycling cannot handle high levels of contamination or plastic mixtures,[3] which means that it cannot handle all the plastic that goes through a Materials Recovery Facility (MRF). A MRF typically sorts the plastic into pure PET and HDPE bales with the rest going into a #1-7 mixed plastic bales. While the PET and HDPE bales are high quality and can be sold at a premium on the open market[4], the mixed plastics are considered low-value and often incinerated or landfilled.[5] Surveys of MRFs in the U.S. have found that on average 25% of the plastic entering a MRF ends up in this mixed plastic bale.[6] The mixed plastic bales represent an attractive feedstock for chemical recycling technologies such as pyrolysis.[7]

Pyrolysis has high feedstock flexibility in that a pyrolysis reactor can pyrolyze a mixture of plastics, such as PP, HDPE, LDPE, and PS, at the same time.[7, 8] Pyrolysis is also capable of pyrolyzing hard to recycle plastics, with some studies reporting that it can handle up to 20% contamination from food residues.[5] While incineration is also capable of processing hard to recycle mixed plastics, it can only produce heat and electricity. Pyrolysis, on the other hand, can produce a wide range of hydrocarbon products, including wax, oil, aromatics, ethylene, and propylene.[9] These products are more valuable than those of incineration and can also be used as a feedstock for new plastics production, contributing to a circular economy. Life cycle assessments of different plastic pyrolysis processes have found that it has consistently lower GHG emissions when compared to incineration.[10-14] Incinerating plastics can cause a myriad of environmental issues including formation of dioxins, fly ash, and other toxins.[15, 16] From both an economic and environmental perspective, pyrolysis is superior compared to incineration for recycling mixed plastic wastes.

Despite these advantages, pyrolysis still faces challenges preventing commercial implantation. Past techno-economic analyses have found that security of feedstock supply and operating capacity are two of the biggest challenges.[1, 5, 7, 9, 17] Larrain, et al.[1] found that a slow pyrolysis plant for mixed polyolefins needed a minimum capacity of 70 kt/yr to be

---

[3] In preparation for submission to *ACS Sustainable Chemistry and Engineering*. Kulas, D; Zolghadr, A; Chaudhari, U; Shonnard, D. Economic and Environmental Analysis of Plastics Pyrolysis After Secondary Sortation of Mixed Plastic Waste

economically feasible. Pyrolysis yields at 460-500 ºC were 40% naphtha, 34% wax, and 11% gas. The gas was co-combusted internally to provide the thermal and electrical energy requirements for the pyrolysis reaction, which was calculated to be 1.71 MJ/kg plastic. They found that the process economics were most sensitive to feedstock availability, product prices, and capital investment. Another recent analysis by Yadav, et al.[5] agreed with this finding, reporting that the pyrolysis process is highly sensitive to feedstock and capital costs. In particular, the high assumed feedstock cost of $0.6/kg drove the minimum selling price (MSP) of the pyro-naphtha product to $2.18/kg, which is 4.3 times higher than that of fossil naphtha. The feedstock's contribution to the MSP ($1.50/kg) was three times that of the pyrolysis process costs ($0.50/kg). Overall a wide range of feedstock costs have been assumed in the pyrolysis literature, with some studies assuming no cost[7, 17, 18] and others assuming costs over $450/MT.[5, 19] Perhaps not surprisingly, the studies assuming no feedstock cost were found to be very profitable, with Fivga and Dimitrou[7] calculating the production cost of pyrolysis fuel to be about 10 times lower than market fuel prices at a scale of 84 kt/yr. Lubongo, et al.[17] agreed with this assessment, finding that paying no feedstock costs for pyrolysis of waste plastic into heavy and light oil was profitable at scales from 10.5 to 35 kt/yr. Buying plastic waste at market price, which in this study was assumed to be $88/MT, was only profitable at the 35 kt/yr scale. A study by Gracida-Alvarez, et al.[9] found that separating out value-added chemicals like ethylene, propylene, and aromatics from the pyrolysis products can offset the high feedstock costs, with a maximum calculated feedstock cost of $460/MT being profitable. The increased capital cost of the separation train can also hurt the process economics though, as found by Westerhout, et al.[18]

Most TEA studies of polyolefin pyrolysis assume an operating capacity near 100 kt/yr.[7, 10, 20-22] However, the commercial pyrolysis plants currently in operation generally have a maximum capacity of 35 kt/yr.[4, 17, 23] There are a few plants currently under construction by QuantaFuel[24] and Brightmark[25] that have a maximum scale of 100 kt/yr. These are planned to become fully operational in the coming years. It is vitally important, then, to consider the effect of operating capacity when analyzing the pyrolysis process economic results. Large plants are generally more profitable due to economies of scale.[7, 17] Fivga and Dimitrou[7] found that scaling up their pyrolysis process from 0.8 kt/yr to 840 kt/yr significantly increased the profitability of the process, with the highest scale producing revenue with a positive NPV within year one of operation. Other TEA studies have reported minimum capacities for economic feasibility of 70 kt/yr[1] and 35 kt/yr[17] respectively.

While LCAs are very common for evaluating plastic waste scenarios, most limit their analysis to only mechanical recycling, landfilling, and incineration.[10, 26, 27] Those that have analyzed chemical recycling as a scenario have found positive results with GHG emission savings from limiting the use of fossil derived virgin material.[10-14] Employing heat integration and renewable electricity are two process optimizations that have been found to further minimize the environmental impacts.[5, 10] In particular, Gracida-Alvarez, et al.[10] found that performing heat integration on the pyrolysis process caused the GHG emissions for all products to be equal or lower than their fossil equivalents. In addition to GHG emissions, pyrolysis may also have positive results in other impact categories. When compared to incineration, pyrolysis produces much less sulfur and nitrogen oxides, dioxins,

and other toxins.[7, 15, 16] In addition, advanced chemical recycling technologies like pyrolysis may help reduce the leakage of waste plastic to the ocean.[10] Increasing the economic value of waste plastic could in turn cause waste plastic to be a valuable resource that is better managed. This could potentially decease the leakage to the ocean and coastal sediments, thus reducing the negative impacts on marine ecosystems.[10, 28, 29]

In this paper we present the novel idea of combining liquid-phase pyrolysis with a post-MRF secondary sort of mixed plastic waste bales. Advanced sorting technologies, featuring improved sensing capabilities, robotic systems for separating various resin types, and artificial intelligence, are being developed in order to handle and separate previously hard to recover plastics. These difficult plastics, which include large amounts of polyethylene terephthalate, polypropylene, and polyethylene, typically end up in #1-7 mixed plastic bales which are then either landfilled or incinerated for energy recovery. Advanced sorting technologies are able to separate the valuable plastic out of these mixed bales creating a lower cost mixed feedstock of HDPE and PP for pyrolysis.

Few studies combine the TEA/LCA analysis, making it difficult to get a full picture of the process sustainability. Coupling the TEA and LCA analysis gives understanding into the relationships and trade-offs between the economic and environmental impacts.[30] In this work a preliminary TEA and LCA analysis of liquid-phase pyrolysis of HDPE and PP separated from mixed #1-7 waste plastic bales is presented. To the best of our knowledge, this is the first study that both analyzes sourcing waste plastics specifically from a secondary sortation of #1-7 mixed plastic bales from a MRF and the liquid-phase pyrolysis product that uses a closed-loop pyrolysis wax solvent.

4.2 Methods

4.2.1 Feedstock

The feedstock for this work is mixed plastic bales #1-7, which contain the partially sorted plastic that leaves a material recovery facility (MRF). The bales have been sorted to be relatively pure plastic (98% plastic, 2% garbage on average) and contain numerous different plastic types (Figure 1). Data received from a MRF in Emmet County, Michigan shows the 2-year average makeup of the mixed plastic bales (Figure 1). The top contributors by mass were found to be polyethylene terephthalate (PET; 40% ± 11%), polypropylene (PP; 36% ± 7%), and high-density polyethylene (HDPE; 15% ± 10%). A recent audit performed by RRS[31] on mixed plastic bales at 9 different MRFs found similar amounts of PP (31%) and HDPE (15%) of plastics to the Emmet County data. The audit reported significantly less PET (22%) than Emmet County and found that there was a large variation in PET makeup between the different MRFs. For this analysis we assumed that the Emmet County audit data presented in Figure 4.1 is representative of the typical mixed plastic bale. The largest resin type in the mixed bale is PET (40%), followed by PP (36%), and PE (15%), totaling 91% of the bale mass. The remainder of the mixed bale is PS/PVC/PETG (6%), garbage (2%) and Aluminum (1%).

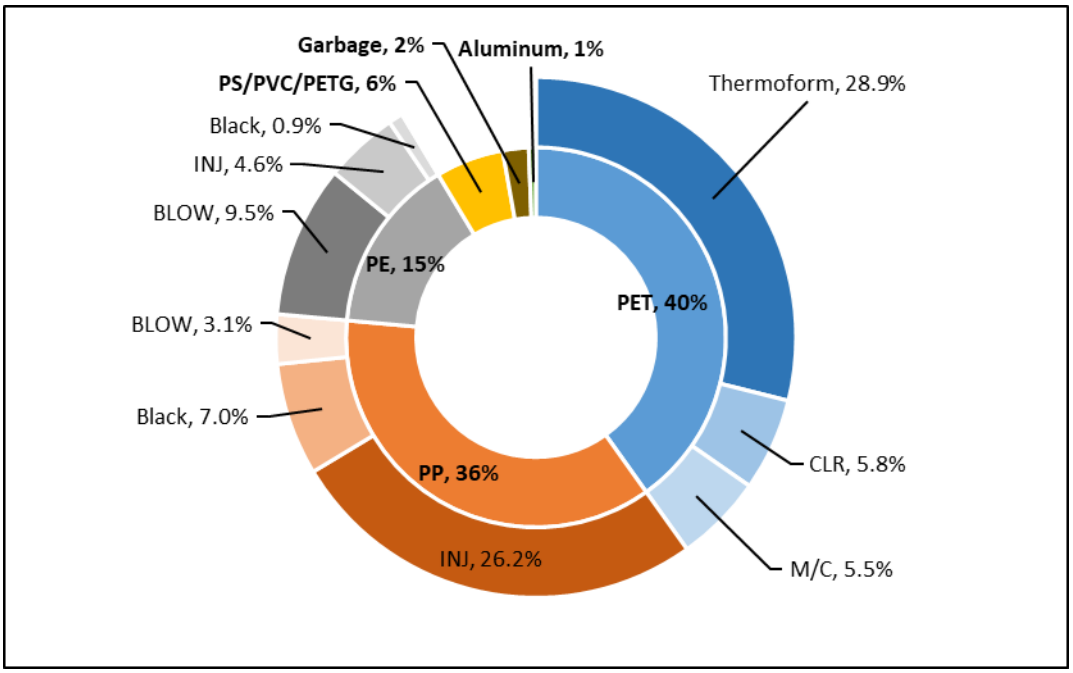

Figure 4.1 Average composition of bale #1-7 from Emmet County MRF (Michigan). The inside circle shows the breakdown by plastic type while the outside circle details the type of each individual plastic and the process that the resins is processed through. Types of PET include thermoform, clear (CLR) and mixed color (M/C). Types of PP and HDPE include black, injection molded (INJ), and blow molded (BLOW).

An additional sorting process is necessary to remove the HDPE and PP from the PET and other mixed plastics and contaminants. Due to the lack of data in the current literature on secondary sorting, the costs and environmental impacts are assumed to be the same as the primary sort at a MRF.[32, 33] We believe that this is a conservative assumption likely to over predict-costs and environmental impacts because the original MRF inputs more complex feeds and contains many addition unit operations compared to a secondary sortation process. The waste from the secondary sorting process, which contains the materials that are not HDPE and PP, is assumed to go to landfill in the base case scenario. A scenario was studied to see how recovering the PET, mostly thermoform PET, in addition to the HDPE and PP would affect the economic and environmental results. Overall, a flowrate of 20 MT/hr of mixed plastic bales is needed to supply the pyrolysis process with 10 MT/hr of HDPE and PP. This results in an annual feed capacity of 84 kt/yr, which is similar in magnitude to other technical studies in this field.[7, 10, 20-22]

4.2.2 Process Simulation

The modeled plastic pyrolysis process, presented in Figure 4.2, continuously converts 10 metric tons (MT) per hour of waste HDPE and PP plastic into three products: wax, oil, and gas. The wax product is recycled back to the dissolution tank as a solvent for the mixed waste plastic feed. The oil product is the main product for this study while the gas product is a co-product.

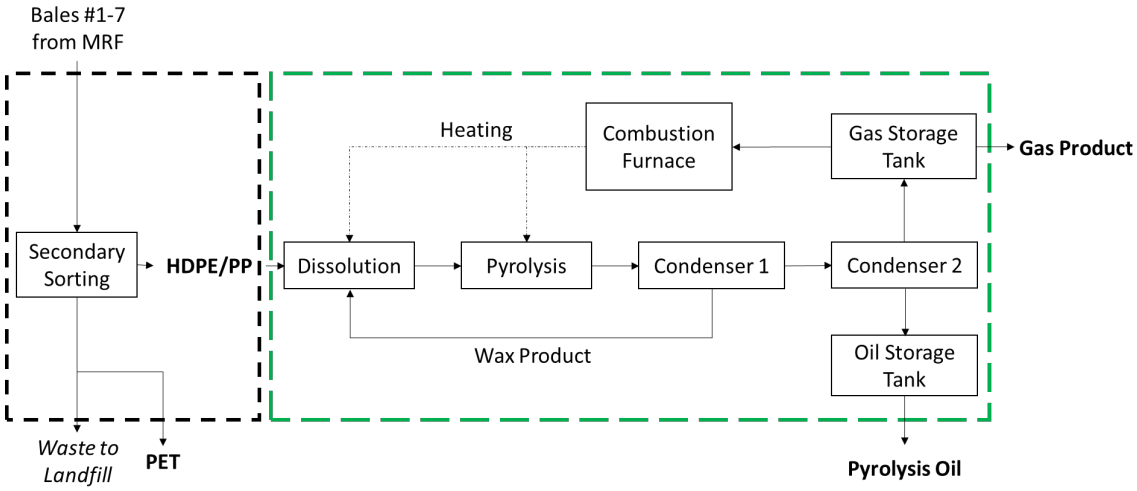

Figure 4.2 Process flow diagram of the modeled pyrolysis process. The black box (left) was modeled using cost and environmental impact data from the literature[32, 33, 36] while the green box (right) was modeled in ASPEN Plus.

An Aspen Plus process model, based on the process flow diagram in Figure 4.2, was developed and implemented. The Aspen Plus model utilizes the Peng-Robinson thermodynamic package due to its reliability in modelling processes that involve hydrocarbon mixtures.[9, 34] The plastic feedstock is modeled as a solid based on proximate and ultimate analysis from He, et al.[35]

4.2.2.1 Dissolution

The clean and sorted waste plastic at 25 ℃ enters the stirred dissolution tank where it dissolves in hot recycled pyrolysis wax at a 1:1 wt% ratio at 240℃.[37] The energy requirements for mixing are calculated using literature correlations[38] based on the measured viscosity of the dissolved mixture.[37] We have observed during pilot scale (0.25 kg/hr) experiments[39] that the dissolution process takes around 6 hours to complete and assume that the scaled-up process behaves similarly. From an operational perspective, it would make sense to have multiple dissolution tanks operating in semi-batch mode. In one tank the plastic would be loaded and dissolved into the recycle wax solvent while the other tank, which was previously loaded, is drained into the pyrolysis reactor. Every 6 hours the two tanks switch roles. This avoids the potential for partially dissolved plastic pieces to get into the pyrolysis reactor which could happen with the continuous use of one dissolution tank.

4.2.2.2 Pyrolysis Reactor

The pyrolysis reactor is operated at 600 ºC with a 3 second vapor residence time.[40] The pyrolysis reaction is modeled as a yield reactor in Aspen Plus, with product yields taken from experimental pilot scale data.[39] The pyrolysis reaction yields can be found in Table C.1 in Appendix C. It has been shown that plastics pyrolysis produces primarily alkenes with minor amounts of alkadienes and alkanes[40], but in this analysis as a simplification

step, was modeled as only alkenes. These conditions of reaction temperature and vapor residence time were chosen primarily to produce a wax yield of 50 wt.%. This is because one requirement of this process concept is that wax yield must be 50 wt.% in order to keep the wax recycle loop sustainable. Lower wax production would require the purchase of make-up paraffin wax or raising the dissolution temperature to compensate, while higher wax production would decrease the production of the desired oil product. Since published micro-scale[40] and unpublished internal pilot scale experiments have demonstrated that PP produces similar pyrolysis yields as HDPE at 600 ℃, we assume that feedstock variations in the ratio of PP to HDPE will not affect the pyrolysis yields. The simple thermal pyrolysis process concept shown in Figure 4.2 does not contain any catalyst or inert carrier gas.

4.2.2.3 Condensers

The hot pyrolysis vapors flow into a dual condenser set-up. The first condenser is operated at 135 ºC to recover the pyrolysis wax at the required 50 wt.% yield. The second condenser is operated at 25 ºC to separate the liquid pyrolysis oil product from the pyrolysis hydrocarbon gases. The second condenser is cooled using a refrigeration cycle which supplies the cooling heat exchanger fluid at 15 ºC to maintain a minimum of ΔT of 10 ºC within the condenser. The gas product is combusted for internal process heat. The excess gas is compressed into a gas storage tank (145 psig) where it is then sold with an assumed market value of propane ($0.96/gallon; see Figure C.1 in Appendix C).

4.2.3 Techno-Economic Analysis (TEA)

The techno-economic analysis (TEA) was conducted using a 20-year discounted cash flow (DCF) analysis with an IRR of 20%. The key input assumptions for the DCF analysis are listed in Table 4.1. The DCF analysis was used to calculate the minimum selling price (MSP) of the oil product. This was solved for by finding the pyrolysis oil selling price that sets the net present value (NPV) equal to 0.

4.2.3.1 Fixed Capital Investment (FCI)

Capital equipment for the pyrolysis process includes dissolution tanks, pyrolysis reactor, condensers, product storage tanks, heat exchangers, combustion furnace, mixers, pyrolysis gas product compressor, and pumps. Both the dissolution tanks and the storage tanks for the wax and liquid product are assumed to need a mixer. Installed capital costs for all were estimated using literature cost correlations which can be found in Table C.2 in Appendix C.[38]

4.2.3.2 Fixed Costs of Production

The fixed costs of product include labor, fringe benefits, maintenance, and other contingency costs. Three operators were assumed to be needed per shift paid at a yearly rate of $50,000 for all operating capacities analyzed in this work.[38] Engineering, project management, and contingency costs are calculated according to industry standards and are shown in Table 4.1.[38]

Table 4.1 Parameters and assumptions utilized in the base case TEA

Parameter	**Value**
Plant Lifetime[41]	20 years
Operating Capacity	84,000 MT/yr of HDPE/PP
Days Operated Per Year	350 days
Construction Time	1 year
Start-up period	6 months
Discount Rate (IRR)	20%
Income Tax Rate	21%
Inflation	2%
Working Capital (WC) (% of FCI)	15%
Depreciation Method	7-year MACRS
Electricity (US average, industrial)[42]	$0.073/kWh
Cooling Water[43]	$0.16/GJ
Feedstock Cost	$240/MT
Landfill tipping fee[36]	$61/MT
Maintenance	3% of ISBL per year
Rent	1% of FCI per year
Taxes	1% of FCI per year
Insurance Premiums	1% of FCI per year
Research and Development	1% of Revenue per year
General plant overhead	65% of Labor and Maintenance per year
Environmental	1% of FCI per year

4.2.3.3 Operating Costs

Operating costs for the process include feedstock, utilities, and fixed operating costs. The #1-7 mixed plastic bale feedstock is assumed to be purchased at a cost of $20/MT.[4] The secondary sorting necessary to recover the HDPE and PP from the mixed bale is priced at $100/MT of waste plastics processed.[32] Considering the 50% yield of HDPE and PP from the mixed plastic bale gives a feedstock cost of $240/MT of sorted HDPE and PP entering the dissolution tank (double the feedstock and sorting costs). This compares favorably to the price of sorted HDPE from a MRF, which on average is around $400/MT.[4] Sensitivity and scenario analyses presented later evaluate the effects of these assumed sorting costs. Utilities include cooling water and electricity. Heating is supplied by the recycle and combustion of the pyrolysis gas at an assumed efficiency of 80%.[38] Cooling water is needed for the condensers and is priced at $0.16/GJ.[43] Electricity is needed for the mixers, pumps, and pyrolysis product gas compressor and is priced using the average industrial price for electricity in 2021 at $0.073/kWh.[42] Residual plastic and garbage from the mixed plastic bale post-secondary sorting is assumed to be either landfilled or incinerated at a cost of $61/MT.[36] Due to the similar cost in tipping fees between incineration and landfill[44], both routes of disposing waste are treated the same in the TEA. Transportation costs were estimated using the average price of transporting liquid and solids[45] assuming 50 miles of

truck transportation from MRF to the plant. The cost to transport the liquid and gas products to the market is not included in the analysis.

4.2.4 Life Cycle Assessment (LCA) Framework, System Definition, and Modeling Assumptions

The goal of this LCA is to conduct a preliminary analysis using the base case process data from the pyrolysis process to evaluate it's 'cradle-to-gate' impacts. The LCA software used in this study is SimaPro® version 9.0, which provides accessible databases of environmental inventory data, including ecoprofiles specific to the U.S. The LCA methodology followed the ISO standards (ISO 14044). The LCA is limited to two impact assessment methods: global warming potential for all greenhouse gas (GHG) emissions and cumulative energy demand (CED). The GHG emissions impact assessment method used was the IPCC 2013 GWP 100a in SimaPro®. The IPCC 2013 was developed by the Intergovernmental Panel on Climate Change and contains climate change factors with a time horizon of 100 years.

4.2.4.1 LCA System Boundary

All results in the LCA assume a basis of 1 kg of product produced. The pathways investigated in this analysis are multi-output and produce two primary products: pyrolysis oil and pyrolysis gas. The LCA system boundary shown in Figure 4.3 includes only the mixed #1-7 bale to pyrolysis-based product pathways. However, the input #1-7 bale feed contains the environmental burdens from upstream collection and sorting at the MRF. The environmental burdens were divided between the two products, pyrolysis liquid and gas, using energy allocation. The cooling water and refrigerant input were described using appropriate inventory profiles in SimaPro. The electricity inventory profile in SimaPro was updated to represent the 2020 U.S. electricity grid.[46] A full calculation of allocation factors can be found in Table C.3 and Table C.4 in Appendix C and input / inventory tables for the base case LCA can be found in Table 4.2. The pyrolysis process infrastructure of installed equipment is not included in this preliminary analysis.

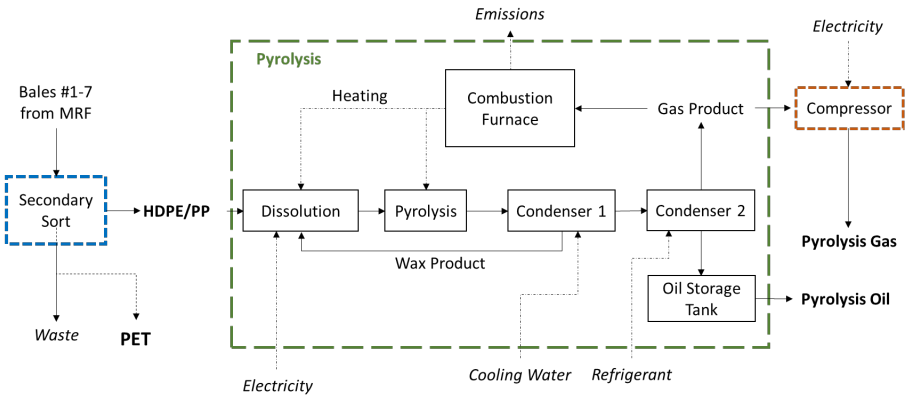

Figure 4.3 System boundary for the base case pyrolysis process. The secondary sorting process, represented by the blue box, uses literature emission factors.[33] The effect of recovering the PET during a secondary sort is analyzed using a scenario analysis.

Emissions from the pyrolysis process, represented by the green box, are energy allocated between the pyrolysis oil and pyrolysis gas. Emissions from the pyrolysis gas compressor apply only to the pyrolysis gas (red box).

4.2.4.2 MRF Collection and Sorting of Feedstock

There is an environmental burden placed on the #1-7 mixed bale from the MRF collection and sorting process. The GHG emissions and energy consumption for the sorting/collection process necessary for creating the mixed bale is modeled using resin-specific results from a report prepared by Franklin Associates.[33] The plastic not recovered is considered waste by both the MRF and this process, and thus has no allocated burden.

4.2.4.3 Secondary Sorting

The #1-7 bale entering the system boundary first goes through a secondary sorting. This separates out the HDPE/PP which is fed to the pyrolysis process. It is assumed that the secondary sorting step has similar emissions to that of the MRF collection/sorting process used for the feedstock burden.[33] While the secondary sort has no collection step, there is a transportation step needed between the MRF and the pyrolysis plant. For this analysis it is assumed that the inventory for feedstock transportation is the same as its original collection for a MRF. For the base case, the literature emissions[33] need a slight adjustment due to sorting yield. A MRF typically has around 20% solid waste[6] which carries no allocated burden. This secondary sort has 50% waste, however, which is approximately double that of a typical MRF. To account for the increase in sorting waste, the assumed emissions are doubled for the sorted HDPE/PP. These emissions are then energy allocated between the oil and gas final product. The waste plastic from the secondary sorting process is assumed to be disposed of to its original destination of landfill or incineration. Since the end-of-life destination for this residual material was not changed by the pyrolysis product, no environmental burden is placed on the pyrolysis products for the waste disposal.

There is also considerable PET (see Figure 4.1) in the #1-7 bale that possibly could be recovered as an additional product. A scenario analysis was conducted to see the effect of recovered PET as a secondary product that could be sold to PET recycling processes. Including the PET as a product decreases the secondary sorting waste down to 10%, which is comparable to the residual generation in a typical MRF. For this case, the emissions from the Franklin Report[33] are used for the two respective products: HDPE/PP and PET. The recovered PET leaves the system boundary after the secondary sorting step and does not affect any of the downstream processes (see Figure 4.3).

4.2.4.4 Pyrolysis Process

The pyrolysis process includes dissolution, pyrolysis reaction, and condensation. Electricity is used for the dissolution tank mixer and is modeled based on the 2020 US average grid.[46] Cooling water is used for the condensers. Heat for the dissolution tank and pyrolysis reaction is provided by combusting a portion of the pyrolysis gas, which generates CO_2 emissions. All the emissions from the pyrolysis process are energy allocated between the oil and gas products. Since the wax product is contained in a closed loop recycle inside the system boundary, it is not included in the energy allocation.

The pyrolysis gas product that is not burned for process heat is compressed and sold as a propane substitute. Electricity needed for the compressor is modeled based on the 2020 US average grid and allocated entirely to the sold gas product.[46]

Table 4.2 LCA inventory table for 1 kg of production of pyrolysis oil and pyrolysis gas for the base case. Each input was modeled using a SimaPro ecoprofile or literature data.

Products	Pyrolysis Oil	Pyrolysis Gas	Unit
Material Inputs			
Water, completely softened, at plant/US- US-EI U (for refrigeration)	97.69	107.38	kg
Water, completely softened, at plant/US- US-EI U (for condenser 1)	152.07	167.15	kg
Pyrolysis Gas[a]	0.12	0.13	kg
Process Energy Inputs			
Electricity, medium voltage, US[b] (For dissolution tank mixer)	3.07E-02	3.37E-02	kWh
Electricity, medium voltage, US[b] (For wax product tank mixer)	6.12E-03	6.72E-03	kWh
Electricity, medium voltage, US[b] (For liquid product tank mixer)	5.58E-03	6.13E-03	kWh
Electricity, medium voltage, US[b] (For feed and wax recycle pump)	4.29E-04	4.72E-04	kWh
Electricity, medium voltage, US[b] (For refrigeration)	1.41E-02	1.55E-02	kWh
Electricity, medium voltage, US[b] (For gas compressor)	0	7.41E-02	kWh
Sorting Process			
MRF collection/sorting[c]	1.07	1.18	kg of plastic
Secondary sorting[c]	2.15	2.36	kg of plastic
Disposal Credit			
Landfilling[d] or Incineration[e]	-1.07	-1.18	kg of plastic

[a]Pyrolysis gas has GHG emissions of 3.28 kg CO_2/kg gas

[b]Electricity has GHG emissions of 0.423 kg CO_2/kwh and a CED of 1.7 MJ/kWh[46]

[c]Sorting/Collection has GHG emissions of 0.10 kg CO_2/kg plastic and a CED of 1.52 MJ/kg plastic[33]

[d]Landfilling has GHG emissions of 0.022 kg CO_2/kg plastic and a CED of 0.31 MJ/kg plastic[47, 48]

[e]Incineration has GHG emissions of 1.42 kg CO_2/kg plastic and a CED of -21.90 MJ/kg plastic[47, 48]

4.2.4.5 Credits for Avoiding Landfill or Incineration

It is assumed that the "business-as-usual" usage for the #1-7 bale is to be treated as a waste and disposed of in either a landfill or by incineration for energy recovery. Thus, a credit is taken due to the avoided emissions of landfilling or incinerating the plastic in the mixed bale. The GHG emission factors for landfilling and incineration with energy recovery are from the EPA WARM model; 0.022 kg CO_2 eq/kg plastic and 1.42 kg CO_2 eq/kg plastic, respectively.[47, 48]

4.3 Results

4.3.1 Simulation results

The base case pyrolysis process modeled in Aspen Plus pyrolyzes 168,000 MT/yr of the 1:1 HDPE/PP and pyrolysis wax mixture (Figure 4.4). Pyrolysis yields are 50 wt.% wax, 22 wt.% oil, and 28 wt.% gas. The wax is recycled back to the dissolution tank to be used as the solvent at a 1:1 ratio with the feed HDPE and PP. A portion of the gas product (19%) is burned for internal process heat while the remaining 81% is sold as a product. Overall, the modeled pyrolysis process produces 37,000 MT/yr of oil and 38,000 MT/yr of gas to be sold. The model output composition of the three pyrolysis products, broken down by mass percentage of each carbon number, is presented in Figure 4.5. The major peaks for each of the three products are C1-C6 for gas, C5-C11 for oil, and C11-C30 for wax. The oil product is very similar in carbon number composition to naphtha (C5-C10)[4] and is considered as a naphtha alternative for this study.

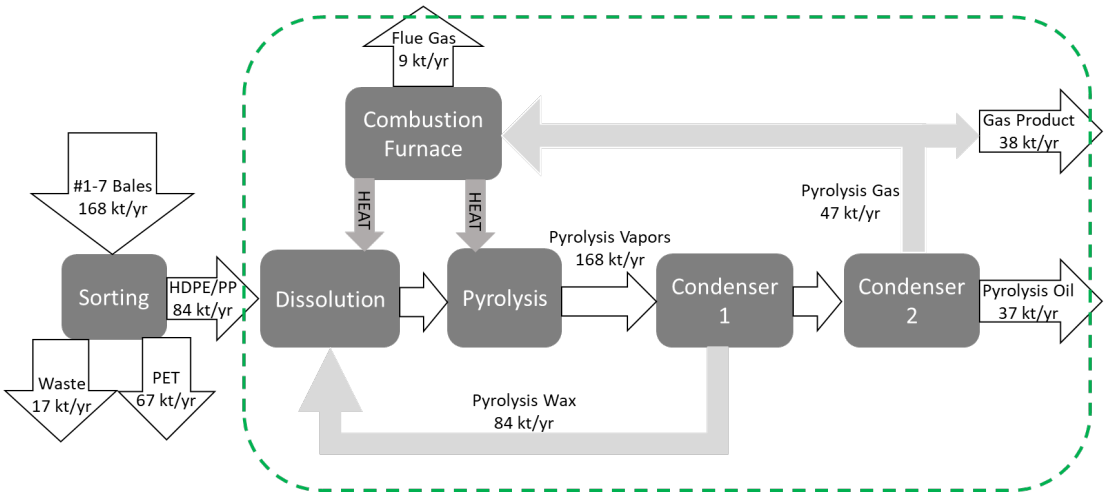

Figure 4.4 Hydrocarbon mass flows through the pyrolysis process. The dotted line contains what is modeled in Aspen Plus. The air required for the combustion furnace is not shown.

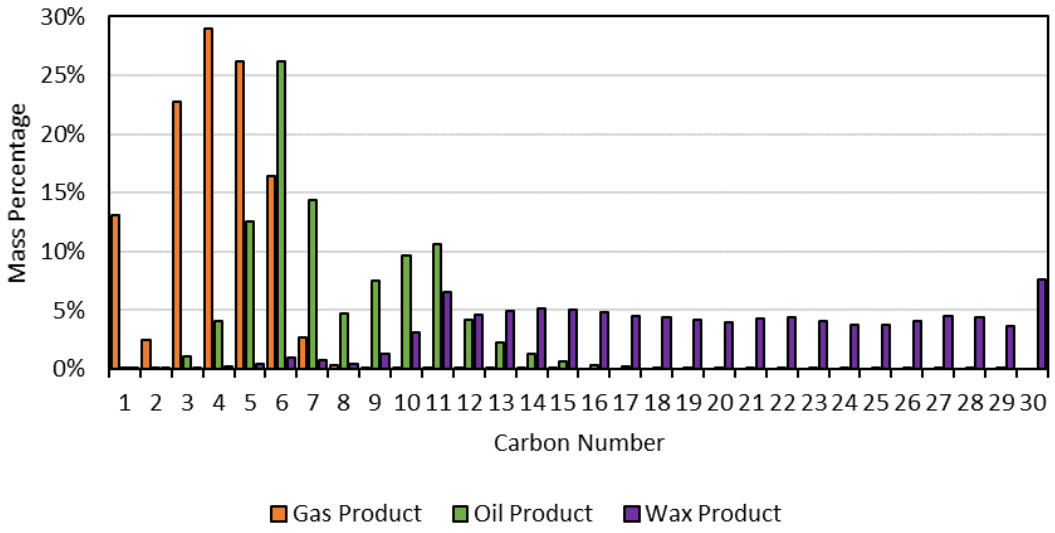

Figure 4.5 Mass contribution by carbon number to each of the three pyrolysis products

4.3.2 Techno-economic results

4.3.2.1 Minimum Selling Price (MSP) of Base Case

A 20-year discounted cash flow model was used to solve for the MSP of the pyrolysis oil for the base case (Figure 4.6) using a spreadsheet analysis. The pyrolysis oil's MSP was calculated to be \$592/MT, which is similar to but slightly higher than the 5-year average price for petroleum naphtha (\$561/MT).[49] The largest contributor to MSP is the feedstock cost (\$20.5 million/yr, \$553/MT), which is primarily due to the high price of the secondary sorting the mixed plastic bales. Other significant expenses include fixed capital investment (FCI) (\$39 million installed), waste disposal costs (\$5 million/yr), and fixed costs of production (FCOP) of \$3 million/yr. Utilities (\$0.5 million/yr) are very minor as heating is supplied through combustion of a portion of the pyrolysis gas product. Top installed capital costs include tanks (\$12 million), gas compressor (\$8 million), heaters (\$7 million), pyrolysis reactor (\$4 million), and mixers (\$3 million). The process capital costs per MT of PP/HDPE pyrolyzed on an annual basis are \$464/MT/yr. This is higher than comparable processes that consist only of a reactor and simple separation sequence.[5, 7, 8] For example, Fivga and Dimitritiou[7] calculated a capital cost of \$200/MT/yr of waste plastics pyrolyzed with a scale of 70,000 MT/yr. The increase in capital costs for our study is probably due to the recycle of the wax solvent, which effectively doubles both throughput and equipment size for the pyrolysis process and the first condenser. The pyrolysis gas not burned for process heating is sold at the 5-year average wholesale price of propane for \$0.96/gallon[50] (\$18.7 million/yr in gas sales). The results presented in Figure 4.6 are based upon industry specific assumptions which are uncertain at this level of technology readiness.[1] A sensitivity analysis and scenario analysis are presented in the following sections to analyze the pyrolysis oils MSP if the underlying parameters change.

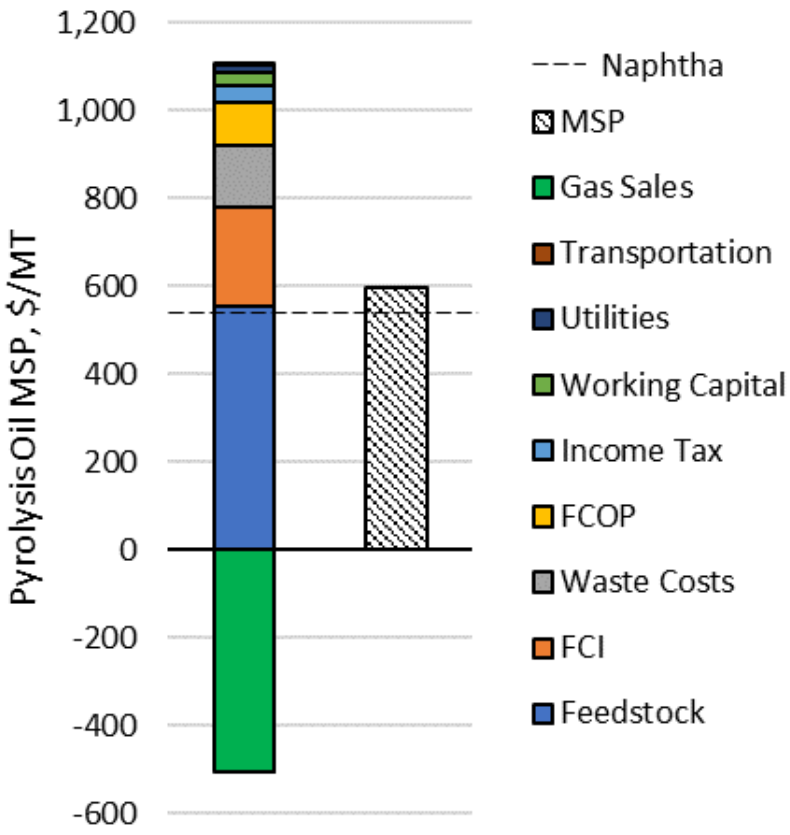

Figure 4.6 Breakdown of the various cost contributors to the MSP of pyrolysis oil in the base case. The dashed line represents the 5-year average price of naphtha ($561/MT).

4.3.2.2 Sensitivity Analysis

A one-at-the-time parameter sensitivity analysis was conducted to analyze the effect of the key economic inputs on the MSP of the pyrolysis oil (Figure 4.7). The pyrolysis oil MSP was calculated after independently varying each input to a lower value(-15%) and a higher value (+15%). This type of analysis exposes which variables have a dominant effect on the MSP and thus require a more thorough evaluation.[1] The tested parameters are pyrolysis gas selling price, transportation costs, utilities cost, general plant overhead and cost of labor (FCOP), waste disposal cost, capital investment, discount rate, and feedstock cost. Figure 4.7 shows that feedstock cost and pyrolysis gas selling price have a greater impact on the MSP than discount rate, FCI, and waste costs. The remaining variables have an impact lower than 1%.

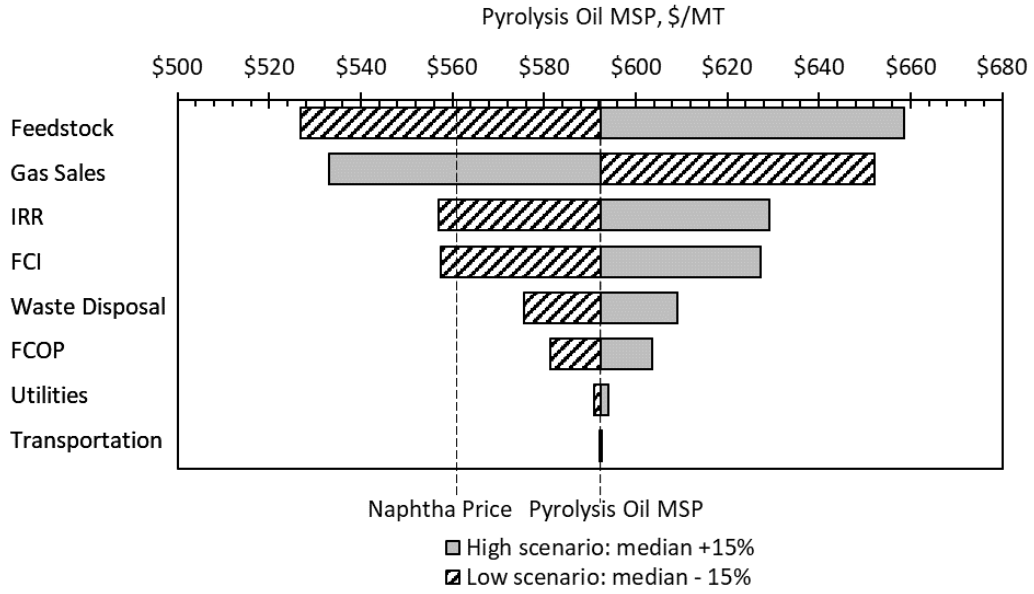

Figure 4.7 One-at-a-time sensitivity analysis of key input variables on the economic outcomes. Each input is independently varied ± 15%. Feedstock costs were varied from $17.4 to $23.6 million/yr, gas sales from $15.9 to $21.5 million/yr, IRR from 17% to 23%, FCI from $33.2 to $44.9 million installed, waste disposal from $4.4 to $5.9 million/yr, FCOP from $2.8 to $3.8 million/yr, utilities from $0.4 to $0.6 million/yr, and transportation from $24,000 to $33,000 per year. Both the naphtha 5-year average price ($561/MT) and the pyrolysis oil base case MSP ($592/MT) are marked on the graph using vertical dashed lines.

4.3.2.3 Scenario Analysis: Effect of Processing Capacity

In order to analyze the effect of processing capacity, the capital investment for smaller processing capacities (B) was scaled using equation 1[38], with an exponent for pyrolysis plants of 0.69[51] and the FCI for the base case 84 kt/yr plant.

$$FCI_B = FCI_{84} * \left(\frac{Capacity_B}{84\ kt}\right)^{0.69} \quad (1)$$

Since transportation is a very minor contributor to MSP (Figure 4.6), this analysis did not consider the effect of processing capacity on the distance to transport bales to the facilities of different size, and their ultimate effects on MSP. The inflection point for the relationship between processing capacity and MSP is observed to be around 20,000 MT/yr of HDPE and PP pyrolyzed (Figure 4.8). At capacities below 20,000 MT/yr the MSP increases rapidly to above $1,000/MT. At plant capacities above 20,000 MT/yr the benefit from economies of scale is more limited, with the oil's MSP only improving $130/MT (from $720/MT to $590/MT) when increasing from a scale of 20,000 MT/yr to 84,000 MT/yr. Being able to operate at a capacity at or above 20,000 MT/yr is crucial to the economic feasibility of the proposed process in the base case.

A recent study by RRS found that mixed plastic bales on average account for 3 wt.% of a MRF's products.[6] The average MRF size in the United States has a yearly throughput of around 100,000 MT/yr.[6, 52] Multiplying these numbers gives a 3,000 MT/yr production of mixed plastic bales from a single MRF, which is well below the critical capacity of 20,000 MT/yr for the pyrolysis process. This average number (MRF size) is lowered by older single stream MRFs that have lower processing capacity.[52] There are several larger MRFs with throughput capacities over 300,000 MT/yr that could supply close to 10,000 MT/yr of mixed plastic bales to the pyrolysis process. In order to operate at the capacities found most economical in Figure 4.8, the pyrolysis plant would need to be sourced from multiple MRFs. One reason for this is the low plastic recycling rate in the United States (8.5% collected for recycle in 2018).[32] There is a lot of unrealized plastic feedstock that is currently transported straight to landfills without even traveling through a MRF. As advanced automatic sorting technologies develop, they may make it easier for plastic that was previously sent to landfill to be now sorted out and recycled. An increase in recycle rates, whether it comes from improved sorting technologies or changes in policy and consumer behavior, would improve the ability to feed a pyrolysis plant at the required operating capacities. The global demand of naphtha is 378 million MT/yr,[5] which is approximately 10,000 times larger than the pyrolysis oil output from the proposed base case plant. This indicates that the production of pyrolysis oil from chemical recycling of waste plastic bales is not likely to cause disruptions in the global market for naphtha.

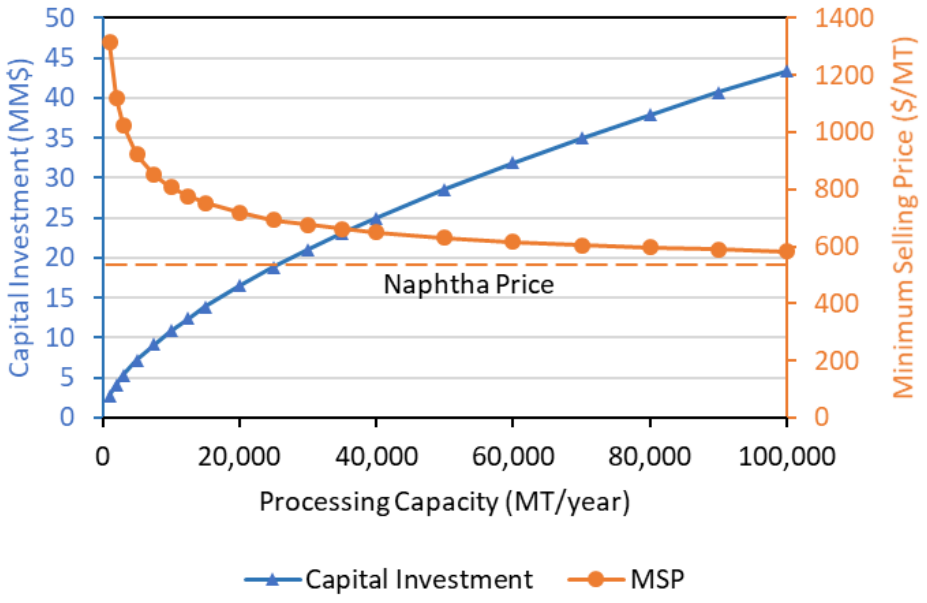

Figure 4.8 The effect of processing capacity on minimum selling price (orange) and capital investment (blue). The naphtha 5-year average price ($561/MT) is marked with a horizontal dashed line.

4.3.2.4 Scenario Analysis: Effect of Feedstock Cost

Figure 4.9 shows the sensitivity of the pyrolysis oil's MSP to two of the top cost contributors shown in Figure 4.7: processing capacity and feedstock cost. Of these two, the feedstock cost has a more significant effect on MSP. A 50% decrease in the assumed sorting cost would decrease the feedstock cost from \$240/MT to \$140/MT, resulting in a \$200/MT decrease in the MSP for the base case processing capacity. Figure 4.9 shows that the base case operating capacity needs a feedstock cost less than \$200/MT to be profitable compared to the average price of naphtha. A capacity of 10,000 MT/yr would need a feedstock cost less than \$100/MT to be profitable. An alternative feedstock option would be to purchase pure HDPE bales directly from the MRF. While these bales would not require a secondary sortation, they cost between \$400-800/MT[4], which would not be economical at any of the operating capacities included in this analysis.

4.3.2.5 Scenario Analysis: Gas Product Usage and Heat Integration

The second most sensitive variable after feedstock costs for the process' economics is the sale of pyrolysis gas (Figure 4.7). There are three possible uses for the pyrolysis gas: combusted for internal process heat, sold as a propane substitute, or converted to electricity which can then be sold. In the base case (Scenario A in Figure 4.10) the pyrolysis gas is combusted for process heat with the excess gas sold as a propane substitute. Five other scenarios for the pyrolysis gas were also analyzed using the discounted cash flow to calculate it's impact on the MSP. Generating electricity from the combustion of the pyrolysis gas (Scenario B in Figure 4.10) would increase the FCI by \$14 million installed and decrease annual gas sales by \$7 million/yr.

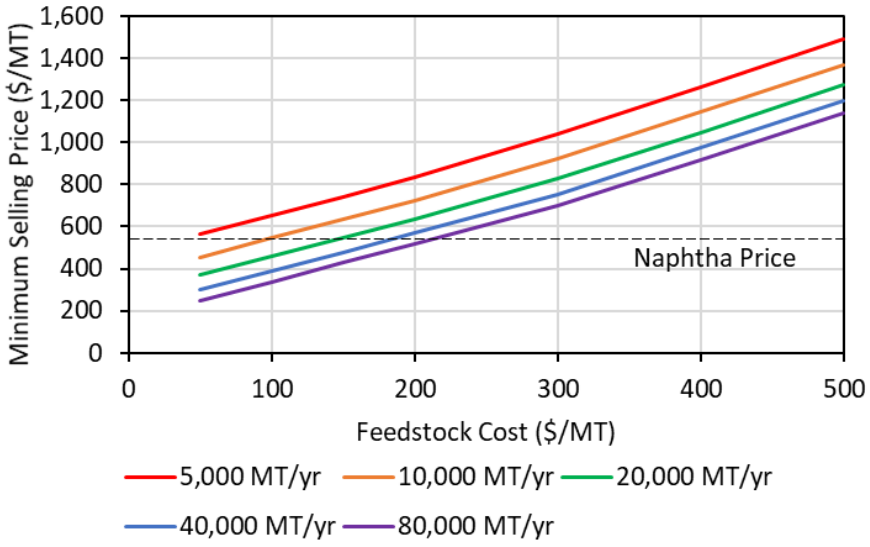

Figure 4.9 Effect of feedstock cost and processing capacity on the minimum selling price of the pyrolysis oil. The base case feedstock cost is \$244/MT and processing capacity is 80,000 MT/yr. The 5-year average price for naphtha (\$561/MT) is marked with a horizontal dashed line.

Using the pyrolysis to generate electricity is not cost effective, as it significantly increases the pyrolysis oil's MSP to $900/MT. There are two reasons for this. First, the capital equipment necessary for converting gas into electricity, priced at a construction cost of $1,078/kW[53] for a total of $24.7 million, is more expensive than to compress and store it ($10.5 million). Second, the assumed generation of electricity is only 40% from pyrolysis gas, creating just 30% the annual sales of pyrolysis gas ($5.7 million/yr for electricity vs $18.7 million/yr for pyrolysis gas). The electricity sales were priced at the 2021 average wholesale price of $58.08/MWh.[54]

Another option (Scenario C in Figure 4.10) would be to use purchased electricity to heat the pyrolysis process while selling all the pyrolysis gas. This change increases both the gas sales (+$4.7 million/yr) and utilities (+$7 million/yr) while not changing the capital costs. The cost of electric heating is higher than the increase in gas sales, leading to a $65/MT increase in the MSP when compared to the base case.

Scenarios D-F in Figure 4.10 repeat scenarios A-C but with heat integration added. Heat integration has a dual economic benefit to the pyrolysis process. First, it decreases utilities consumption for both heating and cooling. Since the heating in this process is provided internally through the combustion of pyrolysis gas, the second benefit is increased gas sales. Less pyrolysis gas is needed for the decreased heating demand which allows more gas to be sold. A pinch analysis identified one match where heat integration could be applied to the process. The pyrolysis vapors exiting the reactor are cooled from 600 to 135 °C in Condenser 1. There is a considerable amount of energy that could be recaptured here and used to heat the pyrolysis feed stream that is heated from 240 to 600 °C between the dissolution tank and pyrolysis reactor. Adding this additional heat exchanger reduces the heating and cooling demand by 50% while increasing the FCI by $5 million. This decreases the MSP by $22/MT down to $570/MT (Scenario D in Figure 4.10). Scenarios E (heat integration with gas product sold as electricity) and F (heat integration with electrical heating and gas product sold) each have a similar slight decrease in MSP when compared to scenario B and C, respectively. Overall, the most economical use of the pyrolysis gas is to have heat integration to reduce the amount needed for process heat and to sell the rest. Only scenario D shows similar MSP when compared to the 5-year average price of naphtha ($561/MT), thus showing the benefits of heat integration.

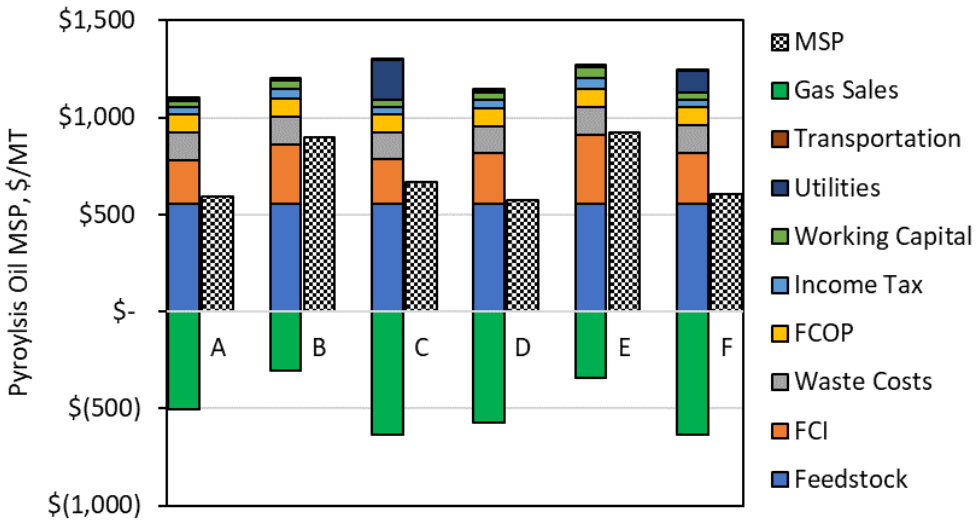

Figure 4.10 MSP price for gas product usage scenarios. The six different scenarios are (A) base case, (B) gas product sold as electricity, (C) electrical heating with gas product sold as propane, (D) heat integration with gas product sold as propane, (E) heat integration with gas product sold as electricity, (F) heat integration with electrical heating and gas product sold as propane.

4.3.2.6 Scenario Analysis: PET Recovery

A considerable amount (40%) of the feed #1-7 plastic bales consists of PET (Figure 4.1). In the base case, the PET is treated as a waste and disposed into a landfill. There may be substantial value within this waste PET stream, however, that could improve the pyrolysis process economics. A scenario analysis was conducted to understand the effect of recovering and selling the PET on the economic outcome. Since it is unknown what amount of the PET is recoverable and what the market value it would have, a range of values are presented in Figure 4.11. It was assumed that no additional sorting costs are required to recover the PET, since robotic sorting systems can be adjusted to sense and sort different resins on the same line. Figure 4.11 shows that selling the sorted PET significantly lowers the MSP of pyrolysis oil. Selling the PET has dual economic benefits. In addition to the increased revenue, waste disposal costs are decreased from avoiding paying the tipping fee to landfill the residue PET. It should be noted that MRF audits have found large variations for the PET content within the mixed plastic bales from different MRFs.[31] Figure 4.11 shows that even recovering low amounts of PET (0-40% recovered) has a large impact on the pyrolysis oil's MSP. Assuming a poor PET recovery of 20% and a low selling price of $25/MT PET still lowers the MSP from $592/MT to $567/MT when compared to the base case. This demonstrates the high potential of sorting the PET to make this process more profitable.

The recovered PET primarily consists of thermoform packaging (Figure 4.1). PET thermoform recycling a quickly developing industry, with 55,000 MT recycled in the US and Canada in 2019.[55] Currently the majority of recycled thermoforms end up in PET bottle bales processed by reclaimers. There is an upper limit to the amount of thermoforms

allowed by reclaimers in recycled PET resin though. Excess PET thermoform ends up in the mixed plastic bales where it is either landfilled or incinerated. Process technologies are currently being researched to overcome the technical challengers of recycling thermoform plastics.[56-58] The sorted thermoform PET in the mixed bale could serve as a cheap feedstock to enable future chemical recycling technologies. A recent TEA of PET chemical recycling[59] found that the operating costs are dominated by high feedstock cost of PET flakes sourced from bottle recyclers.[60] They assumed $660/MT in that study, which is substantially larger than any of the selling prices presented in Figure 4.11. A sensitivity analysis performed on the PET chemical recycling process found that lowering the feedstock cost from $660/MT to $200/MT would decrease the MSP of terephthalic acid monomer from $1.93/kg to $1.20/kg.[59] Thus, recovering the PET during the secondary sort could economically benefit both the proposed pyrolysis process and possible future PET chemical recycling technologies.

4.3.3 Life Cycle Assessment (LCA) Results

Four different scenarios were analyzed on the environmental burden of the pyrolysis products (Table 4.3). The differences between the scenarios all deal with assumptions about the feedstock. The first variable studied was the avoided disposal of the plastic feedstock. It was assumed that the plastic feedstock alternative destination if it wasn't sold to this pyrolysis plant was a landfill or incineration facility. The emission factors for landfilling and incineration are significantly different, with landfilling plastic having a GWP of 0.022 kg CO_2 eq/kg plastic while incinerating plastic has 1.42 kg CO_2 eq/kg plastic.[47, 48]

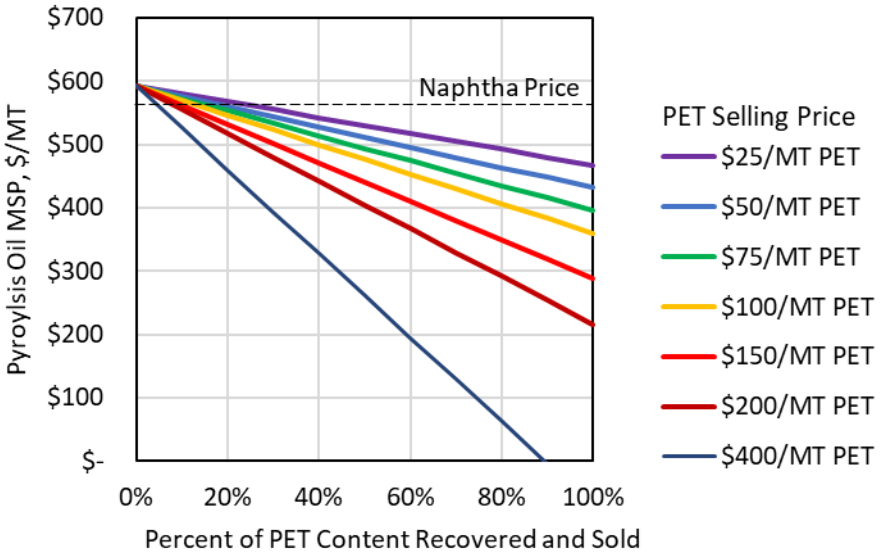

Figure 4.11 Effect of recovering and selling the PET on the base case pyrolysis oil MSP. Both the PET selling price (legend) and the amount of PET recovered (x-axis) are analyzed. The 5-year average naphtha price ($561/MT) is marked with a horizontal dashed line.

Table 4.3 Assumptions made for the four LCA scenarios. Each scenario is modeled with and without heat integration.

Scenario	Avoided Destination for Feedstock	PET Recovered
1	Landfill	0%
2	Incineration	0%
3	Landfill	100%
4	Incineration	100%

The second variable studied was the PET recovery. It is not clear whether the PET in the #1-7 bale can be recovered in a state that they'd have a market value. Two options were analyzed for this variable: recovering all the PET and recovering no PET. In addition, each scenario was analyzed with and without heat integration of the pyrolysis process. The complete scenarios analyzed in this section are shown in Table 4.3.

4.3.3.1 Greenhouse Gas (GHG) Emissions

The GHG emissions from the pyrolysis process are shown in Figure 4.12 for the four scenarios presented in Table 4.3. The results are presented for each of the three products from the process (pyrolysis oil, pyrolysis gas, and PET) and for each product, values are presented for the main life cycle stages. The assumption of which feedstock destination was avoided has a significant effect on the final LCA results since incinerating plastic has an emissions factor about 20 times greater than landfilling. In scenario 2 and 4, the credit for avoiding incineration overwhelms the emissions from the pyrolysis process, which are also significant. In other studies, similar to ours, avoiding incineration generates significant emissions credits in waste plastics pyrolysis LCAs.[61, 62] The majority of the pyrolysis emissions come from burning the pyrolysis gas for internal process heat. They are high due to the recycle of the plastic wax, which lowers the overall product yield per pass through the pyrolysis reactor. This is a disadvantage on the LCA results compared to single pass reactors, however heat integration is a strategy to lower the pyrolysis emissions by recycling most of the heat captured in the first condenser and recycle it back to preheat the feed into the reactor. The GHG emissions for this plastic pyrolysis process are significantly lower, however, than for incineration of plastics. Recovering the PET as a product was found to have a minor effect on the GHG emissions, slightly improving the emissions for pyrolysis oil and pyrolysis gas products. The benefits of the PET product are two-fold. First, the additional product helps share the environmental burden of the feedstock and sorting process. Second, it reduces the amount of waste needed to be disposed of. For the scenarios without heat integration, GHG emissions are lower for the pyrolysis oil and gas than their fossil equivalents of naphtha (0.35-0.69 kg CO_2 eq/kg) and propane (0.64 kg CO_2 eq/kg) when assuming that incineration is avoided when mixed bales are fed to the pyrolysis process, and higher when assuming landfilling. Adding heat integration causes the pyrolysis oil to have GHG emissions equivalent or better than the low end of the industry range for fossil naphtha. A similar effect is seen for pyrolysis gas when compared to fossil propane. The heat integrated case is a fairer comparison to the fossil products as industrial petrol-chemical facilities always have some level of heat integration implemented.

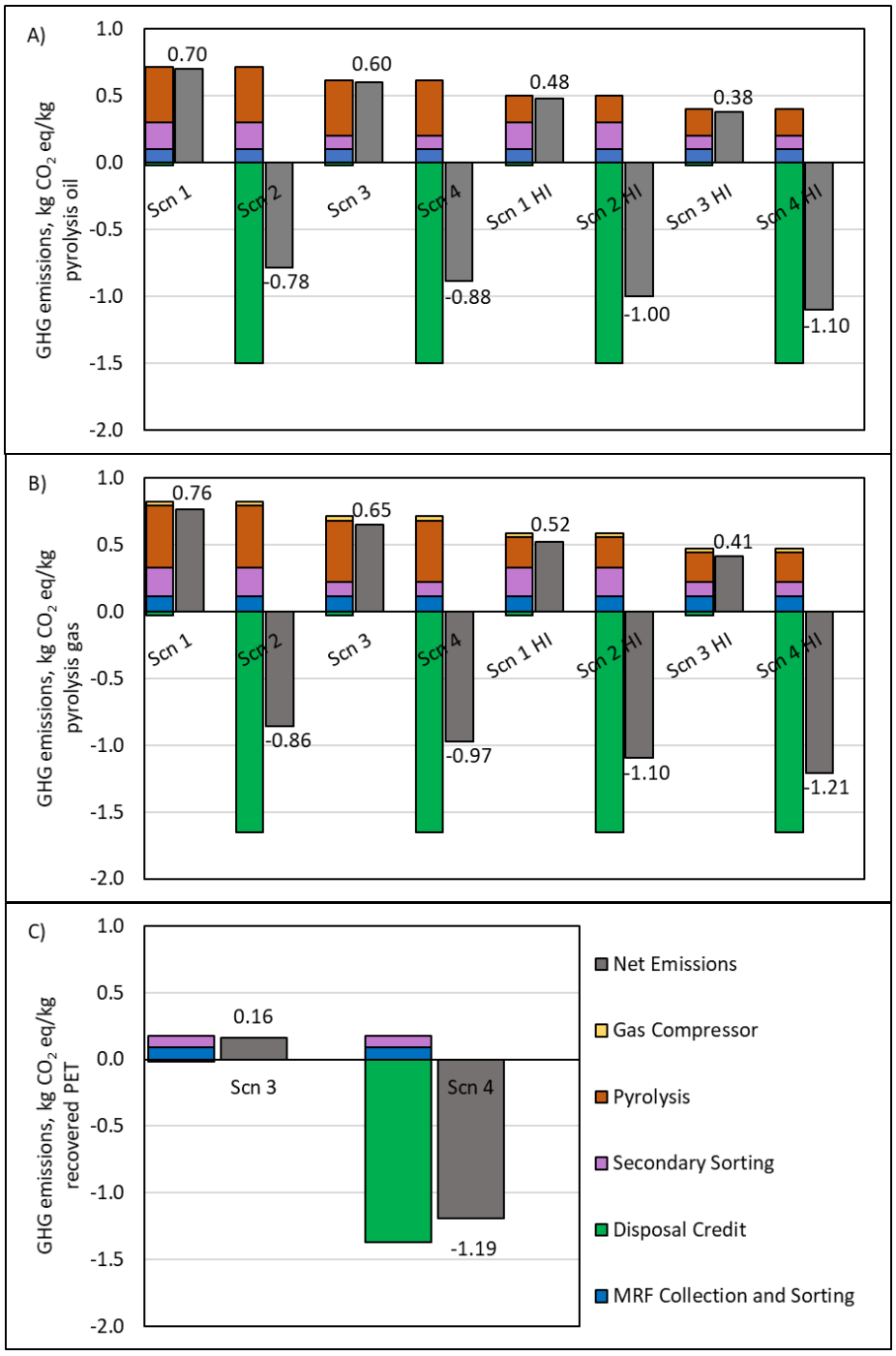

Figure 4.12 GHG emissions for the 3 products from the modeled process: pyrolysis oil (A), pyrolysis gas (B), and recovered PET (C). Each of the four scenarios are shown with and without heat integration for pyrolysis oil and gas. Heat integration does not have an effect on the GHG emissions of recovered PET. "Disposal Credit" represents either landfilling or incineration with energy recovery in the separate scenarios.

4.3.3.2 Cumulative Energy Demand (CED)

The cumulative energy demand of the process, shown in Figure 4.13, follows the same overall trends as the GHG emissions. One difference is the impact of the disposal credit taken for avoiding incineration. Incinerating plastic produces an energy credit due to the electricity produced. This gives incineration (-21.8 MJ/kg plastic) a much lower energy consumption than landfilling (0.31 MJ/kg plastic).

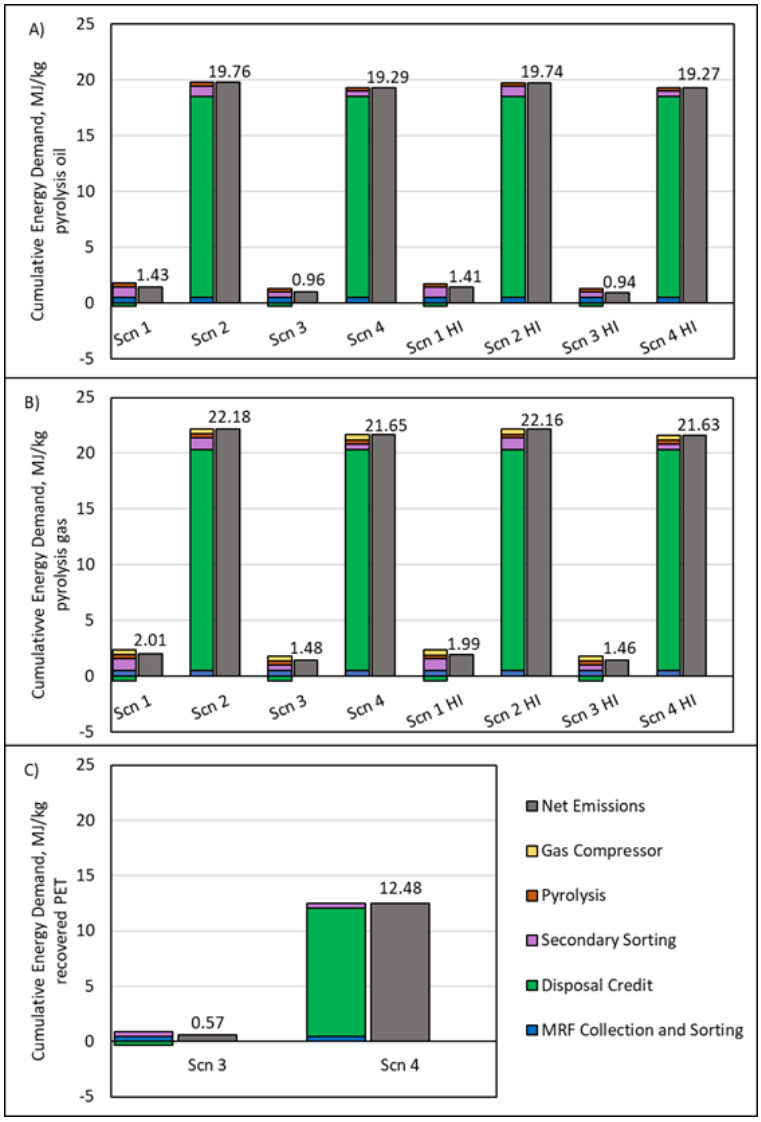

Figure 4.13 Cumulative energy demand for the 3 products from the modeled process: pyrolysis oil (A), pyrolysis gas (B), and recovered PET (C). Each of the four scenarios are shown with and without heat integration for pyrolysis oil and gas. Heat integration does not have an effect on the GHG emissions of recovered PET. "Disposal Credit" represents either landfilling or incineration with energy recovery in the separate scenarios.

Neither the sorting nor pyrolysis process have high energy demand. This is due to the recycling and combustion of the pyrolysis gas, which limits the amount of external energy needed for the process. Overall, the cumulative energy demand is much lower for the pyrolysis oil and gas than their fossil equivalents of naphtha (50.3 MJ/kg) and propane (55.9 MJ/kg).

4.3.3.3 Eco-efficiency: Combining TEA and LCA Results

The majority of the emissions for the pyrolysis process come from combusting the pyrolysis gas to produce process heat. Implementing heat integration in the process decreases the amount of pyrolysis gas needed for combustion by 50%. This has a positive effect on both the process economics and the pyrolysis oil GHG emissions (Figure 4.14). Switching from pyrolysis gas heating to electrical heating has a negative effect on both the economics and GHG emissions. This is because the current US electrical grid has slightly more emissions than combustion of pyrolysis gas in supplying the required heating duty. Looking toward the future, a continued increase in renewable energy's contribution to the electrical grid would lower GHG emissions. A recent study by Gracida-Alvarez, et al.[10] found that using cleaner energy sources such as hydropower, nuclear, solar, or wind causes a 70-94% reduction in GHG emissions when compared to the current electric grid, dependent on product and energy source. In the best case, where the electrical grid is completely renewable, the emissions from pyrolysis heating could be close to zero.

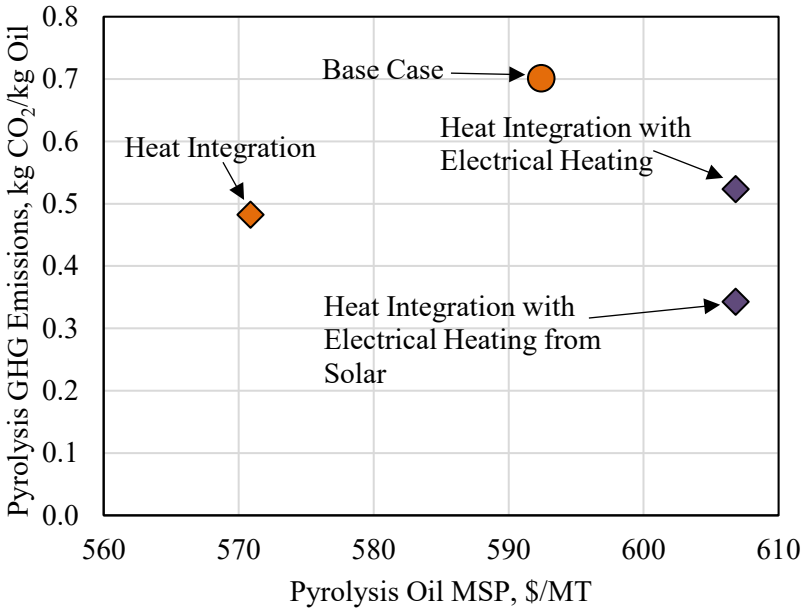

Figure 4.14 GHG emissions vs MSP for pyrolysis oil scenario 1 (landfilling; no PET recovered and sold) for different heating scenarios. Both the base case and heat integration use pyrolysis gas for heating the dissolution tank and pyrolysis reactor. The other two cases use electrical heating, with one using the current US average electrical grid and the other using a renewable energy source such as solar to generate the electricity.

Assuming that all the pyrolysis heating is provided by solar power reduces the GHG emissions of the pyrolysis process (excluding sorting) to 0.07 kg CO_2 eq per kg pyrolysis oil. Using electricity for heat is still worse economically than using pyrolysis gas for heat, perhaps creating a future trade-off if the electrical grid continues to become greener. Excluding PET sales, the heat integrated case compares favorably both economically and environmentally to fossil naphtha, with a MSP similar to naphtha's market value ($561/MT) and GHG emissions on the low end on the range for fossil naphtha (0.35-0.65 kg CO_2 eq/kg naphtha).

4.4 Conclusions and Future Work

The base-case scenario presented herein processed 84,000 MT/yr of waste HDPE/PP into wax, oil, and gas products using a pyrolysis process with a liquid feed approach. The HDPE/PP is sourced from a secondary sort of #1-7 mixed plastic bales from a MRF. The wax product is recycled as the dissolution solvent for the waste plastic, creating a liquid feed into the pyrolysis reactor. The MSP to produce the pyrolysis oil is $592/MT in the sub-optimum base case, which is similar to the 5-year average selling price of naphtha ($561/MT), a commodity that it is expected to displace in the market. This result is most sensitive to feedstock costs, pyrolysis gas sales, operating capacity, and waste costs. It was found that the proposed plant is most profitable if the feedstock costs drop below $200/MT and/or the PET is recovered from the mixed bales and sold into the secondary materials market for at least $25/MT. For the LCA, the pyrolysis gas and oil products have similar GHG emissions to their fossil-equivalent products for the process base case. When a credit for avoiding incineration of the mixed plastic bale is taken into consideration, the pyrolysis products have negative GHG emissions. Implementing heat integration and decarbonizing the electric grid also have a positive impact on the GHG emissions, although heat integration did not benefit the MSP very much. Future work includes additional TEA and LCA research into the secondary sort process. It was found that recovering PET in addition to the HDPE/PP during the secondary sort could significantly improve the economic results of this process while also potentially enabling PET chemical recycling technologies. Additional scenarios could analyze variations in #1-7 bales composition, pyrolysis yield, and co-locating the plant at a petrol-chemical facility. In this work the #1-7 bales composition was assumed to be 40% PET, 36% PP, and 15% HDPE. Literature data indicates that there are large variations in the mixed plastic composition between different MRFs.[31] Lower PP/HDPE content in the feedstock would increase sorting and waste costs while decreasing throughput in the pyrolysis reactor. More research is needed to understand what levels of variation occur between MRFs and whether there are seasonal variations in plastic composition within individual MRFs. Variations in PP/HDPE composition along with possible contamination that the sorting process failed to remove could also affect pyrolysis yield. In this study it was assumed that the sorting process perfectly removed all contamination. This assumption is probably an idealization and more research is needed to understand just how contamination would affect the pyrolysis yields of this process. Co-locating the pyrolysis process at a petrol-chemical facility would eliminate the need for oil and gas product transportation. The oil and gas product would both be sold to the petrol-chemical facility as a feedstock for higher-value chemical/plastic production within the petrol-chemical facility. This would change the value of the gas product, which is currently

assumed to be sold as a propane substitute. In summary, pyrolysis oil for the heat integrated case compares favorably both economically and environmentally to fossil naphtha. Future improvements to the process, such as recovering PET and co-locating the plant next to a petrol-chemical facility, may further improve the economics and environmental burdens of pyrolysis oil.

4.5 Acknowledgments

We thank Lindsey Walker from Emmet County Recycling for providing information on the composition of #1-7 mixed plastic bales.

Funding: This work was supported by the Defense Advanced Research Projects Agency ReSource program cooperative agreement HR00112020033. The views, opinions and/or findings expressed are those of the author and should not be interpreted as representing the official views or policies of the Department of Defense or the U.S. Government.

4.6 References

1. Larrain, M.; Van Passel, S.; Thomassen, G.; Kresovic, U.; Alderweireldt, N.; Moerman, E.; Billen, P., Economic performance of pyrolysis of mixed plastic waste: Open-loop versus closed-loop recycling. *Journal of Cleaner Production* **2020,** *270*, 122442. DOI: 10.1016/j.jclepro.2020.122442

2. National Overview: Facts and Figures on Materials, Wastes and Recycling. https://www.epa.gov/facts-and-figures-about-materials-waste-and-recycling/national-overview-facts-and-figures-materials#recycling (accessed June 2022).

3. Ignatyev, I. A.; Thielemans, W.; Vander Beke, B., Recycling of polymers: a review. *ChemSusChem* **2014,** *7* (6), 1579-1593. DOI: 10.1002/cssc.201300898

4. Li, H.; Aguirre-Villegas, H. A.; Allen, R. D.; Bai, X.; Benson, C. H.; Beckham, G. T.; Bradshaw, S. L.; Brown, J. L.; Brown, R. C.; Castillo, M. A. S., Expanding Plastics Recycling Technologies: Chemical Aspects, Technology Status and Challenges. *ChemRxiv* **2022**. DOI: 10.26434/chemrxiv-2022-9wqz0-v2

5. Yadav, G.; Singh, A.; Nicholson, S. R.; Beckham, G. T. *Techno-Economic Analysis and Life Cycle Assessment for Pyrolysis of Mixed Waste Plastics*; National Renewable Energy Lab.(NREL), Golden, CO (United States): 2022.

6. Dimino, R.; Timpane, M. *Economic Impact of Beverage Container Deposits on Municipal Recycling Processing Costs*; National Waste & Recycling Association, 2022.

7. Fivga, A.; Dimitriou, I., Pyrolysis of plastic waste for production of heavy fuel substitute: A techno-economic assessment. *Energy* **2018,** *149*, 865-874. DOI: 10.1016/j.energy.2018.02.094

8. Sahu, J.; Mahalik, K.; Nam, H. K.; Ling, T. Y.; Woon, T. S.; bin Abdul Rahman, M. S.; Mohanty, Y.; Jayakumar, N.; Jamuar, S., Feasibility study for catalytic cracking of waste plastic to produce fuel oil with reference to M alaysia and simulation using ASPEN Plus. *Environmental Progress & Sustainable Energy* **2014,** *33* (1), 298-307. DOI: 10.1002/ep.11748

9. Gracida-Alvarez, U. R.; Winjobi, O.; Sacramento-Rivero, J. C.; Shonnard, D. R., System analyses of high-value chemicals and fuels from a waste high-density polyethylene refinery. Part 1: Conceptual design and techno-economic assessment. *ACS Sustainable Chemistry & Engineering* **2019,** *7* (22), 18254-18266. DOI: 10.1021/acssuschemeng.9b04763

10. Gracida-Alvarez, U. R.; Winjobi, O.; Sacramento-Rivero, J. C.; Shonnard, D. R., System Analyses of High-Value Chemicals and Fuels from a Waste High-Density Polyethylene Refinery. Part 2: Carbon Footprint Analysis and Regional Electricity Effects. *ACS Sustainable Chemistry & Engineering* **2019,** *7* (22), 18267-18278. DOI: 10.1021/acssuschemeng.9b04764

11. Perugini, F.; Mastellone, M. L.; Arena, U., A life cycle assessment of mechanical and feedstock recycling options for management of plastic packaging wastes. *Environmental Progress* **2005,** *24* (2), 137-154. DOI: 10.1002/ep.10078

12. Alston, S. M.; Arnold, J. C., Environmental impact of pyrolysis of mixed WEEE plastics part 2: life cycle assessment. *Environmental science & technology* **2011,** *45* (21), 9386-9392. DOI: 10.1021/es2016654

13. Al-Salem, S.; Evangelisti, S.; Lettieri, P., Life cycle assessment of alternative technologies for municipal solid waste and plastic solid waste management in the Greater London area. *Chemical Engineering Journal* **2014,** *244*, 391-402. DOI: 10.1016/j.cej.2014.01.066

14. Gear, M.; Sadhukhan, J.; Thorpe, R.; Clift, R.; Seville, J.; Keast, M., A life cycle assessment data analysis toolkit for the design of novel processes–A case study for a thermal cracking process for mixed plastic waste. *Journal of cleaner production* **2018,** *180*, 735-747. DOI: 10.1016/j.jclepro.2018.01.015

15. McKay, G., Dioxin characterisation, formation and minimisation during municipal solid waste (MSW) incineration. *Chemical engineering journal* **2002,** *86* (3), 343-368. DOI: 10.1016/S1385-8947(01)00228-5

16. Li, Q.; Meng, A.; Jia, J.; Zhang, Y., Investigation of heavy metal partitioning influenced by flue gas moisture and chlorine content during waste incineration. *Journal of Environmental Sciences* **2010,** *22* (5), 760-768. DOI: 10.1016/s1001-0742(09)60174-1

17. Lubongo, C.; Congdon, T.; McWhinnie, J.; Alexandridis, P., Economic feasibility of plastic waste conversion to fuel using pyrolysis. *Sustainable Chemistry and Pharmacy* **2022,** *27*, 100683. DOI: 10.1016/j.scp.2022.100683

18. Westerhout, R.; Van Koningsbruggen, M.; Van Der Ham, A. G.; Kuipers, J.; Van Swaaij, W. P. M., Techno-economic evaluation of high temperature pyrolysis processes for mixed plastic waste. *Chemical Engineering Research and Design* **1998,** *76* (3), 427-439. DOI: 10.1205/026387698524857

19. Santillán, A. V.; Sanchez, J. F.; Pimentel, M. P.; Montoya, A. C., Olefins and ethanol from polyolefins: analysis of potential chemical recycling of poly (ethylene) Mexican case. *International Journal of Chemical Reactor Engineering* **2016,** *14* (6), 1289-1300. DOI: 10.1515/ijcre-2015-0217

20. Bora, R. R.; Wang, R.; You, F., Waste polypropylene plastic recycling toward climate change mitigation and circular economy: energy, environmental, and technoeconomic perspectives. *ACS Sustainable Chemistry & Engineering* **2020,** *8* (43), 16350-16363. DOI: 10.1021/acssuschemeng.0c06311

21. Panda, A. K.; Singh, R. K.; Mishra, D., Thermolysis of waste plastics to liquid fuel: A suitable method for plastic waste management and manufacture of value added products—A world prospective. *Renewable and Sustainable Energy Reviews* **2010,** *14* (1), 233-248. DOI: 10.1016/j.rser.2009.07.005

22. Jiang, G.; Wang, J.; Al-Salem, S. M.; Leeke, G. A., Molten solar salt pyrolysis of mixed plastic waste: process simulation and technoeconomic evaluation. *Energy & Fuels* **2020,** *34* (6), 7397-7409. DOI: 10.1021/acs.energyfuels.0c01052

23. Alliance, O. R. *Plastics-to-fuel project developer's guide*; Hong Kong: 2015.

24. Mannion-Gibson, A., Quantafuel expands into the UK to help solve plastic waste problem. Quantafuel: 2021.

25. Jiang, H.; Celeste, E.; Stephanis, B. How waste solutions company Brightmark is converting plastic waste into fuel. https://www.businessinsider.com/brightmark-plastic-waste-fuel-pollution-2020-10 (accessed June 27 2022).

26. Lazarevic, D.; Aoustin, E.; Buclet, N.; Brandt, N., Plastic waste management in the context of a European recycling society: Comparing results and uncertainties in a life cycle perspective. *Resources, Conservation and Recycling* **2010,** *55* (2), 246-259. DOI: 10.1016/j.resconrec.2010.09.014

27. Rigamonti, L.; Grosso, M.; Møller, J.; Sanchez, V. M.; Magnani, S.; Christensen, T. H., Environmental evaluation of plastic waste management scenarios. *Resources, Conservation and Recycling* **2014,** *85*, 42-53. DOI: 10.1016/j.resconrec.2013.12.012

28. Jambeck, J. R.; Geyer, R.; Wilcox, C.; Siegler, T. R.; Perryman, M.; Andrady, A.; Narayan, R.; Law, K. L., Plastic waste inputs from land into the ocean. *Science* **2015,** *347* (6223), 768-771. DOI: 10.1126/science.1260352

29. Brandon, J. A.; Jones, W.; Ohman, M. D., Multidecadal increase in plastic particles in coastal ocean sediments. *Science advances* **2019,** *5* (9). DOI: 10.1126/sciadv.aax0587

30. Nicholson, S. R.; Rorrer, J. E.; Singh, A.; Konev, M. O.; Rorrer, N. A.; Carpenter, A. C.; Jacobsen, A. J.; Román-Leshkov, Y.; Beckham, G. T., The critical role of process analysis in chemical recycling and upcycling of waste plastics. *Annual Review of Chemical and Biomolecular Engineering* **2022,** *13*, 301-324. DOI: 10.1146/annurev-chembioeng-100521-085846

31. Kurzynowski, B.; Dimino, R.; Goodal, C. *#3-7 Bale Audit Results*; RRS: 2021.

32. Chaudhari, U. S.; Lin, Y.; Thompson, V. S.; Handler, R. M.; Pearce, J. M.; Caneba, G.; Muhuri, P.; Watkins, D.; Shonnard, D. R., Systems analysis approach to polyethylene terephthalate and olefin plastics supply chains in the circular economy: A review of data sets and models. *ACS Sustainable Chemistry & Engineering* **2021,** *9* (22), 7403-7421. DOI: 10.1021/acssuschemeng.0c08622

33. Associates, F. *Life Cycle Impacts for Postconsumer Recycled Resins: PET, HDPE, and PP*; The Association of Plastic Recyclers: 2018.

34. Wu, J.; Prausnitz, J. M., Phase equilibria for systems containing hydrocarbons, water, and salt: An extended Peng− Robinson equation of state. *Industrial & Engineering Chemistry Research* **1998,** *37* (5), 1634-1643. DOI: 10.1021/ie9706370

35. He, M.; Xiao, B.; Hu, Z.; Liu, S.; Guo, X.; Luo, S., Syngas production from catalytic gasification of waste polyethylene: Influence of temperature on gas yield and composition. *International Journal of Hydrogen Energy* **2009,** *34* (3), 1342-1348. DOI: 10.1016/j.ijhydene.2008.12.023

36. Milbrandt, A.; Coney, K.; Badgett, A.; Beckham, G. T., Quantification and evaluation of plastic waste in the United States. *Resources, Conservation and Recycling* **2022,** *183*. DOI: 10.1016/j.resconrec.2022.106363

37. Zolghadr, A.; Foroozandehfar, A.; Kulas, D. G.; Shonnard, D., Study of the Viscosity and Thermal Characteristics of Polyolefins/Solvent Mixtures: Applications for Plastic Pyrolysis. *ACS omega* **2021,** *6* (48), 32832-32840. DOI: 10.1021/acsomega.1c04809

38. Towler, G.; Sinnott, R. K., *Chemical engineering design: principles, practice and economics of plant and process design*. Elsevier: 2012.

39. Kulas, D.; Zolghadr, A.; Shonnard, D., Liquid-Fed Waste Plastic Pyrolysis Pilot Plant: Effect of Reactor Volume on Product Yields. *Journal of Analytical and Applied Pyrolysis* **2022,** *166*, 105601. DOI: 10.1016/j.jaap.2022.105601

40. Kulas, D. G.; Zolghadr, A.; Shonnard, D., Micropyrolysis of Polyethylene and Polypropylene Prior to Bioconversion: The Effect of Reactor Temperature and Vapor Residence Time on Product Distribution. *ACS Sustainable Chemistry & Engineering* **2021,** *9* (43), 14443-14450. DOI: 10.1021/acssuschemeng.1c04705

41. Swanson, R. M.; Platon, A.; Satrio, J.; Brown, R.; Hsu, D. D. *Techno-economic analysis of biofuels production based on gasification*; National Renewable Energy Lab.(NREL), Golden, CO (United States): 2010.

42. Average Prices of Electricity to Ultimate Customers. https://www.eia.gov/totalenergy/data/monthly/pdf/sec9_11.pdf.

43. Estimator-User's, A. C. C., Guide (V8. 0). Aspen Technology, Inc.: Burlington, MA: 2012.

44. Baptista, A. I.; Perovich, A. *US municipal solid waste incinerators: An industry in decline*; The Tishman Environment and Design Center at The New School: 2019.

45. Current Freight Rates. https://www.tcicapital.com/tci-insights/current-freight-trends/ (accessed April 2021).

46. Electric Power Annual 2020. https://www.eia.gov/electricity/annual/ (accessed June 2022).

47. Documentation for Greenhouse Gas Emission and Energy Factors Used in the Waste Reduction Model (WARM), Containers, Packaging, and Non-Durable Good Materials Chapters. EPA, U. S., Ed. 2020.

48. Documentation for Greenhouse Gas Emission and Energy Factors Used in the Waste Reduction Model (WARM), Management Practices Chapters. EPA, U. S., Ed. 2020.

49. Naphtha. https://tradingeconomics.com/commodity/naphtha (accessed June 27 2022).

50. Weekly Heating Oil and Propane Prices (October - March). https://www.eia.gov/dnav/pet/pet_pri_wfr_a_EPLLPA_PWR_dpgal_m.htm (accessed June 2022).

51. Kuppens, T.; Van Dael, M.; Vanreppelen, K.; Thewys, T.; Yperman, J.; Carleer, R.; Schreurs, S.; Van Passel, S., Techno-economic assessment of fast pyrolysis for the valorization of short rotation coppice cultivated for phytoextraction. *Journal of Cleaner Production* **2015,** *88*, 336-344. DOI: 10.1016/j.jclepro.2014.07.023

52. Powell, J. Sortation by the Numbers. https://resource-recycling.com/recycling/2018/10/01/sortation-by-the-numbers/#:~:text=MRF%20plants%20vary%20widely%20in%20size&text=First%2C%20the%20majority%20of%20MRFs,being%20over%20200%2C000%20square%20feet. (accessed May 2022).

53. Construction cost data for electric generators installed in 2019. https://www.eia.gov/electricity/generatorcosts/ (accessed May 2022).

54. Wholesale Electricity and Natural Gas Market Data. https://www.eia.gov/electricity/wholesale/ (accessed June 16 2022).

55. NAPCOR *2020 PET Thermoform Recycling: A Progress Report*; 2021.

56. Zenda, K.; Funazukuri, T., Depolymerization of poly (ethylene terephthalate) in dilute aqueous ammonia solution under hydrothermal conditions. *Journal of Chemical Technology & Biotechnology: International Research in Process, Environmental & Clean Technology* **2008,** *83* (10), 1381-1386. DOI: 10.1002/jctb.1951

57. Lange, J.-P., Managing plastic waste─ sorting, recycling, disposal, and product redesign. *ACS Sustainable Chemistry & Engineering* **2021,** *9* (47), 15722-15738. DOI: 10.1021/acssuschemeng.1c05013

58. Raheem, A. B.; Noor, Z. Z.; Hassan, A.; Abd Hamid, M. K.; Samsudin, S. A.; Sabeen, A. H., Current developments in chemical recycling of post-consumer polyethylene terephthalate wastes for new materials production: A review. *Journal of Cleaner Production* **2019,** *225*, 1052-1064. DOI: 10.1016/j.jclepro.2019.04.019

59. Singh, A.; Rorrer, N. A.; Nicholson, S. R.; Erickson, E.; DesVeaux, J. S.; Avelino, A. F.; Lamers, P.; Bhatt, A.; Zhang, Y.; Avery, G., Techno-economic, life-cycle, and socioeconomic impact analysis of enzymatic recycling of poly (ethylene terephthalate). *Joule* **2021,** *5* (9), 2479-2503. DOI: 10.1016/j.joule.2021.06.015

60. *Cleaning the rPET Stream: How we scale post-consumer recycled PET in the US*; Closed Loop Partners: 2017.

61. Krüger, C.; Russ, M.; Gonzalez, M.; Horlacher, M. *Evaluation of pyrolysis with LCA–3 case studies*; BASF: 2020.

62. Jeswani, H.; Krüger, C.; Russ, M.; Horlacher, M.; Antony, F.; Hann, S.; Azapagic, A., Life cycle environmental impacts of chemical recycling via pyrolysis of mixed plastic waste in comparison with mechanical recycling and energy recovery. *Science of the Total Environment* **2021,** *769*. DOI: 10.1016/j.scitotenv.2020.144483

5 Conclusions and Future Work

This dissertation investigated the technical, economic, and environmental feasibility of using a novel liquid-fed fast pyrolysis process to recycle waste polyolefin plastic from a circular economy perspective. The research was split into three scales: micro, pilot, and system.

Chapter 2 presents the work at the microscale level where the utility of conventional micropyrolysis was extended through the addition of a tubular vapor residence time reactor downstream of the pyroprobe in order to analyze the fundamental reaction kinetics. A key outcome of this work was a scalable lumped kinetic model that predicts product distribution as a function of vapor residence time (1.4 – 5.6 s) and temperature (550-600 °C) for polyolefin plastics. At low temperatures (550 °C) and short VRT (1.4 s), the pyrolysis products included a wide range of liquid (C5-C20 hydrocarbons) and wax products (C21-C30 hydrocarbons) were produced. Increasing temperature and VRT produced higher proportions of gas (C2-C4 hydrocarbons) along with the generation of aromatics products.

In Chapter 3 the pilot scale research is presented to achieve "proof of concept" as well as to compare the pilot scale products to those at the micropyrolysis scale. It was found that residence time had a significant effect on product distribution. Increasing pilot plant pyrolysis residence time from 1 to 4.5 seconds caused a 9 wt. % drop in wax production, 5% drop in heavy oil, a 11 wt. % increase in light oil production, and a 4 wt.% increase in gas production. A multiphysics model was created which incorporates and extends the kinetic model presented in Chapter 2 with momentum, mass and heat transport to predict vapor residence time and temperatures within the pyrolysis reactor. The trends for product distribution as a function of VRT were found to be consistent between both the pilot plant and micropyrolysis systems, demonstrating that the pilot system can be "tuned" to produce the desired pyrolysis product similar to the tuning possible at the micropyrolysis scale.

Finally, in Chapter 4, the novel pyrolysis process, developed through laboratory research and pilot scale experiments, was modeled through process simulation and assessment. A process simulation of the proposed concept was conducted using generated pyrolysis yield data from Chapter 3. A techno-economic analysis and life cycle assessment of the process found favorable economic and environmental results for pyrolysis oil when compared to fossil naphtha at an operating capacity of 84,000 MT/yr. The heat integrated process had a pyrolysis oil minimum selling price (MSP) of $572/MT which is similar to the 5-year average selling price of petroleum naphtha ($561/MT). The economic results were found to be most sensitive to waste plastics feedstock costs, pyrolysis gas sales, operating capacity, and waste disposal costs. It was found that the proposed plant is profitable if the feedstock costs drop below $200/MT and/or the PET in the mixed waste plastic bales is recovered and sold into the secondary materials market for at least $25/MT. For the LCA, the pyrolysis gas and oil products have similar GHG emissions and lower CED when compared to their fossil-equivalent products for the process base case. When a credit for avoiding incineration of the mixed plastic bale is taken into consideration, the pyrolysis products have negative GHG emissions. Implementing heat integration and decarbonizing

the electric grid also have a positive impact on the GHG emissions, although these changes have a smaller effect on the pyrolysis oil's MSP.

Future work for the micropyrolysis apparatus includes examining the effect of mixed plastics (HDPE, LDPE, PP) and contamination (food contact contamination, paper, cardboard, etc.) on the underlying kinetics, the presence of unwanted elements in the products (O, S, Cl, etc.) and distribution of products among gas, liquid, and wax products. A wider range of temperatures needs investigation using micropyrolysis so that predictions of pyrolysis kinetics can occur over a wide range of temperatures, from 450-600°C and a wide range of vapor residence times. The resulting dataset will allow more accurate determination of kinetic parameters. Additional research is also needed to close a mass balance on the micropyrolysis experimental apparatus by understanding and controlling how a portion of the primary pyrolysis product is being trapped in the glass wool within the pyroprobe and whether this system limitation can be minimized. Pilot scale experiments indicate that the micropyrolysis experiments significantly underestimate the formation of the heaviest molecular weight species, which appears to be consistent to what is trapped in the glass wool. One focus on future research with the pilot plant system is to improve the condenser system to achieve better separation between the wax, oil, and gas products. Currently, considerably more overlap is found between the three products than what is thermodynamically predicted by the process simulation. The condensers for recovery of pyrolysis wax, and separately liquid, require more residence time so that the condensation process achieves the equilibrium state. In addition, more research is needed to understand how contamination effects the dissolution process and the quality of the pyrolysis products. Undissolved solids could provide an issue clogging the feeding process. It is not clear what levels and which types of contamination the wax solvent can handle. Understanding this will inform the level of sortation needed by the secondary sort process. Additional pilot-scale pyrolysis research could couple fast pyrolysis with catalytic upgrading of hydrocarbon vapors with the intention of adding functional groups to the C=C bonds in the pyrolysis products. Upgrading of pyrolysis vapors can be directed toward production of high-value pyrolysis products such as lubricants, monomers, and specialty chemicals.

Additional research is also needed to generate more accurate TEAs and LCAs of the secondary sort process. It is currently assumed that the economic costs and environmental burdens for secondary sorting are the same as for a materials recovery facility (MRF). The secondary sorting process is expected to primarily contain automatic sorting while a MRF also contains manually sorting and a variety of non-plastic products. Additional data and modeling of the secondary sorting process would increase the TEA and LCA accuracy. Research is also needed into the ability of the secondary sort to recover PET. A TEA scenario analysis found that recovering PET in addition to the HDPE/PP during the secondary sort could significantly improve the economic results of this process while also potentially enabling PET chemical recycling technologies. The economic benefits are large enough to devote future research towards fully examining this pathway. Additional TEA and LCA scenarios could analyze variations in #1-7 bales composition, pyrolysis yield, and co-locating the plant at a petrol-chemical facility. While in this work the #1-7 bales composition was assumed to be 40% PET, 36% PP, and 15% HDPE, significant compositional variations are present between individual MRFs. Lower PP/HDPE content

in the feedstock would increase sorting and waste costs while decreasing throughput in the pyrolysis reactor. More research is needed to understand what levels of variation occur between MRFs and whether there are seasonal variations in plastic composition within individual MRFs. Variations in PP/HDPE composition along with possible contamination that the sorting process failed to remove could also affect pyrolysis yield. In this study it was assumed that the sorting process perfectly removed all contamination. This assumption is probably an idealization and more research is needed to understand just how contamination would affect the pyrolysis yields of this process. Co-locating the pyrolysis process at a petrochemical facility would eliminate the need for pyrolysis oil and gas product transportation. The oil and gas product would both be sold to the petrochemical facility as a feedstock for higher-value chemical/plastic production within the petrochemical facility. This would change the value of the gas product, which is currently assumed to be sold as a propane substitute. In summary, pyrolysis oil for the heat integrated case compares favorably both economically and environmentally to fossil naphtha. Future improvements to the process, such as recovering PET and co-locating the plant next to a petrochemical facility, may further improve the economics and lower environmental burdens of pyrolysis oil.

A Supporting Information for Chapter 2

Micropyrolysis of Polyethylene and Polypropylene Prior to Bioconversion: The Effect of Reactor Temperature and Vapor Residence Time on Product Distribution

A.1 Schematic of two-stage micropyrolysis reactor

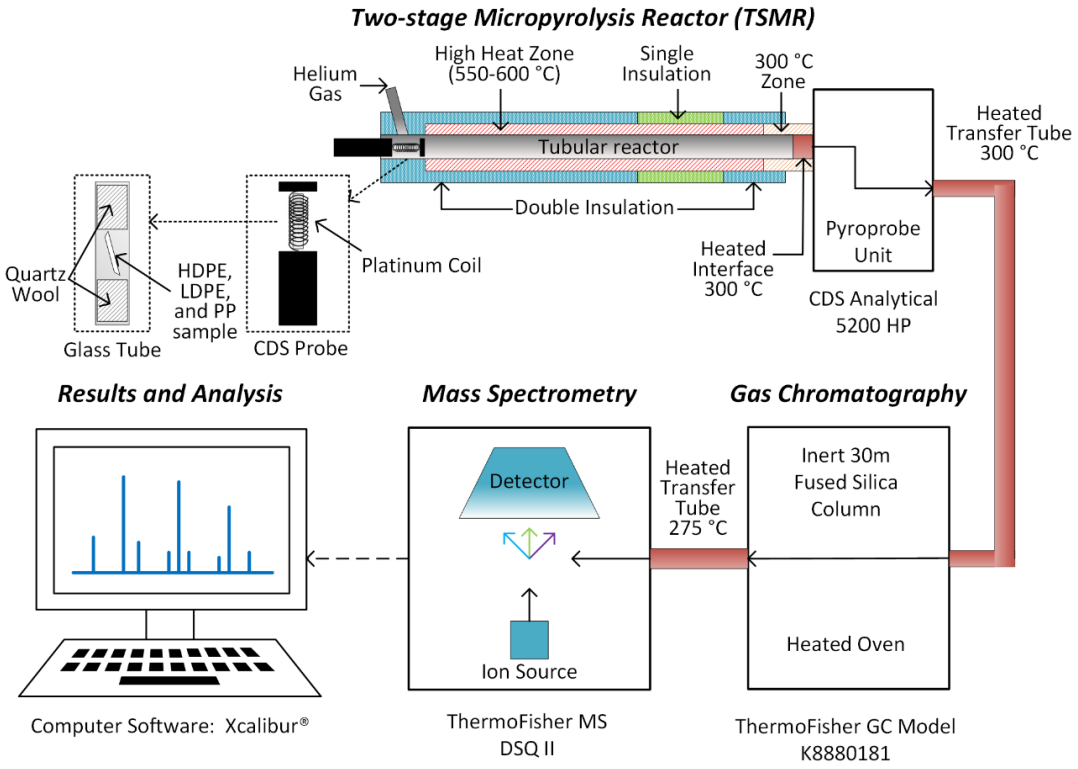

Figure A.1 Detailed schematic of the two-stage micropyrolysis experimental setup

A.2 Thermogravimetric analysis (TGA) of pyrolysis residue

Thermogravimetric analysis (TGA) was conducted on the pure glass wool and glass wool post-pyrolysis reaction to test if there was any pyrolysis residue for HDPE remaining on the glass wool. The thermogravimetric-based pyrolysis test was performed on a TA Instrument Model Q500. The glass wool sample, weighing 5 mg (nominal), was loaded into a platinum sample pan. The sample was then equilibrated at 40°C and purged in a continuously-flowing stream of nitrogen at a rate of 150 ml/min for 2 h before ramping, ensuring that all air (oxygen) was removed from the furnace before heating. The purged sample was then heated at a rate of 10°C/min until it reached 600°C. The TGA and derivative thermal gravimetric (DTG) curve (Figure A.2) show that weight loss from pure glass wool is less than 1%, showing that glass wool does not degrade at the pyrolysis temperature and is not responsible for any weight loss in the sample. The TGA and DTG results for residue from pyrolysis (Figure A.3) show considerable weight loss from the

pyrolysis products caught in the glass wool. The product distribution contains a variety of heavy components with the primary peak having a similar temperature signature to the pure HDPE (350-490 °C). This indicates that the primary pyrolysis produces products of both much lower molecular weight and similar molecular weight compared to the original resin. We hypothesize that the primary products from pyrolysis are hitting a cold zone inside the capillary tube and forming aerosols in the presence of the helium gas. The glass wool within the cold zone is capturing a portion of these aerosols while others break through and proceed to the tubular reactor where they continue to react and are eventually detected by the GCMS. TGA results were not conducted for residue from pyrolysis of LDPE and PP but it is expected that the results will be consistent for all 3 plastic types. Accounting for the measured weight loss from the TGA results gives a mass balance closure above 80% for the plastic sample (Table A.1). Three weights are used in the mass balance: the initial weight of the plastic sample prior to micropyrolysis, the plastic sample weight lost from pyrolysis, and the pyrolysis residue on the glass wool from TGA after removing the glass wool from the tube. The sample weight lost from pyrolysis was calculated by weighing the sample tube before and after the pyrolysis reaction. Since the glass wool doesn't degrade (Figure A.2) any weight loss must be from pyrolysis vapors leaving the sample tube and going into the tubular reactor. 83% of the initial HDPE sample weight is accounted for after the pyrolysis reaction, leading to a mass balance closure of 83%. The mass balance closure of less than 100% is likely due to the inability to remove all of the glass wool from the microyrolysis tube, based on visual inspection.

Table A.1 Mass Balance of HDPE sample from pyrolysis

Sample	**Weight**
Initial HDPE sample weight	0.00148 g
Sample weight lost from pyrolysis	0.00046 g
Pyrolysis residue in glass wool	0.00077 g
Total sample weight accounted for	0.00123 g
Mass Balance Closure	83%

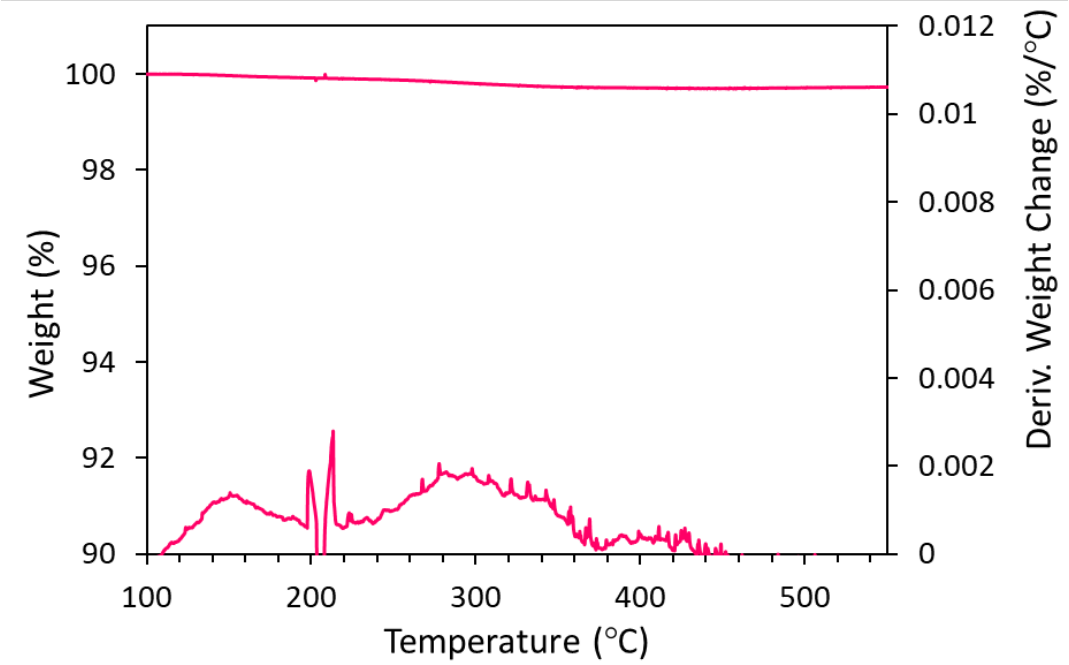

Figure A.2 TGA and DTG curve of pure glass wool

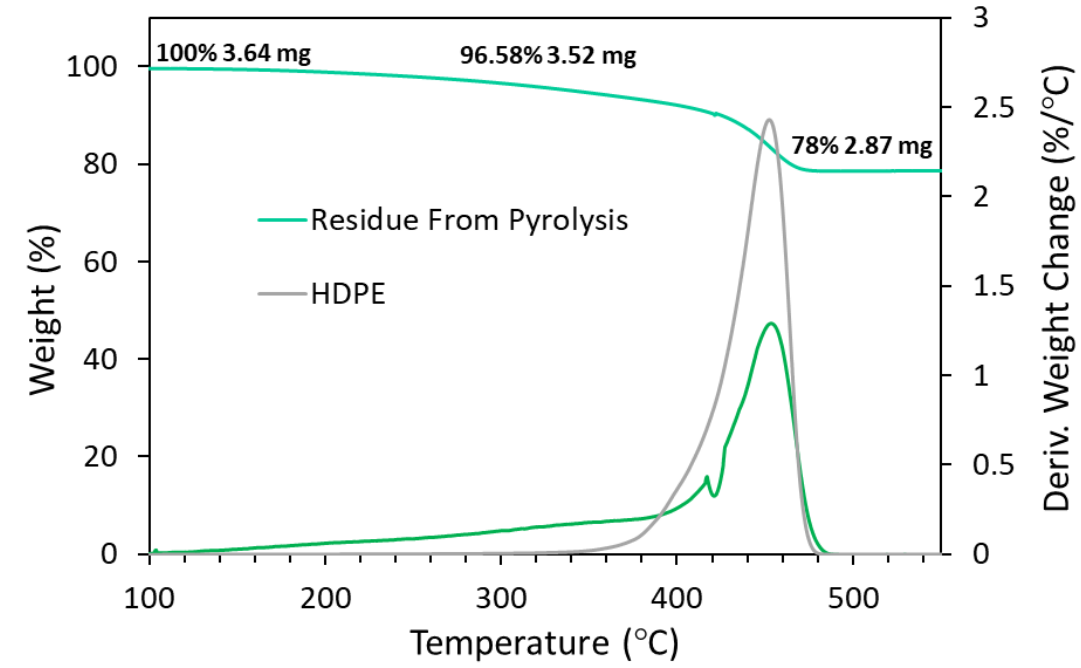

Figure A.3 TGA and DTG curves for residue from pyrolysis and pure HDPE resin. For residue from pyrolysis the remaining weight left after TGA is the glass wool.

A.3 Typical peak structure found in GC-MS results

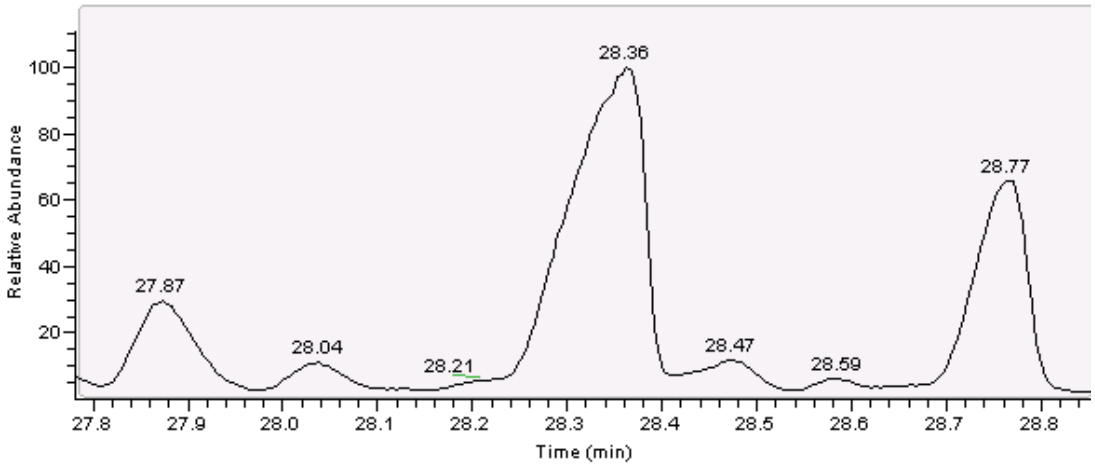

Figure A.4 Typical peak structure found in GCMS. The left peak is 1,9-decadiene (27.87 min), the center peak is 1-decene (28.36 min) and the right peak is decane (28.77 min). Results are from HDPE micropyrolysis at 575 ℃ and 2.8 second vapor residence time.

A.4 Aromatic production

The effect of vapor residence time (VRT) and reactor temperature on total aromatics production (Figure A.5) and benzene production (Figure A.6) for HDPE, LDPE, and PP. Increasing VRT and reactor temperature caused an increase in both aromatics and benzene production.

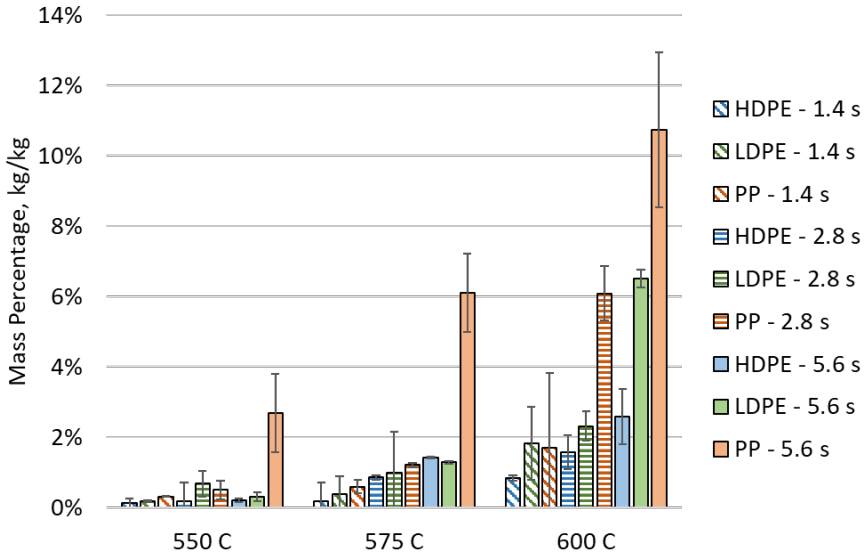

Figure A.5 Effect of vapor residence time and reactor temperature on total aromatics production for HDPE, LDPE, and PP

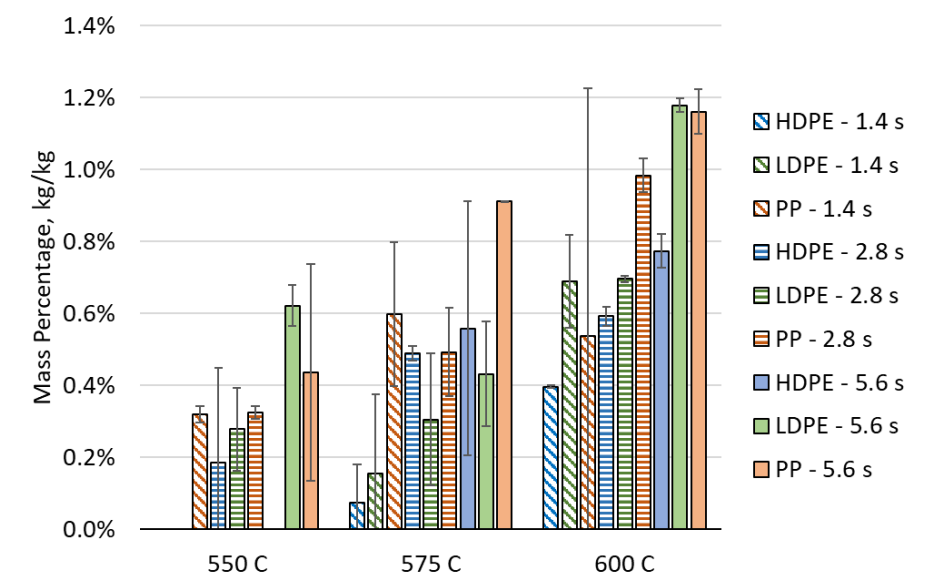

Figure A.6 Effect of vapor residence time and reactor temperature on benzene production for HDPE, LDPE, and PP

A.5 Reaction constants obtained from kinetic model

Table A.2, Table A.3, and Table A.4 show the solved reaction constants for each of the 10 reactions using the Arrhenius parameters presented in Table 2.1 in Chapter 2 at the three reactor temperatures studied in this work (550, 575, and 600 °C).

Table A.2 Reaction constant 'k' for each of the 10 reactions obtained from the kinetic model fit at 550 °C

Reaction constant (s^{-1})	**PP**	**HDPE**	**LDPE**
k_1 (Polymer -> Wax)	20.48	19.15	45.59
k_2 (Polymer -> Heavy Oil)	83.94	63.11	78.70
k_3 (Polymer -> Light Oil)	51.89	38.07	40.99
k_4 (Polymer -> Gas)	60.79	43.73	47.24
k_5 (Wax -> Heavy Oil)	1.84	1.78	3.69
k_6 (Wax -> Gas)	5.83E-07	2.33E-04	1.34E-07
k_7 (Light Oil -> Gas)	1.19E-02	5.29E-02	1.80E-03
k_8 (Heavy Oil -> Light Oil)	0.55	0.63	0.65
k_9 (Wax -> Light Oil)	9.11	4.53	5.66
k_{10} (Gas -> Aromatics)	0.46	0.19	0.52

Table A.3 Reaction constant 'k' for each of the 10 reactions obtained from the kinetic model fit at 575 °C

Reaction constant (s^{-1})	**PP**	**HDPE**	**LDPE**
k_1 (Polymer -> Wax)	48.80	38.10	92.29
k_2 (Polymer -> Heavy Oil)	99.21	79.86	88.85
k_3 (Polymer -> Light Oil)	85.06	54.76	64.80
k_4 (Polymer -> Gas)	66.51	48.12	54.71
k_5 (Wax -> Heavy Oil)	1.90	2.01	4.49
k_6 (Wax -> Gas)	1.92E-06	2.91E-04	1.14E-06
k_7 (Light Oil -> Gas)	1.19E-02	5.39E-02	2.06E-03
k_8 (Heavy Oil -> Light Oil)	1.03	0.82	0.68
k_9 (Wax -> Light Oil)	17.16	5.95	5.94
k_{10} (Gas -> Aromatics)	0.46	0.19	0.52

Table A.4 Reaction constant 'k' for each of the 10 reactions obtained from the kinetic model fit at 600 °C

Reaction constant (s^{-1})	**PP**	**HDPE**	**LDPE**
k_1 (Polymer -> Wax)	110.63	72.85	179.44
k_2 (Polymer -> Heavy Oil)	116.15	99.70	99.61
k_3 (Polymer -> Light Oil)	135.56	77.15	99.79
k_4 (Polymer -> Gas)	72.39	52.66	62.83
k_5 (Wax -> Heavy Oil)	1.96	2.26	5.39
k_6 (Wax -> Gas)	5.93E-06	3.58E-04	8.52E-06
k_7 (Light Oil -> Gas)	1.20E-02	5.48E-02	2.35E-03
k_8 (Heavy Oil -> Light Oil)	1.87	1.06	0.72
k_9 (Wax -> Light Oil)	31.14	7.69	6.21
k_{10} (Gas -> Aromatics)	0.46	0.19	0.52

A.6 Microscopy images of pyroprobe samples

Pictures were taken with stereo microscope camera (10x) of four HDPE plastic micropyrolysis samples to visually ensure complete degradation. The HDPE samples were pyrolyzed inside the pyroprobe for varying lengths of time between 2 and 20 seconds at 575 °C. This was done to get an indication of how long it took for the HDPE sample to completely degrade. At a pyroprobe time of 2 seconds the HDPE is partially degraded. Vapor bubbles are seen trapped in the sample from the rapid cooling at 2 seconds. At 3 seconds the sample has reduced in size indicating further degradation and vaporization. At 5 seconds the sample is completely degraded and is now in the vapor phase. Keeping the pyroprobe heated at 575 °C for the full 20 seconds, as was done in the experimental

methods, ensures that the sample is fully pyrolyzed and no visual residue remains (shown in part D of Figure A.7).

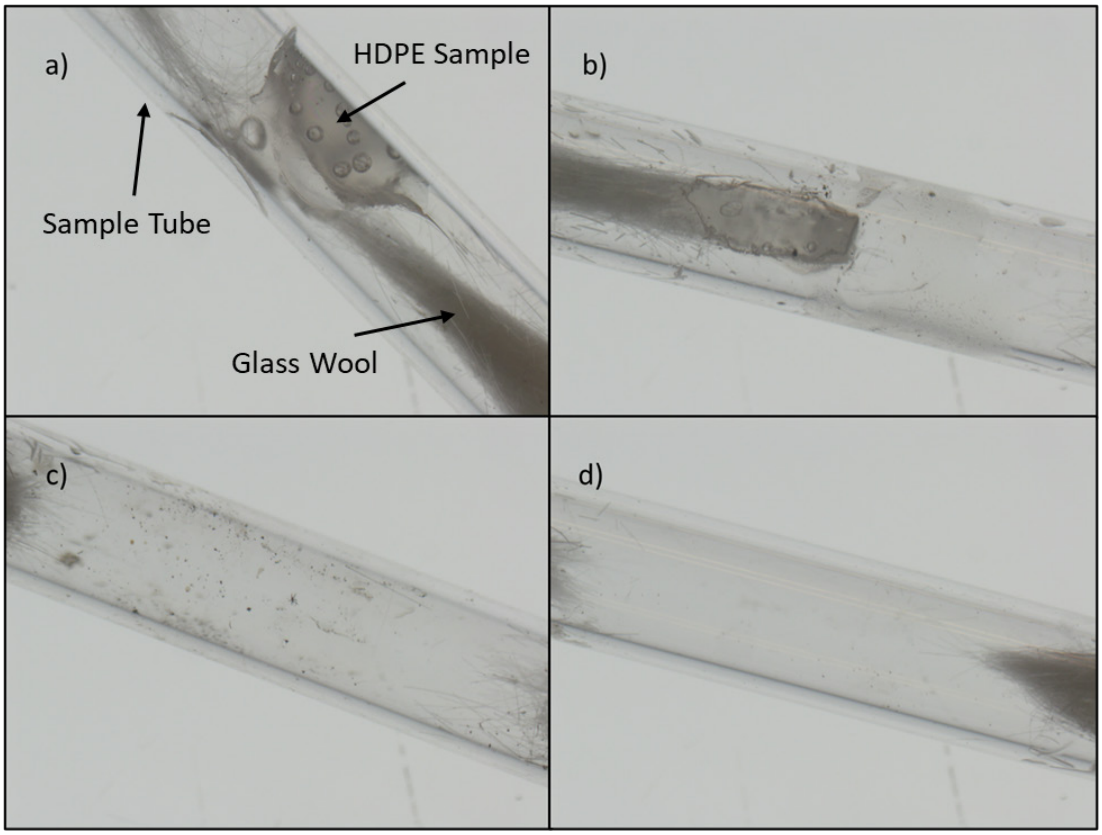

Figure A.7 Amount of degradation of HDPE sample after pyroprobe firing of 2 seconds (a), 3 seconds (b), 5 seconds (c), and 20 seconds (d) at 575 °C

B Supporting Information for Chapter 3

Liquid-Fed Waste Plastic Pyrolysis Pilot Plant: Effect of Reactor Volume on Product Yields

B.1 GC-MS chromatograms of pyrolysis products

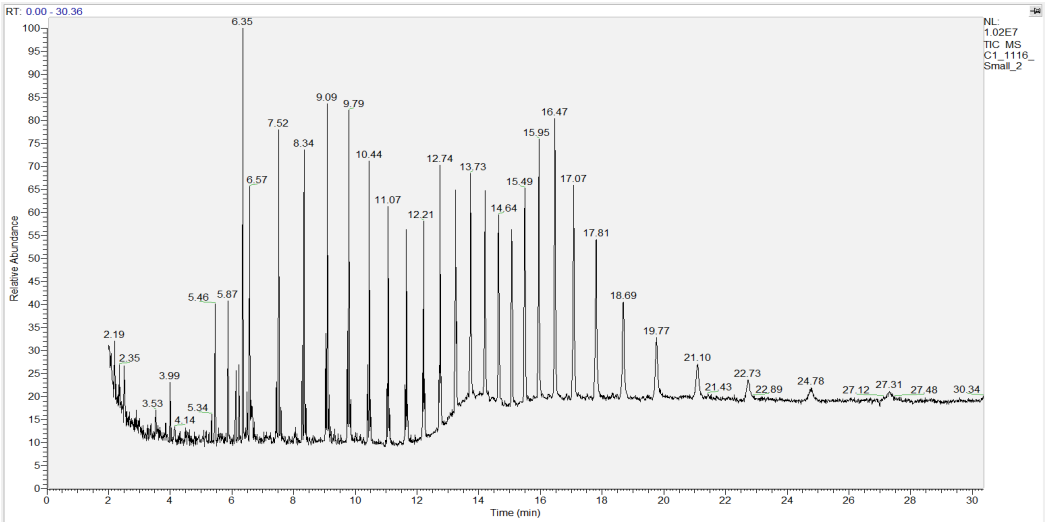

Figure B.1 GC-MS Chromatogram of condenser 1 (C1) product for run 1A. Peaks of interest include 1-decene (5.87 min.), 1-tetradecane (9.09 min.), 1-hexadecane (10.44 min.), 1-octadecene (11.65 min.), and 1-eicosene (12.74 min.). C36 hexene was the largest detected.

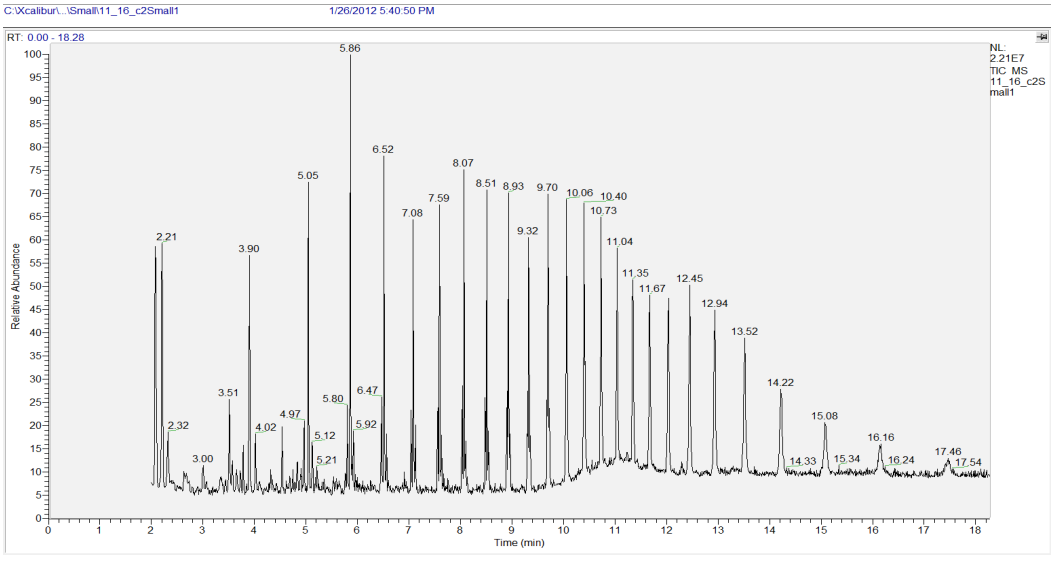

Figure B.2 GC-MS chromatogram of condenser 2 product for run 1A. Peaks of interest include 1-decene (5.86 min.), 1-tetradecane (8.07 min.), 1-hexadecane (8.93 min.), 1-octadecene (9.70 min.), and 1-eicosene (10.40 min.).

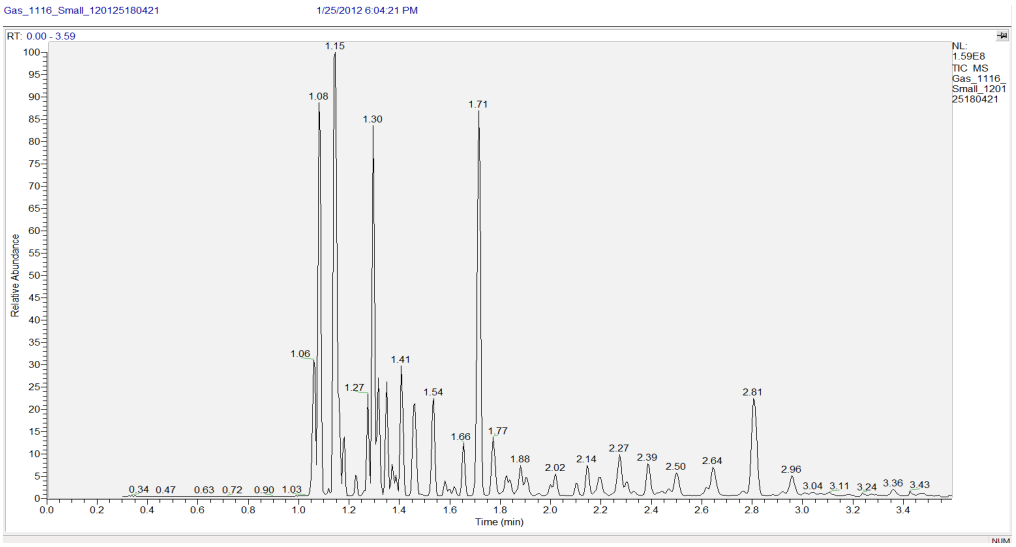

Figure B.3 GC-MS chromatogram of gas product for run 1A. Peaks of interest are ethane (1.06 min.), propene (1.08 min.), butene (1.15 min.), pentene (1.30 min.), hexene (1.71 min.), and heptene (2.81 min).

B.2 Pilot plant condenser design

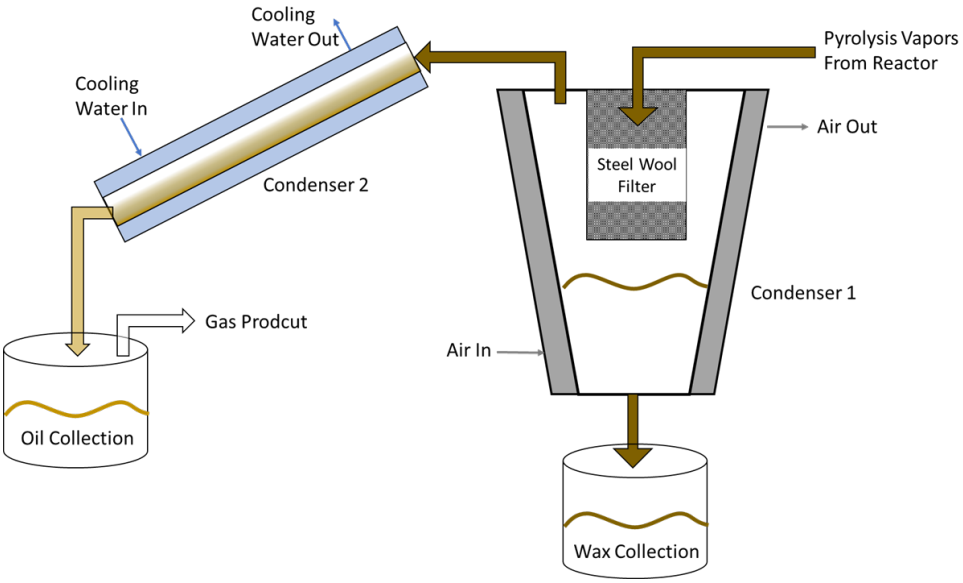

Figure B.4 Pyrolysis vapors flow from the reactor into a steel wool filter inside condenser 1. The steel wool traps any aerosols present and condenses the wax product, which is collected at the bottom of the conical condenser. Air is used as a cooling agent to keep the temperature inside condenser 1 steady at 150 °C. The remaining vapors proceed to the shell and tube condenser 2 where cooling water is used to keep the inside temperature steady at 25 °C. The condensed liquid flows out of the condenser into a collection jar.

B.3 GC-MS calibration curves

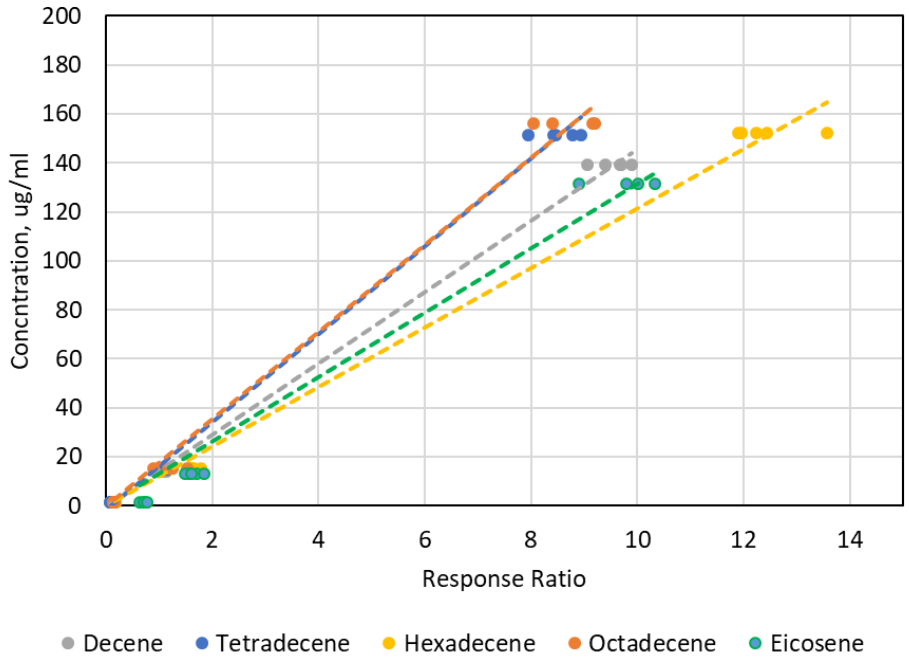

Figure B.5 GC-MS calibration curves for 1-decene, 1-tetradecane, 1-hexadecane, 1-octadecene, and 1-eicosene. The response ratio is the ratio of each compounds peak area relative to the internal standard to correct for injection variations.

B.4 Reaction pathways for lumped kinetic model

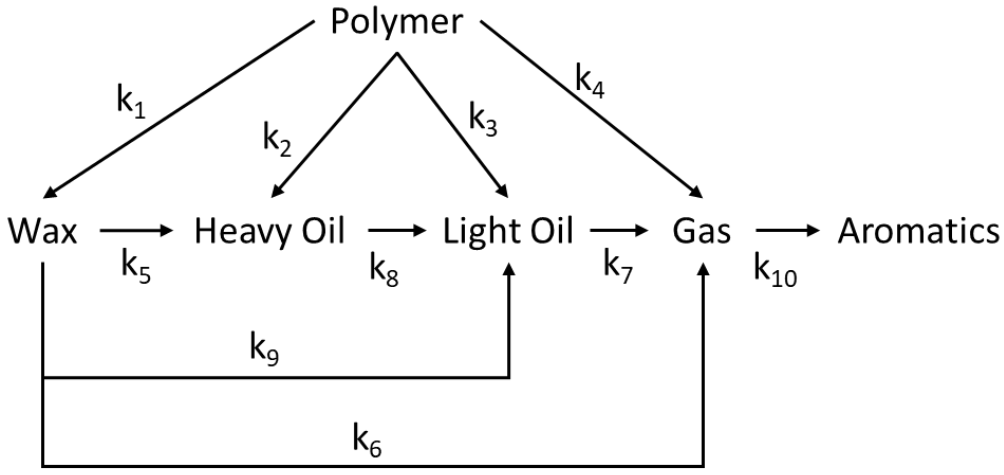

Figure B.6 Reaction pathway diagram for the lumped kinetic model used in the main manuscript. Polymer is the HDPE plastic feedstock, wax is C21+, heavy oil is C11-C20, light oil is C5-C10, gas is C1-C4, and aromatics include BTEX (benzene, toluene, ethylbenzene and xylene).

B.5 Inputs for reactor model

The reactor model was solved using Polymath 6.10. Table B.1, Table B.2, and Table B.3 contain the inputs used in the model.

Table B.1 Modeling inputs for pyrolysis products. The molecular weight (MW) and heat capacity (Cp) were calculated using ASPEN Plus.

Lumped Product	**Representative Compound**	**MW (g/mol)**	**Heat Capacity (J/kg*K)**
Wax	Pentacosene	352	3494
Heavy Oil	Pentadecene	212	3335
Light Oil	Octene	114	3296
Gas	Propene	44	3151
Aromatics	Benzene	78	2545

Table B.2 Heat of reactions (ΔHr) for the 10 lumped pyrolysis reactions used in reactor model

Reaction #	**Reactant**	**Product**	**Δ H_r (J/g)**	**Source**
1-4	HDPE	Wax, heavy oil, light oil, gas	515	[1]
5	Wax	Heavy Oil	455	Aspen Plus
6	Wax	Gas	1926	Aspen Plus
7	Light Oil	Gas	1134	Aspen Plus
8	Heavy Oil	Light Oil	336	Aspen Plus
9	Wax	Light Oil	791	Aspen Plus
10	Gas	Aromatic	294	Aspen Plus

Table B.3 Arrhenius parameters for the ten pyrolysis reaction pathways

	HDPE	
Reaction Constant	**A, 1/s**	**Ea, kJ/mol**
k_1 (Polymer -> Wax)	2.59E+11	1.60E+02
k_2 (Polymer -> Heavy Oil)	1.85E+05	5.46E+01
k_3 (Polymer -> Light Oil)	8.65E+06	8.44E+01
k_4 (Polymer -> Gas)	1.12E+03	2.22E+01
k_5 (Wax -> Heavy Oil)	4.52E+00	2.84E+01
k_6 (Wax -> Gas)	8.40E+01	5.13E+01
k_7 (Light Oil -> Gas)	9.92E-02	4.30E+00
k_8 (Heavy Oil -> Light Oil)	6.28E+03	6.31E+01
k_9 (Wax -> Light Oil)	1.30E+03	6.31E+01
k_{10} (Gas -> Aromatics)	1.90E-01	8.06E-04

B.6 Product distribution from reactor model

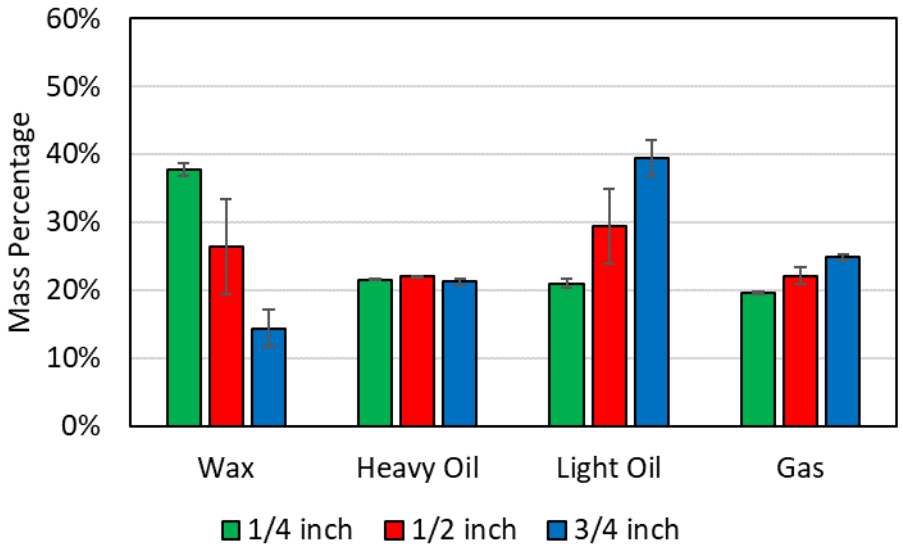

Figure B.7 Lumped product distribution from the reactor model. Each bar represents the average of the two mass flowrates for each reactor volume.

B.7 Temperature traces for ½" and ¼" reactor

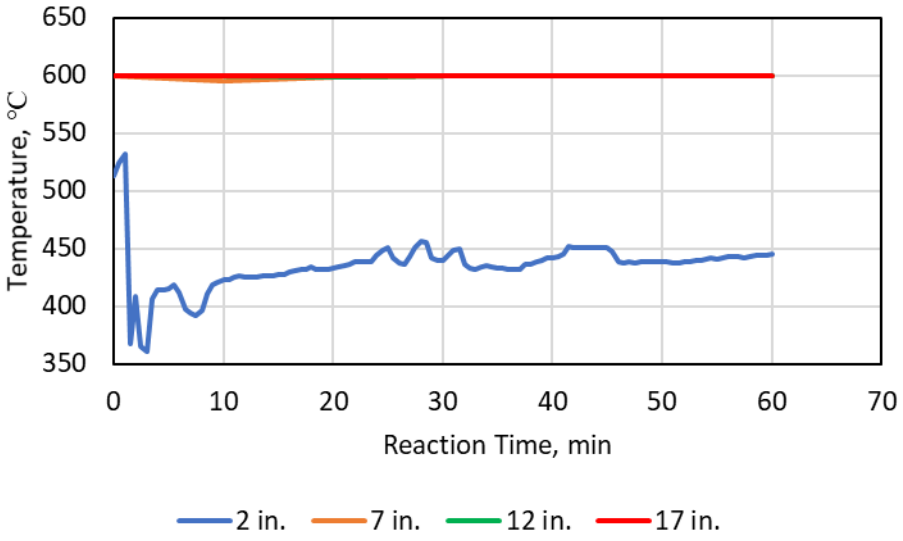

Figure B.8 Reactor temperature profile for pilot plant run #1A using the ¼" ID reactor.

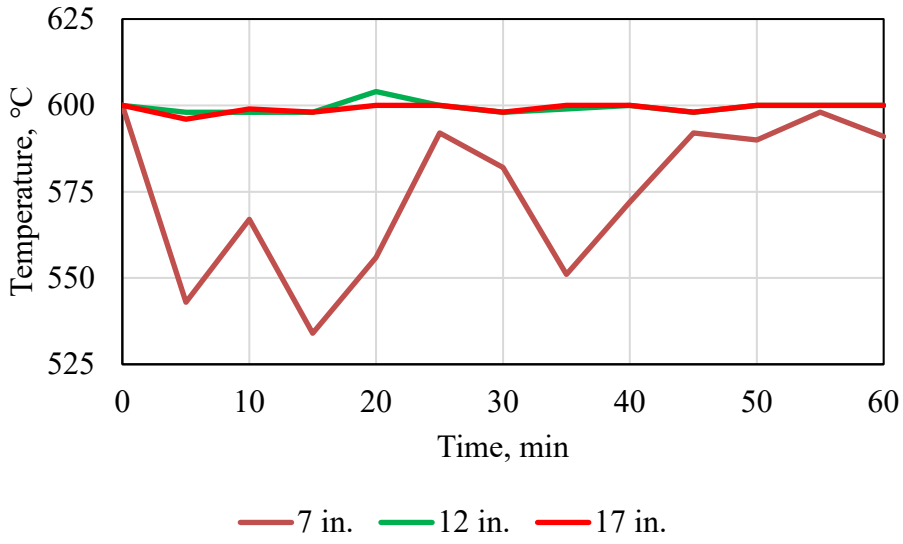

Figure B.9 Reactor temperature profile for pilot plant run #2B using the ½ inch ID reactor.

B.8 Typical peak structure found in GCMS results

The typical peak structure found in GC-MS results consists of a dominant center alkene peak with two minor side peaks (Figure B.10). The left side peak is an alkadiene while the right-side peak is alkane.

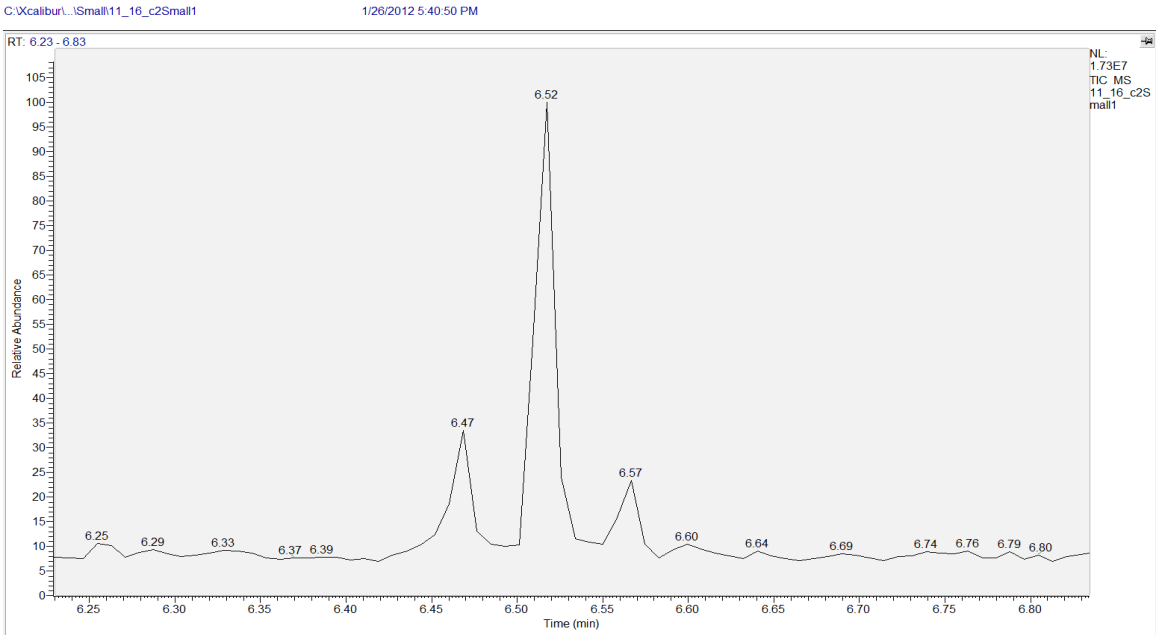

Figure B.10 Typical peak structure found in GC-MS. The left peak is 1,10-undecadiene (6.47 min), the center peak is 1-undecene (6.52 min) and the right peak is undecane (6.57 min). Results are from the condenser 2 product of run 1A.

B.9 References

1. Elordi, G.; Arabiourrutia, M.; Bilbao, J.; Olazar, M., Energetic viability of a polyolefin pyrolysis plant. *Energy & Fuels* **2018,** *32* (3), 3751-3759. DOI: 10.1021/acs.energyfuels.7b03664

C Supporting Information for Chapter 4

Economic and Environmental Analysis of Plastics Pyrolysis After Secondary Sortation of Mixed Plastic Waste

C.1 Five-year average propane price

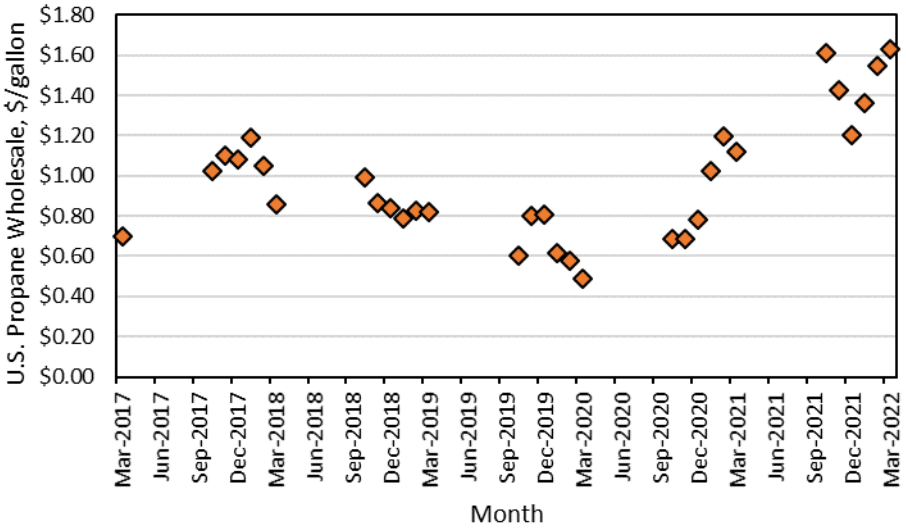

Figure C.1 The average wholesale propane price over the past 5 years is $0.96/gallon.[1]

C.2 Pyrolysis Reactor Yields

Table C.1 Pyrolysis yields of 1:1 HDPE/Pyrolysis Wax Solvent at 600 °C.2 1-Triacontene represents all the mass fractions above C30.

Compound	Mass Fraction	Compound	Mass Fraction	Compound	Mass Fraction
Methane	0.037	1-Undecene	0.056	1-Heneicosene	0.022
Ethylene	0.007	1-Dodecene	0.032	1-Docosene	0.022
Propene	0.066	1-Tridecene	0.030	1-Tricosene	0.020
1-Butene	0.091	1-Tetradecene	0.029	1-Tetracosene	0.019
1-Pentene	0.103	1-Pentadecene	0.027	1-Pentacosene	0.019
1-Hexene	0.109	1-Hexadecene	0.025	1-Hexacosene	0.020
1- Heptene	0.043	1-Heptadecene	0.023	1-Heptacosene	0.023
1-Octene	0.013	1-Octadecene	0.022	1-Octacosene	0.022
1-Nonene	0.023	1-Nonadecene	0.021	1-Nonacosene	0.018
1-Decene	0.037	1-Eicosene	0.020	1-Triacontene	0.038

C.3 Methodology for costing of equipment

The purchased equipment cost of each unit operation was calculated using equation C-1.

$$C_e = \frac{CEPCI_{2019}}{CEPCI_{2010}}(a + bS^n) \quad \text{(C-1)}$$

where C_e is the purchased equipment cost on a U.S Gulf Coast basis, $CEPCI_{2019}$ (607.4) and $CEPCI_{2010}$ (532.9) are time correction factors to account for inflation since the cost correlations were published in 2010[3], a and b are empirical costing parameters based on equipment size, S is the equipment size parameter, and n is an exponential sizing correlation which is specific to each piece of equipment. The costing parametes a, b, S, and n are listed in Table C-2 for each unit operation used in this study. The fixed capital investment (FCI), which accounts for piping, construction, instrumentation, electrical systems, cost of designing the plant, offsites, and contingency, is calculated using equation C-2.

$$FCI = C_e(\text{ISBL})(1 + OSBL)(1 + \text{X} + \text{D\&E}) \quad \text{(C-2)}$$

where ISBL is the Inside Battery Limits factor, OS is the Outside Battery Limits factor, X is contingency factor, and D&E is design and engineering factor. For this study an ISBL of 3.2, OSBL of 1.4, X of 0.1, and D&E of 0.25 was used.

Table C.2 Purchased equipment cost for common plant equipment[3]

Equipment	**Units for Size, S**	**a**	**b**	**n**
Propeller	kW	17,000	1,130	1.05
Tanks (Floating Roof)	m^3	113,000	3,250	0.65
Heaters (Furnaces – Cylindrical)	MW	80,000	109,000	0.8
Heat Exchangers (Double Pipe)	m^2	1,900	2,500	1
Reactor (Jacketed, Agitated)	m^3	61,500	32,500	0.8
Pumps	kW	-1,100	2,100	0.6
Compressor	kW	580,000	20,000	0.6

C.4 LCA allocation factors

Table C.3 Energy allocation factors for pyrolysis oil and pyrolysis gas without heat integration.

Product	**Mass Flow Rate, kg/hr**	**Energy Content, MJ/kg**	**Energy Allocation Factor**
Pyrolysis Oil	4406	42	1.073E-04
Pyrolysis Gas	4467	46.2	1.180E-04

Table C.4 Energy allocation factors for pyrolysis oil and pyrolysis gas with heat integration.

Product	**Mass Flow Rate, kg/hr**	**Energy Content, MJ/kg**	**Energy Allocation Factor**
Pyrolysis Oil	4406	42	1.004E-04
Pyrolysis Gas	5050	46.2	1.104E-04

C.5 References

1. Weekly Heating Oil and Propane Prices (October - March). https://www.eia.gov/dnav/pet/pet_pri_wfr_a_EPLLPA_PWR_dpgal_m.htm (accessed June 2022).

2. Kulas, D.; Zolghadr, A.; Shonnard, D., Liquid-Fed Waste Plastic Pyrolysis Pilot Plant: Effect of Reactor Volume on Product Yields. *Journal of Analytical and Applied Pyrolysis* **2022,** *166*, 105601. DOI: 10.1016/j.jaap.2022.105601

3. Towler, G.; Sinnott, R. K., *Chemical engineering design: principles, practice and economics of plant and process design*. Elsevier: 2012.

D Copyright documentation

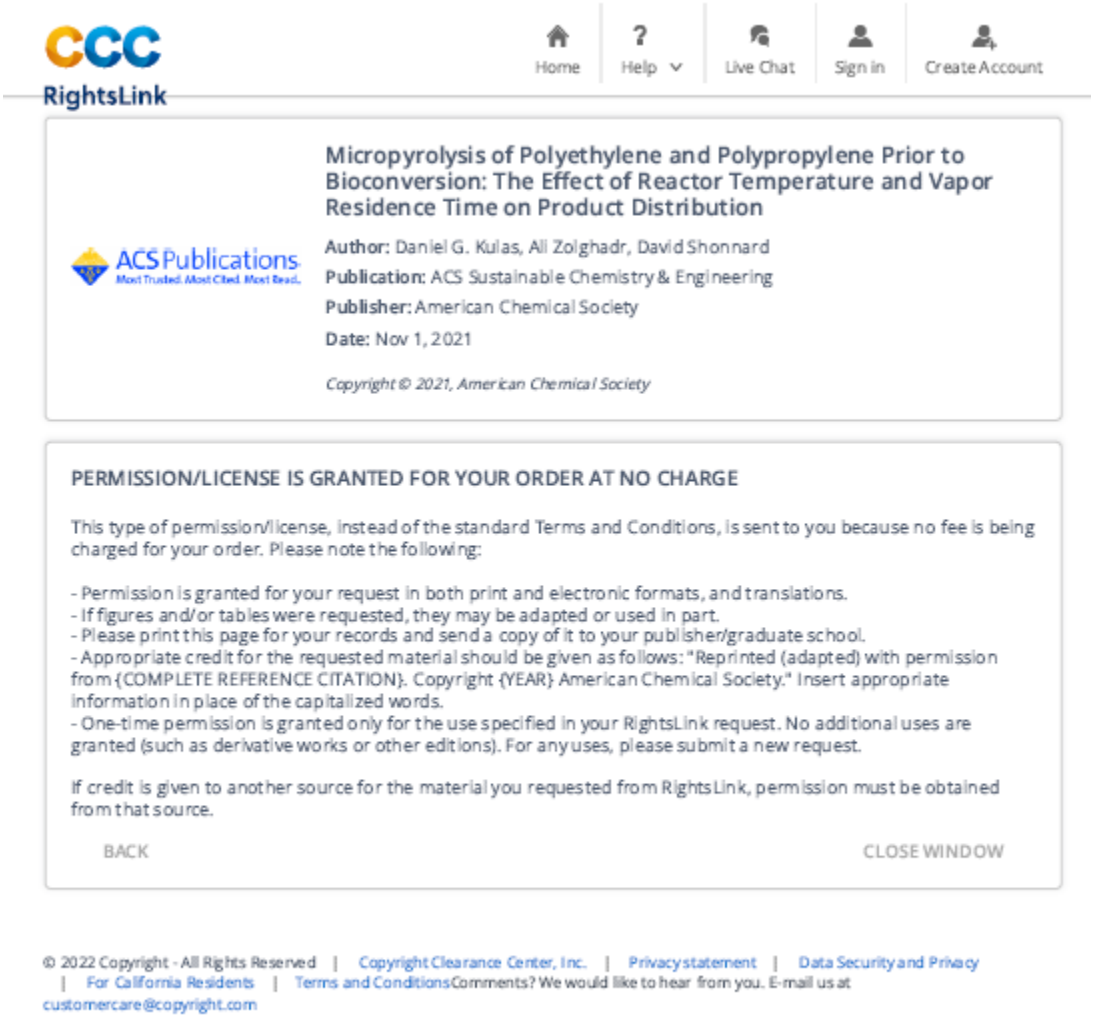

Figure D.1 Copyright clearance for Chapter 2.